AN UPDATED ASSESSMENT OF THE RISK FOR OIL SPILLS IN THE BALTIC SEA AREA

July - 2002

TABLE OF CONTENTS

INTRODUCTION **3**

1. METHODOLOGY AND MODELS **4**

1.1. METHODOLOGY OF MODELLING 4
1.2. GENERAL BEHAVIOR OF OIL IN THE MARINE ENVIRONMENT 6
1.3. THE OIL SPILL MODELLING SYSTEM 8

2. INFORMATION FOR MODELLING **10**

2.1. METEOROLOGICAL INFORMATION 10
2.2. SEA CURRENTS 10
2.3. OIL PROPERTIES 12
2.4. CARTOGRAPHIC BASE 13
2.5. OIL SPILL SCENARIOS DATA 13

3. RESULTS OF OIL SPILL MODELLING **14**

3.1. RISK ZONES EVALUATION 14
3.2. WEATHERING EVALUATION 40
3.3. PROBABILITY OF THE SHORE IMPACT 42

4. LITERATURE **54**

APPENDIX A. 55
MATHEMATICAL MODEL OF THE OIL SPREADING ON THE SEA SURFACE 55
NUMERICAL TECHNIQUE 63
APPENDIX B. 66
3D BAROCLINIC MODEL WITH FREE SURFACE FOR CURRENTS CALCULATION 66
APPENDIX D. 71
LIST OF FILES 71

Introduction

The main objective of this work is evaluation of most important characteristics of the oil spills movement and weathering in the Baltic Sea Area, for selected possible oil spill locations, in the vicinity of main seaports involved in the oil transportation.

The real spill accidents usually are happen in the complicated weather situations, and time period for spill response measures is very limited. For this reason, previously calculated scenarios may provide with as a real support in spill response preparation. The mathematical modelling of oil movement gives a opportunity to evaluate the scale and probability of the sea and shore objects impact by a potential oil spill. As a result of this, specialists on OSR development can optimize their efforts in identification the appropriate resources required for the oil spill response depending on the size and place of the spill. Using the OSR resources model, it may be possible also to evaluate various spill combatting strategies, and drive a solution about OSR resources and equipment conformity to the objectives of response and containment of a possible oil spill.

1. Methodology and Models

1.1. Methodology of Modelling

Two primary modes of oil spill simulations are used: "Trajectory and Fates" which predict the behavior (transport and fates) of an oil spill in specific wind and current conditions, and "Stochastic", which calculates the probable water and shoreline oiling due to typical or historical hydro meteorological conditions for some certain region. In present study, the Trajectory and Fates mode was used for oil spreading and evaporation calculations for different wind conditions. The Stochastic model was used to determine how quickly oil can reach specific coastal regions, and likelihood of oil impact in case of oil spill occur in certain hypothetical points. The stochastic modelling consists of a large number of oil spill scenarios, using actual wind conditions for the Baltic Sea over typical year period. It is assumed that this information accurately represents the possible weather conditions for the region, and, generally speaking, that oil spill has an equal probability of occurrence during the reference time period.

For oil spill impact assessment the transportation route was divided in parts. The basic points for oil spill modelling was chosen in every part of routes. The locations of basic points are shown in **Figure 1, Figure 2**

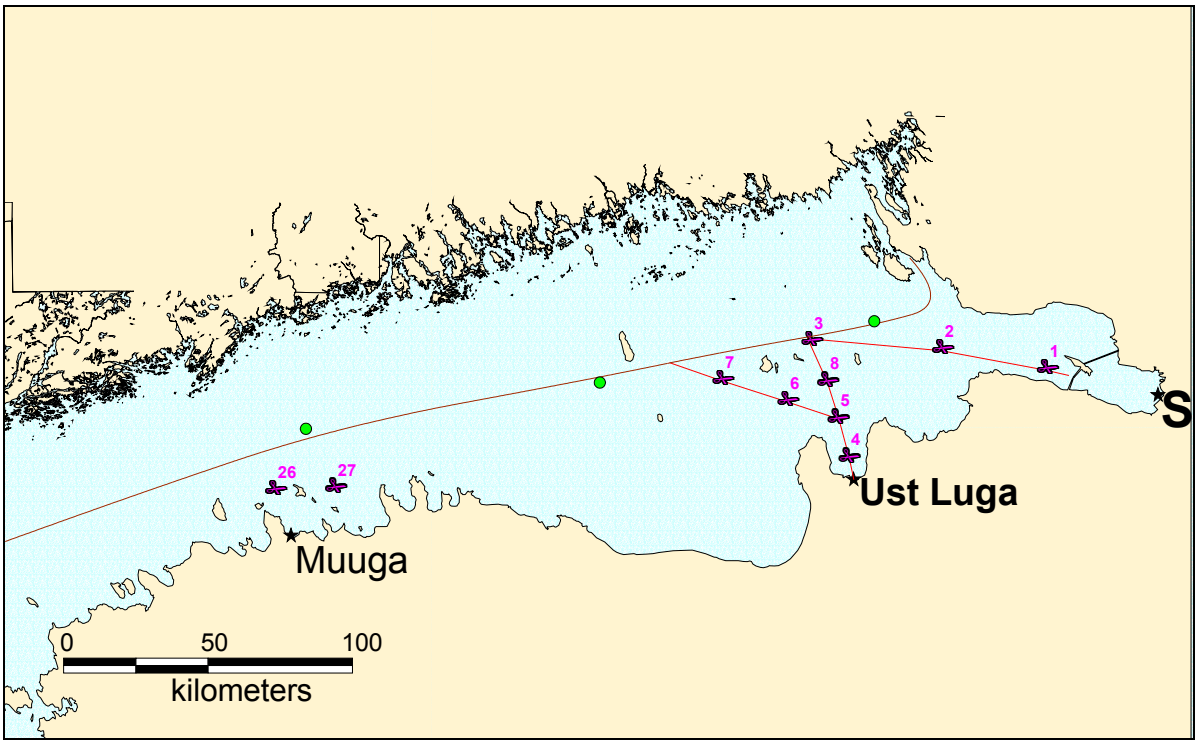

Figure 1. Hypothetical oil spill points locations (Northern part).

Points 1-8 are corresponded to the route segment near the Russian ports St.Petrsburg and Ust Luga, points 26-27 – to Muuga (Estonia).

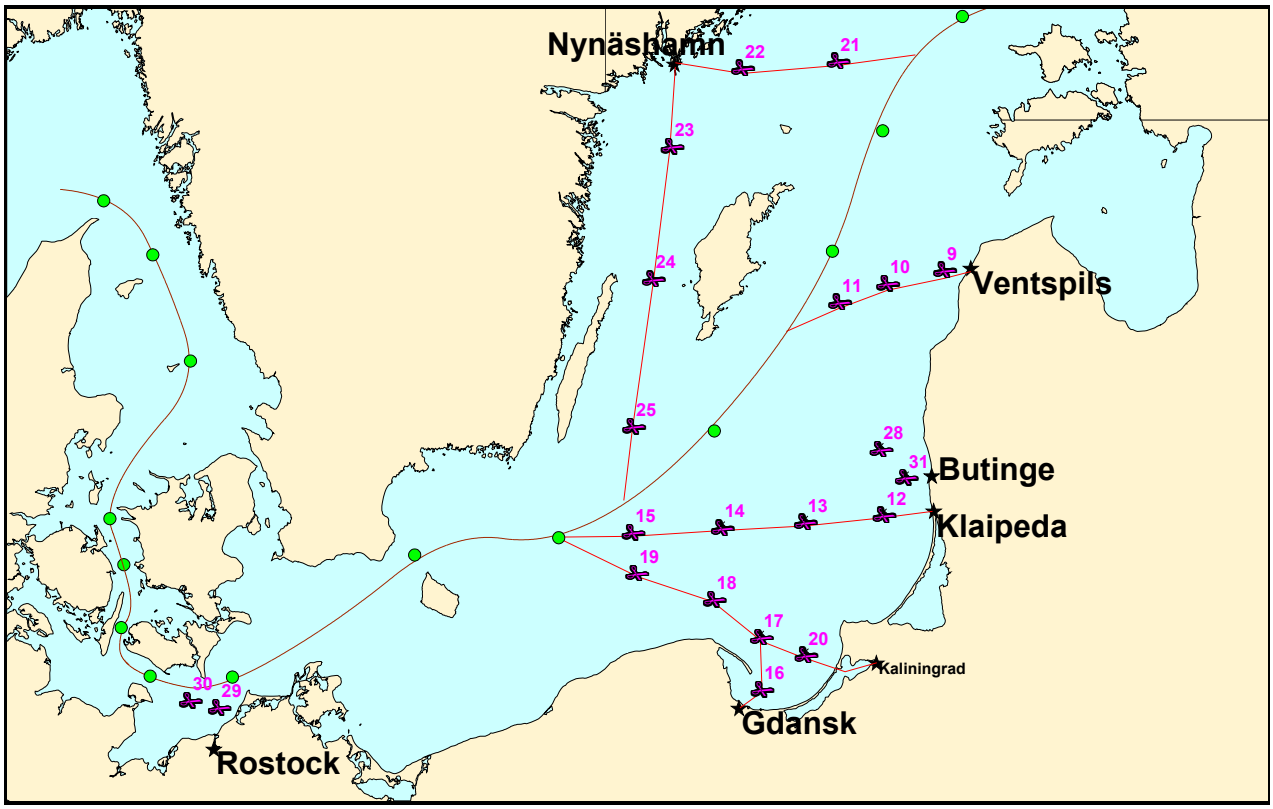

Figure 2. Hypothetical oil spill points locations (Southern part).

It is supposed that an oil spill accident probability does not depend on time within the reference year. About 2500 oil spill scenarios were simulated for each point (about 42500 scenarios in all). The evaluations presented in Chapter 3 are based on these calculation results.

The main stages of these evaluations are as follows

- Hydrometeorological data preparation based on historical records and shortcoming data reconstruction with mathematical models of surface wind, sea currents and ice dynamics
- Oil spill trajectories calculation and subsequent analysis for the purpose of shore and valuable marine objects impact risk evaluation
- Oil spill weathering calculations considering evaporation and natural dispersion processes resulting in partial oil fractions lost with subsequent atmosphere and water column pollution
- Statistical processing of trajectories calculations results to identify oil spill impact risk zones for certain time period in different hydro meteorological conditions
- Oil spill impact probabilities calculations of the specific shoreline sections or valuable marine objects.

For convenience, let us define two important notions used in this report.

Risk zone is area of water where oil can appear in defined time period right from the start of accident (e.g., 1 day, 3 day, etc.), if no response activity will be carried out. Risk zones are determined by statistical processing of the large amount of probable trajectories of oil spills motion depending on hydrometeorological conditions of the region and oil spill parameters.

Scale of Impact defines evaluated spatial characteristics of oil spill (e.g. length, area), changing in time after oil spill accident, depending on spreading, weathering, diffusion, etc. Scale of impact depend on position and type of oil spill source (instantaneous or leak), amount of spilled oil or leakage rate, physic-chemical properties of oil, hydrometeorological conditions. Scale of impact changes considerably depending on shoreline orientation toward wind direction and surface currents pattern.

Statistical estimates and oil weathering calculations results, being examined jointly, give a possibility to understand spatial and temporal scales of possible accident development, risk zones of water area and shore impact, and supposed scale of oil spill impact consequences.

The Oil Spill Modelling System (OSMS) computer program was used for oil spill simulations.

1.2. General Behavior of Oil in the Marine Environment

The shape and position of the oil slick is controlled by metocean (near-water wind) and hydrological (surface currents) conditions in the area at the time of the spill. Three primary processes affecting the behavior of oil spilled on the water are advection, spreading, and weathering. Advection is the process of lateral transport of the oil due to the driving force of winds and currents, and is the primary driving mechanism for oil spills. Spreading is the process by which the area of the oil increases over time due to positive buoyancy, surface tension and diffusion. The physical and chemical change which spilled oil undergoes is known as “weathering”. Knowledge of these processes and how they interact to alter the nature and composition of the oil with time is valuable in preparing and implementing of contingency plan for effective oil spill response.

Description of Oil Fates Processes

- **Evaporation**

is a physical-chemical process resulting in mass transfer of hydrocarbons from the sea surface to the atmosphere. It is the most significant initial weathering process by which all volatile fractions (light ends) of an oil are lost within the first few hours of a spill. Another significant role of evaporation is to change the physical and chemical properties of the oil (e.g., density, viscosity, water content, etc.)

- **Emulsification**

is a physical-chemical process resulting in the formation of water-in-oil emulsions. The formation of emulsions changes the properties and characteristics of oil to a very large degree. Emulsion formation is a result of surfactant like behavior of the polar and asphaltene compounds. These compounds are stabilized in many crude oils by the aromatic solvents. As aromatics get depleted due to weathering, asphaltenes begin to precipitate. Precipitated asphaltenes reduce the surface tension of the oil-water interface and initiate the emulsification process. Water enters the oil phase by the disruption or deformation of the oil-water interface. Deformation of the interface may take place due to turbulence, capillary ripples, Raleigh-Taylor instability and Kelvin-Helmholz instability. Water droplets in the oil phase are stabilized by the precipitated asphaltenes.

- **Entrainment**

Entrainment is a physical process when macroscopic globules of oil are transported from the sea surface into the water column due to breaking waves. Entrained oil is broken into droplets of varying sizes, which spreads and diffuses in the water column. Droplet sizes, droplet buoyancy and turbulence control the stability of entrainment. Breaking waves created by the action of wind and waves on the ocean surface are the primary sources of energy for entrainment. Entrained oil is subjected to enhanced dissolution & bio degradation processes.

- **Dissolution**

Dissolution is a chemical process resulting in mass transfer of hydrocarbons (water-soluble fractions) from oil surface slick and oil droplets to the water column. The mass transfer mechanism is due to molecular diffusion and proceeds at a slower rate compared to evaporation. Dissolution and evaporation are competitive processes.

The dissolved component concentration of hydrocarbons in water under a surface slick shows an initial increase followed by a rapid decrease after some hours due to the evaporative loss of components. Most soluble components are also volatile and direct evaporation from the water column depletes their concentrations in the water column. Dissolution is important where evaporation is low (dispersed oil droplets and ice-covered surfaces). Dissolved hydrocarbons are the most available to biota.

- **Biodegradation**

Biodegradation is a biological-chemical process altering or transforming petroleum hydrocarbons through the action of microbial populations and/or the ingestion or retention by macro organisms.

- **Sedimentation**

Sedimentation is the increase in density of oil due to weathering and interaction with suspended sediments or material of biological origin. The result of sedimentation is the deposition of oil adsorbed sediment particles to the sea floor.

- **Shoreline Interaction**

Interaction of oil with the shoreline affects surface oil transport and weathering process under atmospheric weathering factors.

1.3. The Oil Spill Modelling System

.

OSMS is a computer system for use in oil spill behavior forecasting, response decisions support, planning and training. The system operates on PC Windows 9x/NT/2000 computers, and provides calculations for oil and oil products in the ocean, near the coast and in polar and ice conditions, taking into account the interaction with response facilities. Mathematical and computational pecularities of models in use are represented in Appendix A.

The following oil spill processes are modeled:

- Transport and deformation of an oil slick due to time and spatially varying winds and currents
- Oil spreading at the sea surface due to positive buoyancy
- Diffusion and dispersion of oil on the sea surface and in the water column
- Evaporation of a multi-component mixture of oil

- Sinking of oil in water, and consequent sedimentation
- Formation of oil-in-water emulsion
- Weathering of oil, resulting in changes in density, viscosity, and water content, due to evaporation and emulsification processes
- Stranding of oil and shoreline interaction

Input Data

- Hydrometeorological conditions - winds and currents, changing in time and space
- Temperature of air and water
- Sea state
- Oil properties (i.e., oil fractions content, density, viscosity, surface tension)
- Information about oil spill: co-ordinates of source; time and duration of release; amount of spilled oil or rate of spill for leak source
- Bathymetric map of region in question
- Coastline information: coastline segments represented by a polygonal approximation of the coastline.

2. Information for modelling

2.1. Meteorological information

In the framework of common approach, used for hydrometeorological information selection for oil spill risk assessment calculations, we were intended to meet the requirement of the typical picture representation for specified region. From this point of view, and with regards to required data presence, period (1.06.1993-1.07.1994) was chosen. Meteorological data with 3-h time step were provided by Helsinki University. The example of baric and wind maps is shown at **Figure 3.**

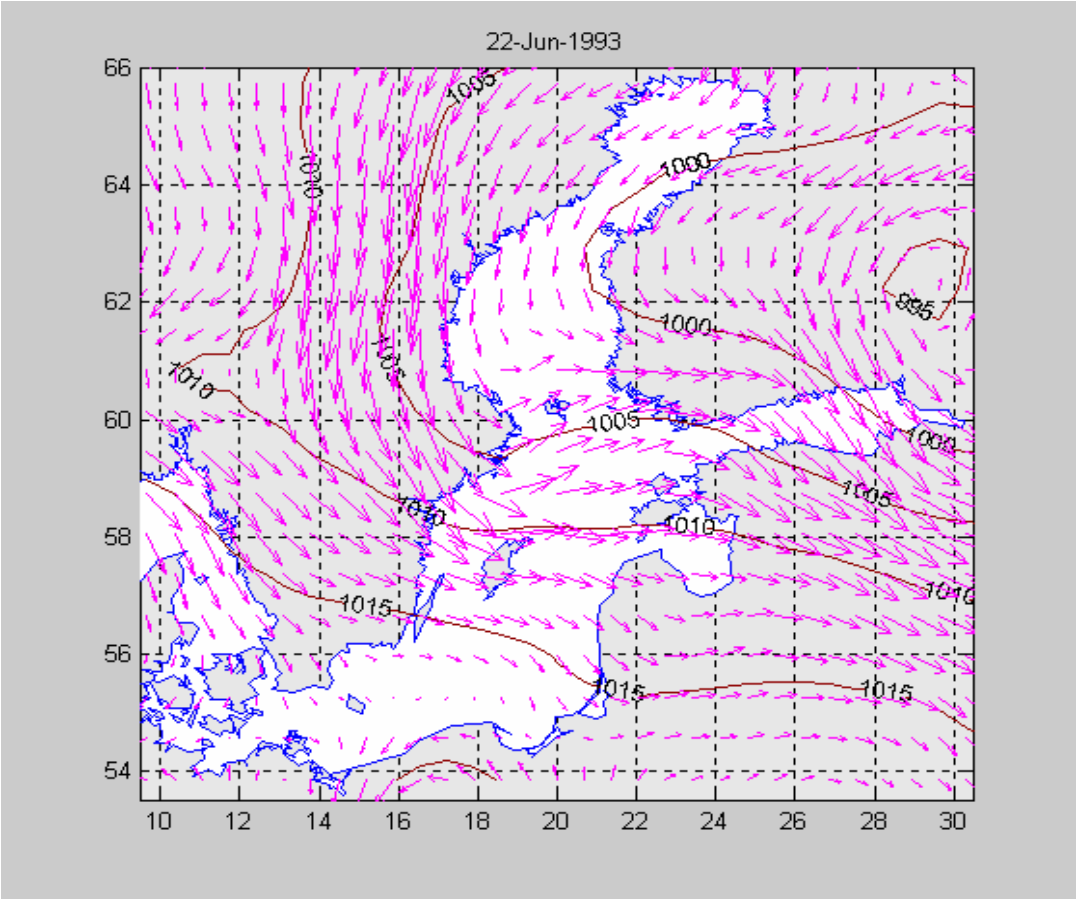

Figure 3 The example of wind and pressure map

2.2. Sea currents

For circulation modelling the 3D baroclinic model with free surface and variable vertical turbulent viscosity coefficient was used (Appendix B). 2920 surface currents fields were obtained with 3 hour time interval at 5 nautical miles mesh with 105x145 cells

dimensions. There is example of calculated surface currents in central Baltic (**Figure 4**) and two its enlarged fragments (**Figure 5, Figure 6**).

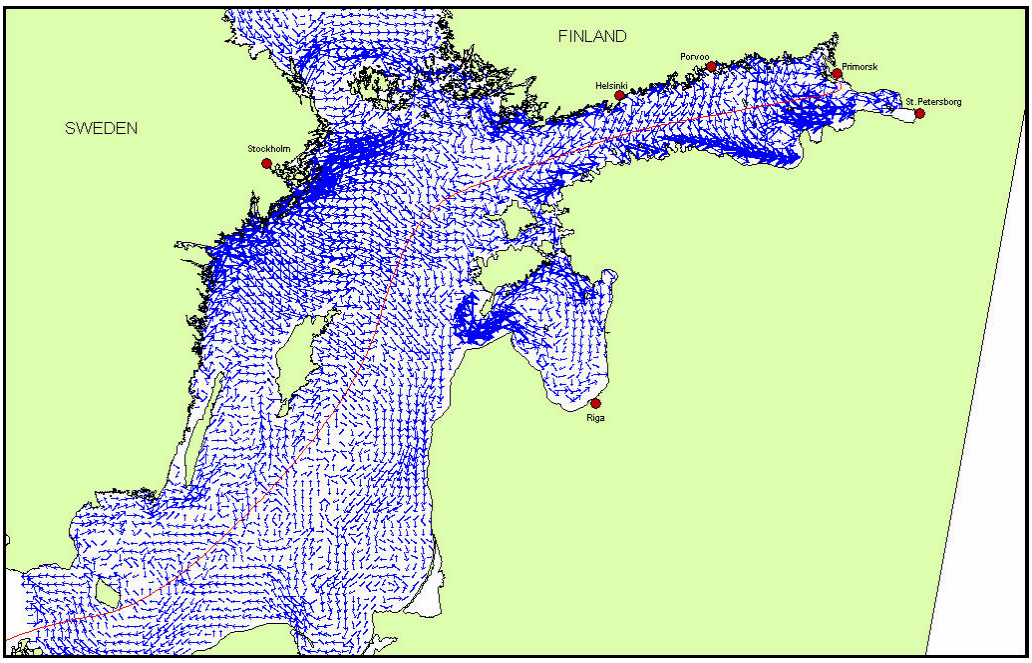

Figure 4 The calculated currents field example for summer season in the Baltic Proper.

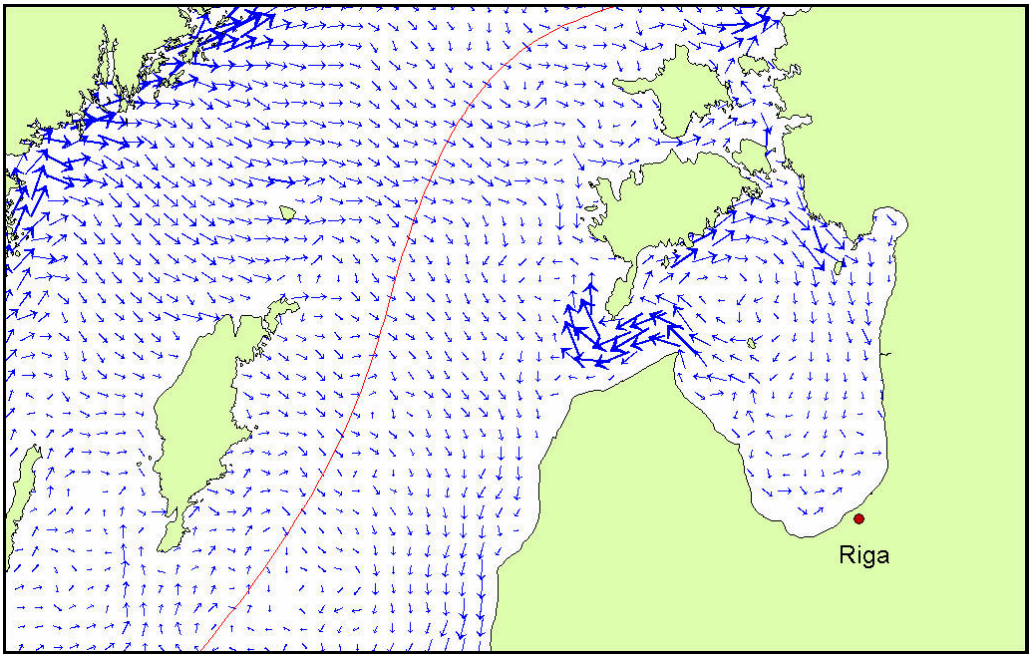

Figure 5 The example of surface current in Gotland island region

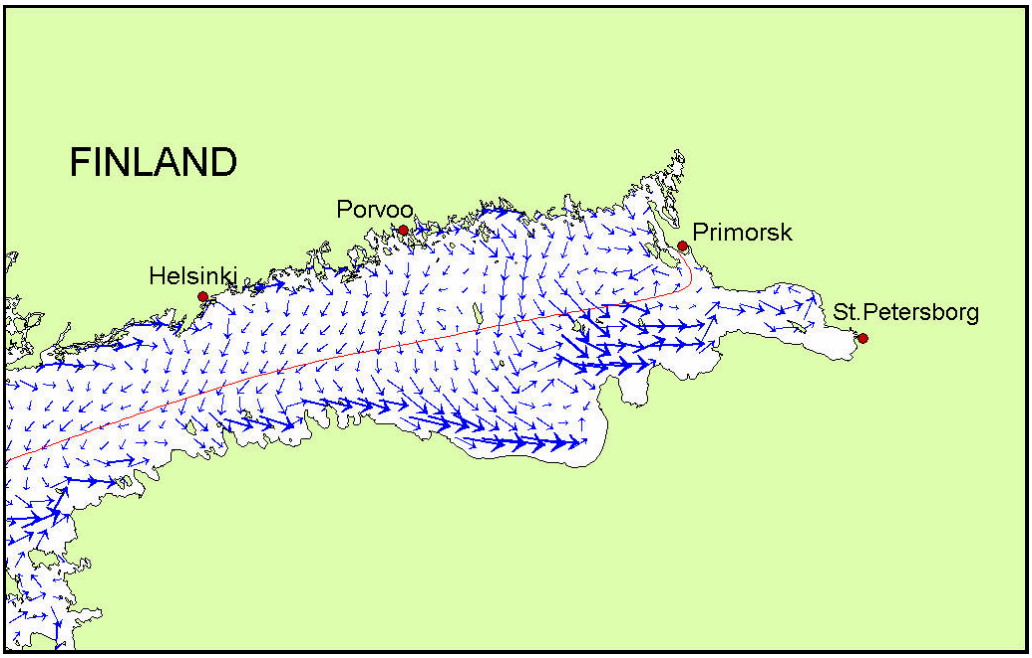

Figure 6 The example of calculated currents field for summer season in the Gulf of Finland

The wind traction stresses and air pressure gradients at sea surface was stated as boundary conditions.

2.3. Oil properties

In oil spill impact risk evaluation, oil or its product must be defined through its physical propertied – density, viscosity, surface tension, and also its fractions content. Oil is represented as a mixture of hydrocarbons with different molecular weights and true boiling points. Oil can be divided by its components in different ways. The common practice is dividing by boiling points temperatures, e.g. as in Russian standard GOST 11011-85 or USA standard ASTM (D-86). The used oil properties are in **Table 1** and **Table 2**.

Table 1 Physical properties of crude oil

Density at 20 ^{0}C	826 kg/m^3
Viscosity, at 20 ^{0}C	**9.13 мм^2/с**

Table 2. **Distillation process features**

Fractions	Boiling point, °C	Weight percent, %
1	100	7.1

Fractions	Boiling point, °C	Weight percent, %
2	150	19.3
3	200	30.4
4	250	40.5
5	300	51.
6	>300	64.2

2.4. Cartographic base

The set of electronic maps in well known MAPINFO® GIS data formats were used as in the oil spill simulations, as in this report preparing. The main Baltic region geographic map was obtained from the Internet site http://www.grida.no/baltic/ (it was developed in the framework of the Baltic region river discharge investigation project, Baltic Drainage Basin Project (BDBP).

2.5. Oil spill scenarios data

Mathematical modelling of the oil spill movement were carried out for 31 point of hypothetical oil spill accident.

	Spill points numbers							
	1	2	3	4	5	6	7	8
Longitude	29.5360	28.9007	28.1083	28.3333	28.2677	27.9629	27.5691	28.2044
Latitude	60.0086	60.0684	60.0931	59.7423	59.8596	59.9124	59.9758	59.9711
	Spill points numbers							
	9	10	11	12	13	14	15	16
Longitude	21.2181	20.5055	19.9053	20.4608	19.4756	18.4360	17.3190	18.9325
Latitude	57.4089	57.3157	57.1880	55.7178	55.6694	55.6297	55.5989	54.5153
	Spill points numbers							
	17	18	19	20	21	22	23	24
Longitude	18.9248	18.3352	17.3655	19.4833	19.8861	18.6914	17.8077	17.5750
Latitude	54.8765	55.1364	55.3170	54.7532	58.8524	58.8032	58.2619	57.3483
	Spill points numbers							
	25	26	27	28	29	30	31	
Longitude	17.3267	24.8597	25.2234	20.4213	12.1382	11.7761	20.7381	
Latitude	56.3289	59.6447	59.6521	56.1710	54.3914	54.4389	55.9748	

The spill of 15000 ton was considered as a largest possible spill during oil transportation by tankers in the Baltic Sea as a result of tanker wreck.

3. Results of oil spill modelling

More than 42500 oil spill scenarios were simulated for risk of oil spill impact evaluation. Hydrometeorological conditions represent typical and extreme Baltic sea conditions. It is supposed, that oil spill accident can occur in arbitrary time moment. On base of wind and pressure data sequences, and simulated by mathematical models currents, a number of equally probable situations were formed. Shifting successively initial time point, within 60 days sequence with 6 hours interval, it is possible to obtain more than 200 different sets of one, two, three (up to 10) days long sequences of wind and currents. The advantage of this approach is that, with good statistical provision of the sequence, a smooth transitions from one "typical" situation to another are naturally ensured.

The results show the areas and times following the spill event when the oil would have a *high probability* of being present on the water surface

All analysis in this report are bared on one year statistics. It seems to need more long-term meteocean data records (e.g., for 10 year) for more thorough oil spill risk evaluation.

3.1. Risk zones evaluation

Based on calculated oil spill trajectories, risk zones were ascertained with the following methodic used. The water area with all possible trajectories around specified spill source is covered by grid. After that, a minimum time of oil spill motion to each grid cell were calculated. Resulting data were used for oil spill possible location zones plotting.

The results show the areas and times following the spill event when the oil would have a *high probability* of being present on the water surface Calculated risk zones for 1 – 10 days and the probabilities of the oil spill impact resilting from hypothetical oil spill accident in the chosen locations are shown in Figure 7-Figure 54. All pictures are arrenged by 3 *ice – free* seasons **1** – *summe*r , **2** – *autumn* , and **4** – *spring*.

Risk zones define the regions where oil spill may occur in the specified period of time, i.e., the risk of oil spill impact out of risk zones is minimal. Risk zones configuration in open sea regions depend on wind spatial and time variability and correspondent currents pattern. In coastal regions near-shore currents and coast line peculiarities affect risk zones configuration.

The probability of oil spill impact within certain risk zone in the specific period of time varies from about 0 to 100%, as it may be seen on the following pictures.

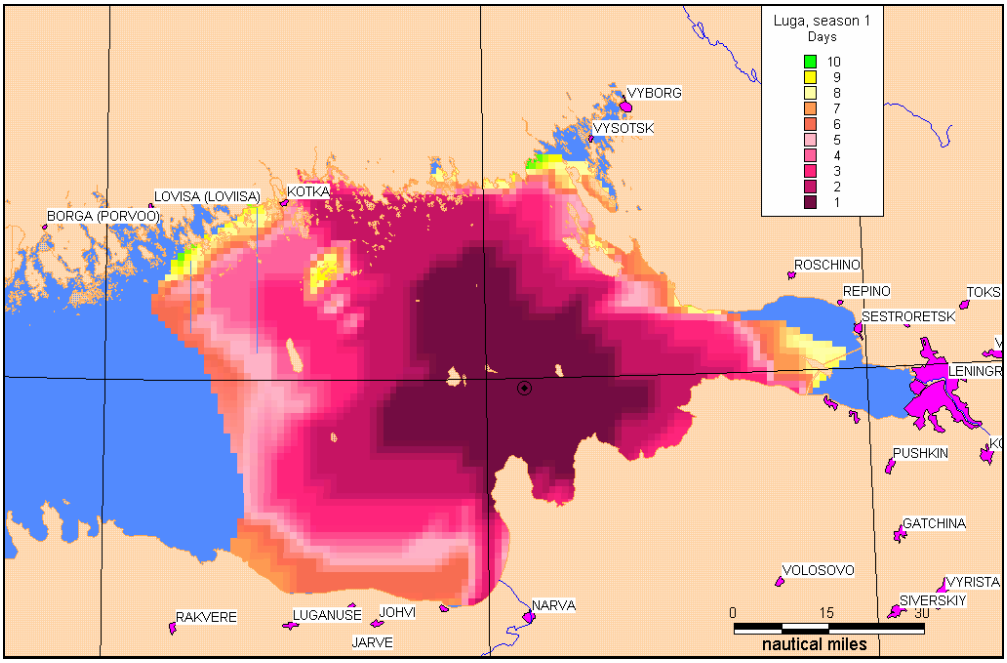

Figure 7 Risk zones for 1-10 days. Point 8. Summer season.

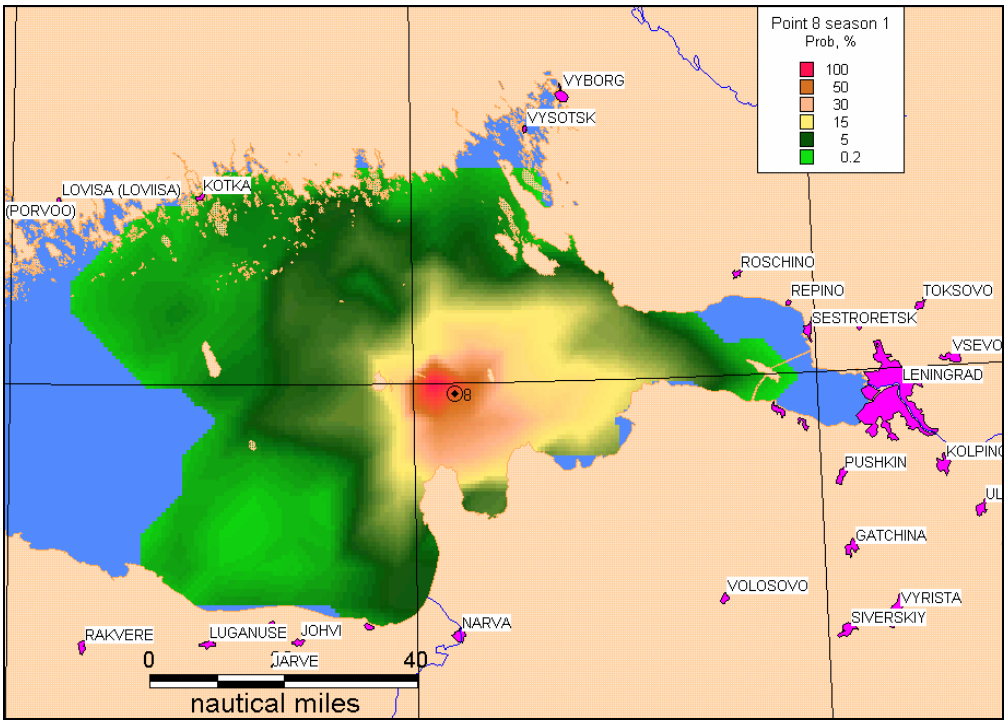

Figure 8 Probability of impact (%). Point 8. Summer season.

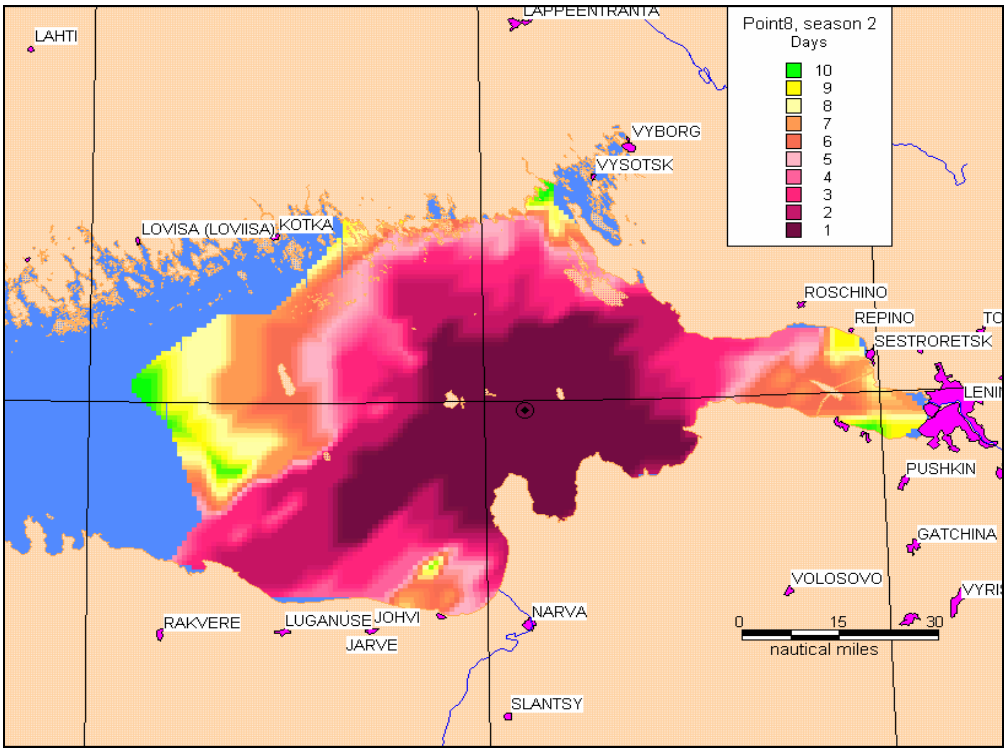

Figure 9 Risk zones for 1-10 days. Point 8. Autumn season.

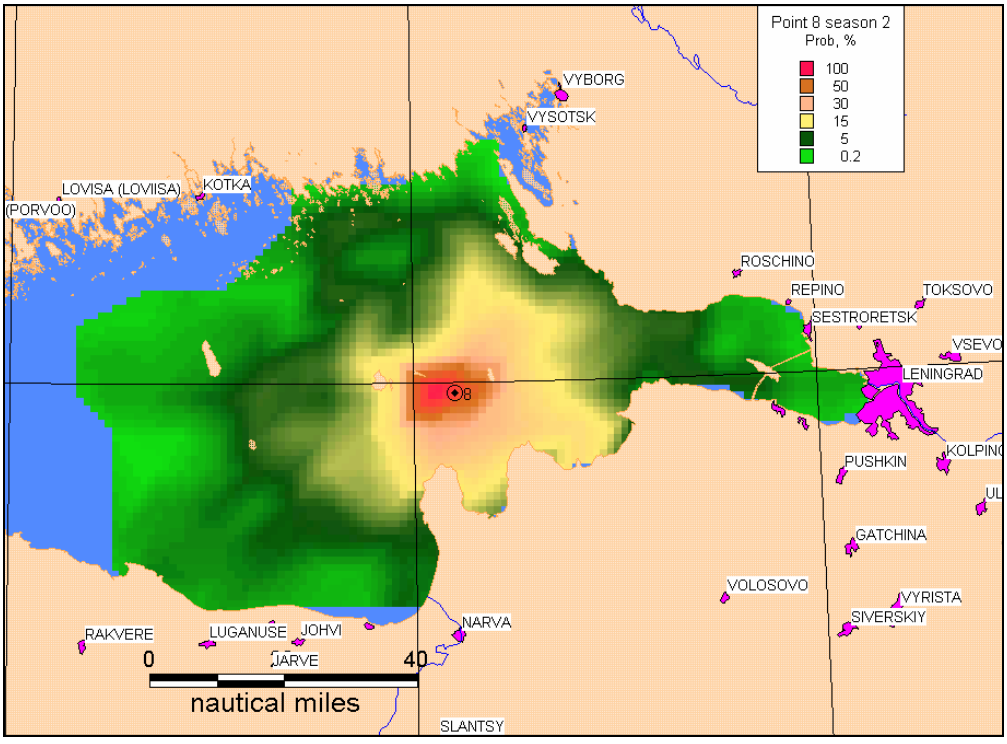

Figure 10 Probability of impact (%). Point 8. Autumn season.

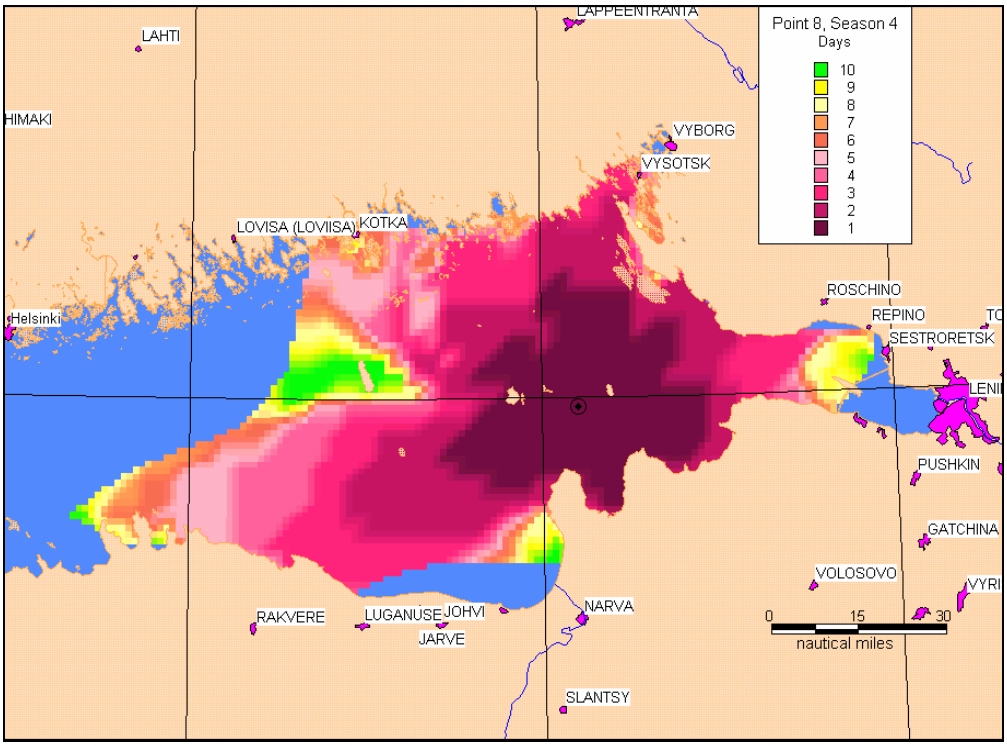

Figure 11 Risk zones for 1-10 days. Point 8. Spring season.

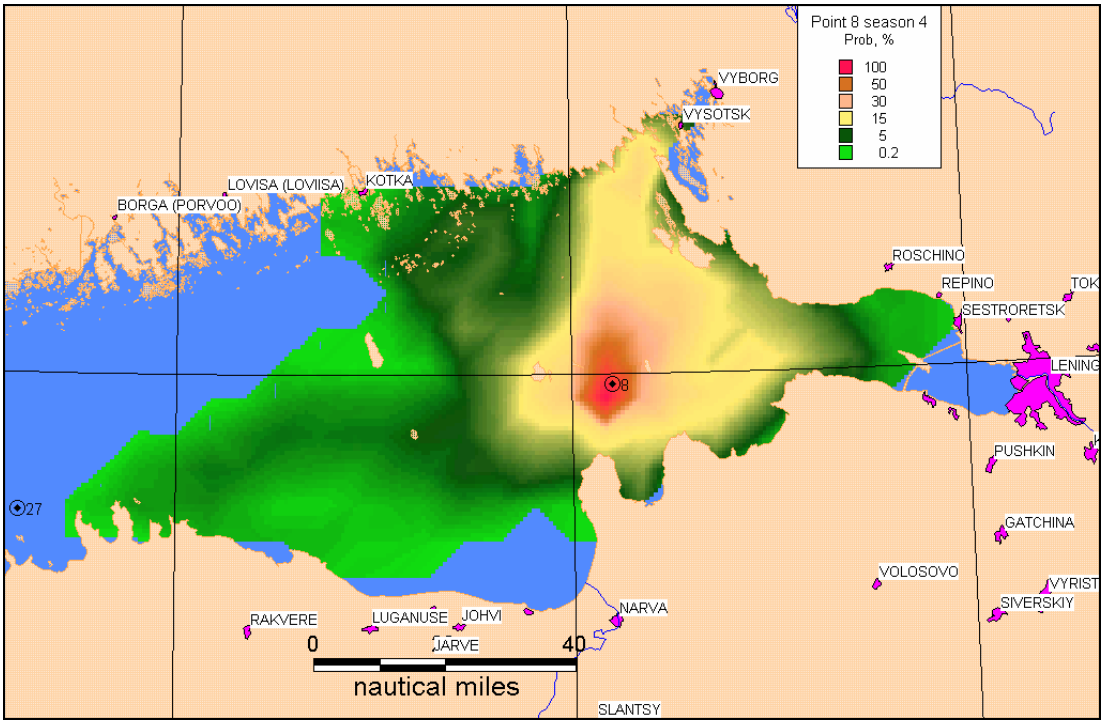

Figure 12 Probability of impact (%). Point 8. Spring season.

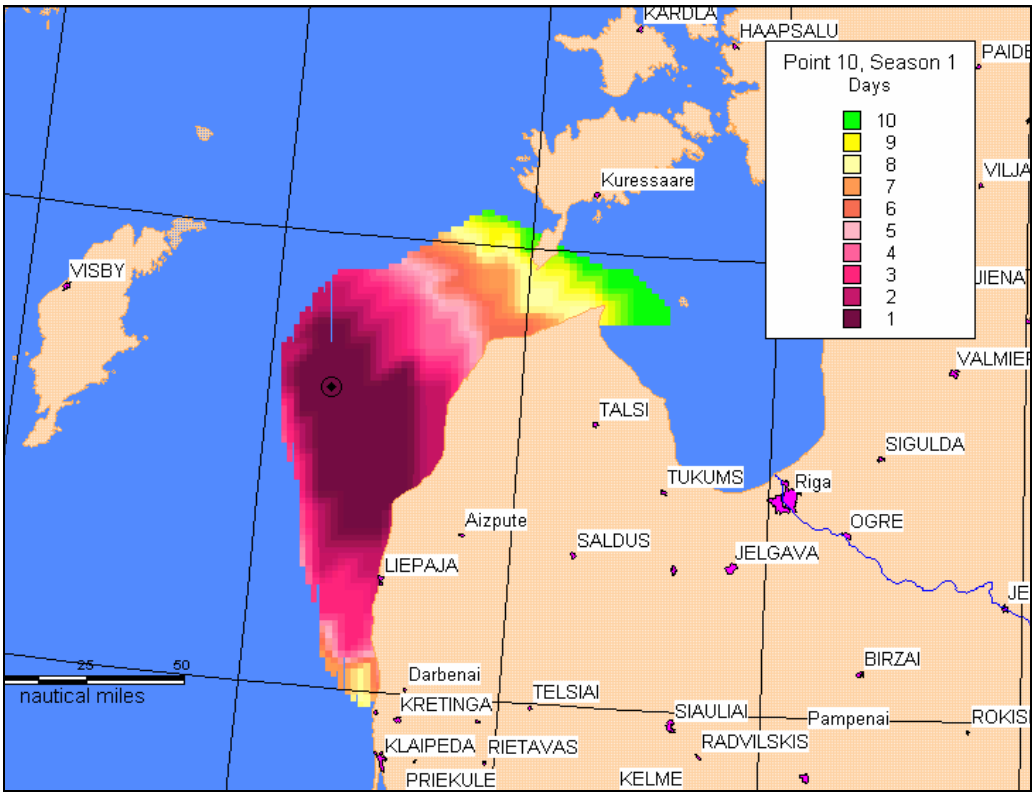

Figure 13 Risk zones for 1-10 days. Point 10. Summer season.

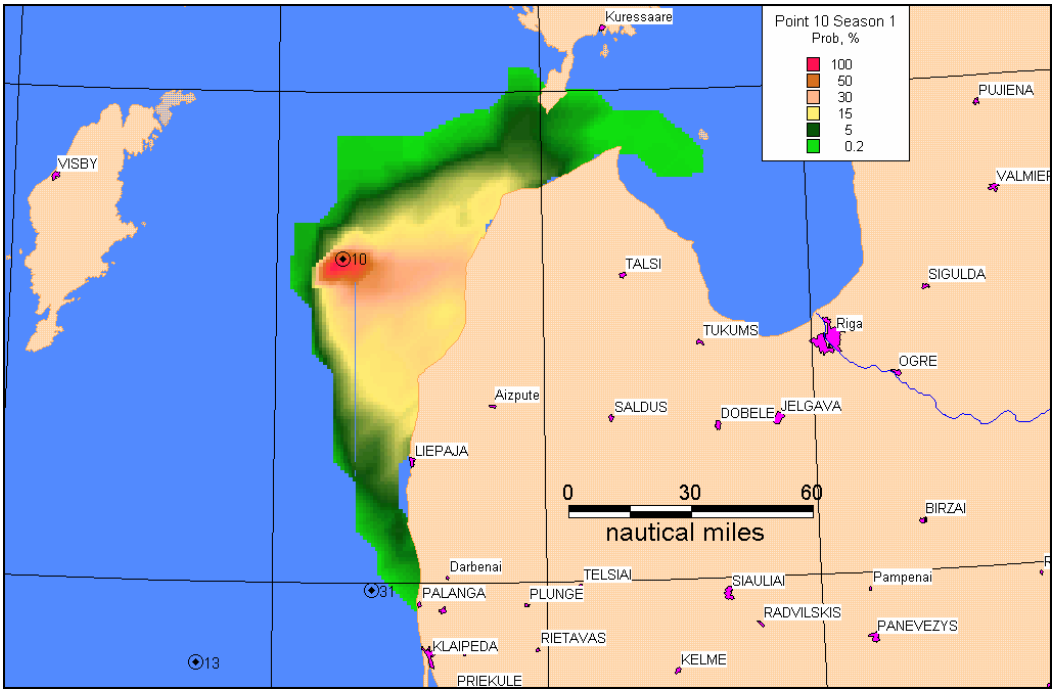

Figure 14 Probability of impact (%). Point 10. Summer season.

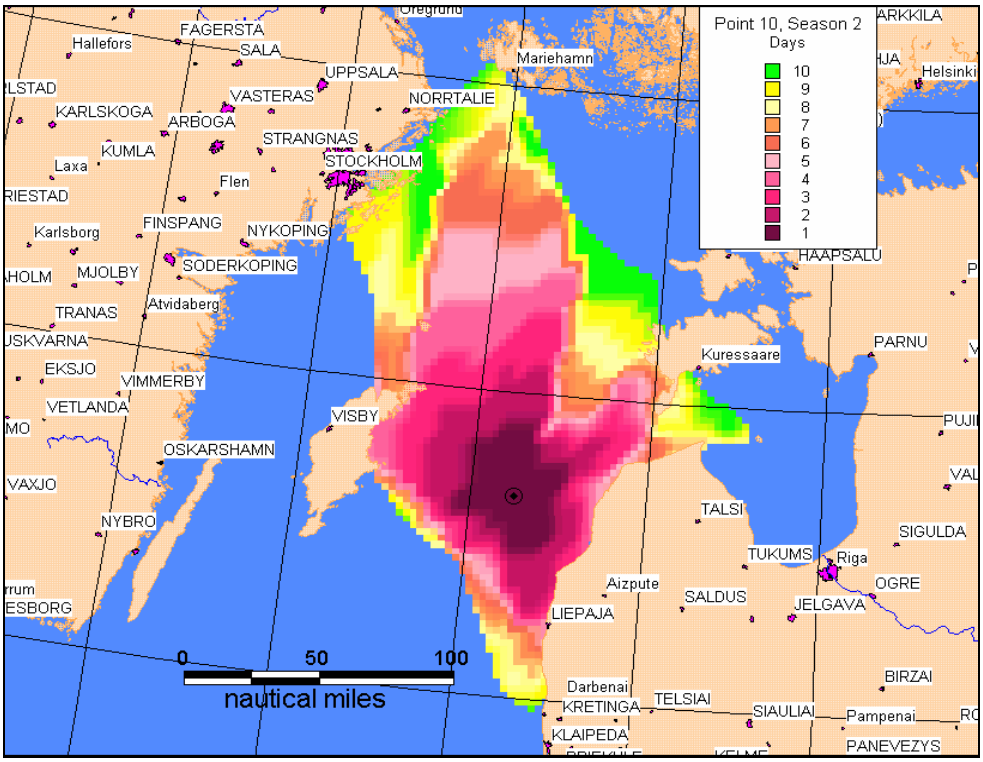

Figure 15 Risk zones for 1-10 days. Point 10. Autumn season.

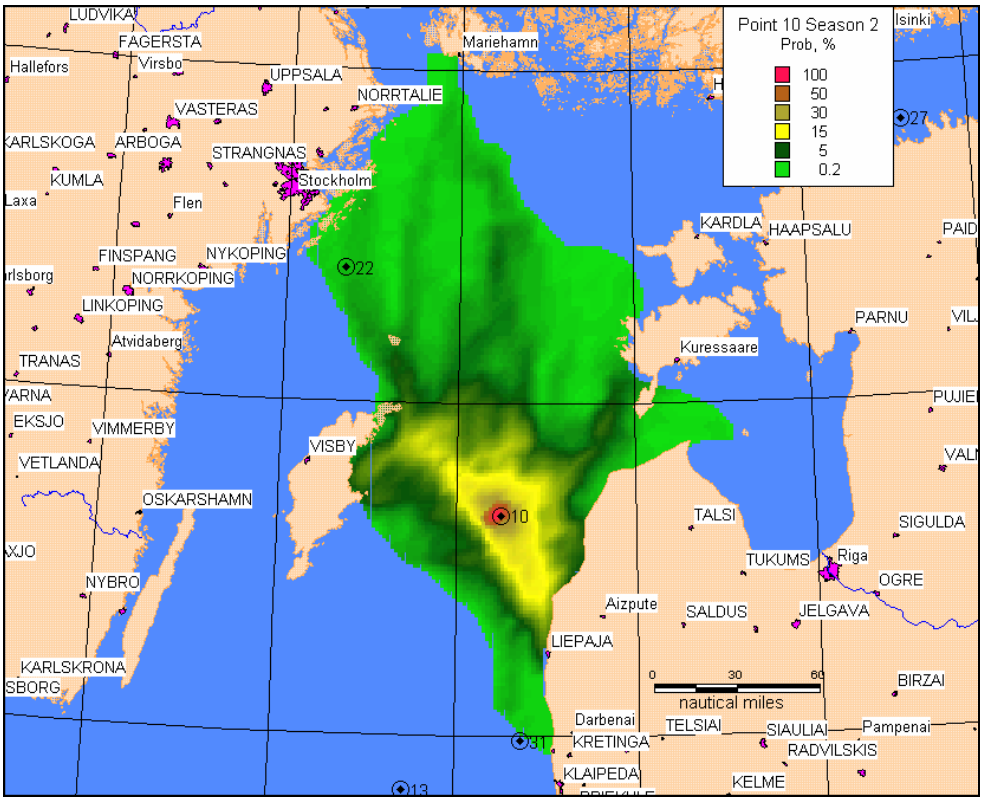

Figure 16 Probability of impact (%). Point 10. Autumn season.

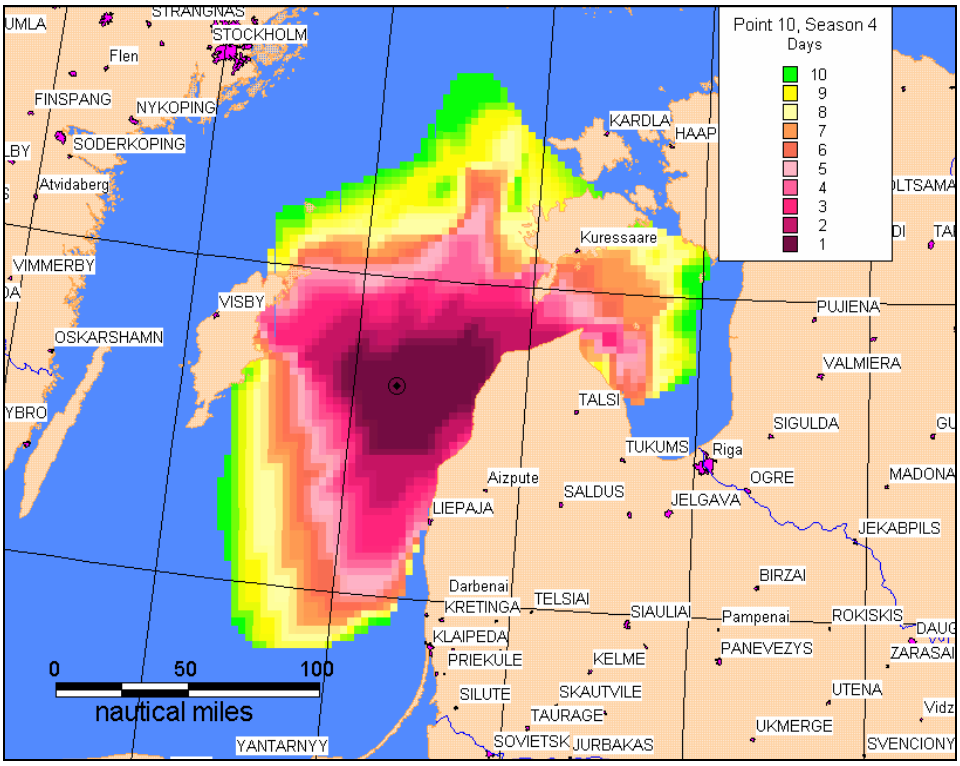

Figure 17 Risk zones for 1-10 days. Point 10. Spring season.

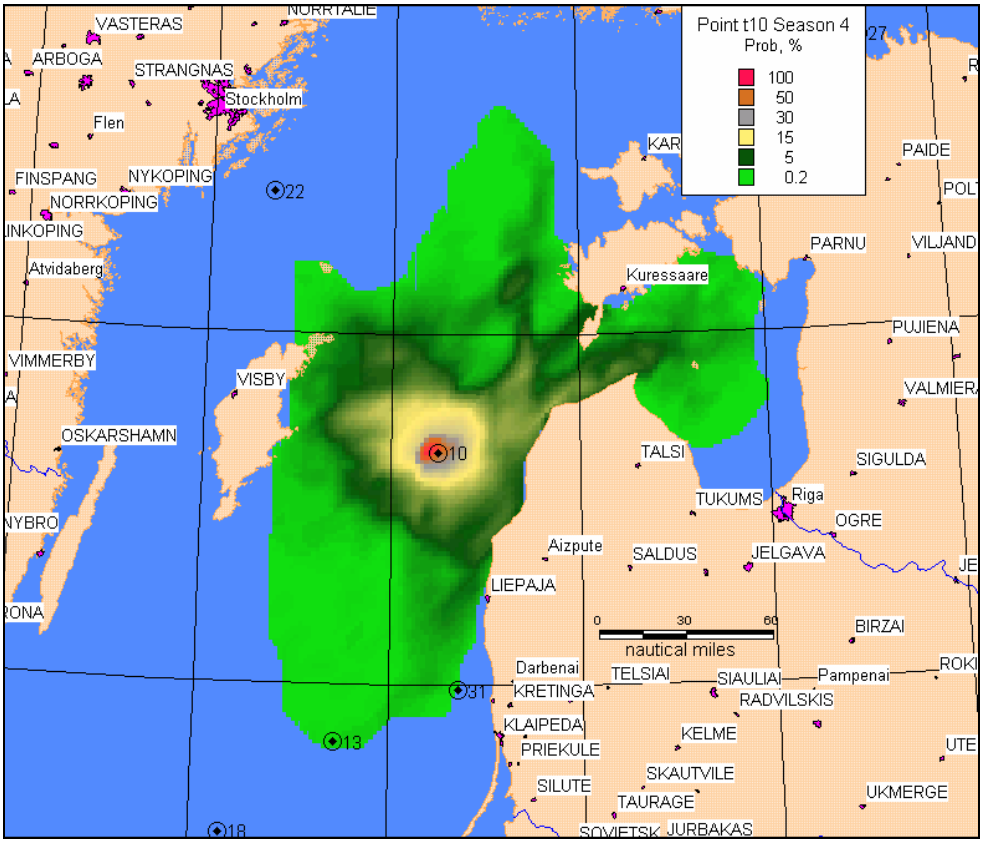

Figure 18 Probability of impact (%). Point 10. Spring season.

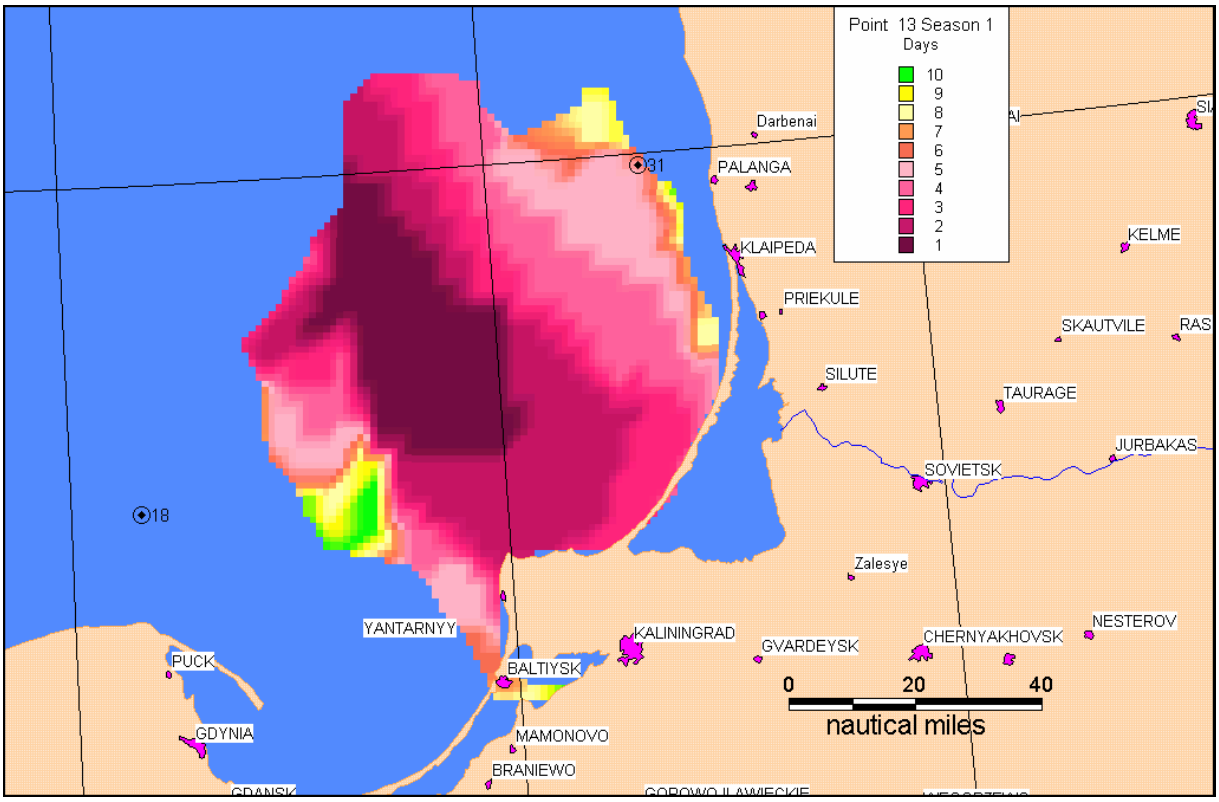

Figure 19 Risk zones for 1-10 days. Point 13. Summer season.

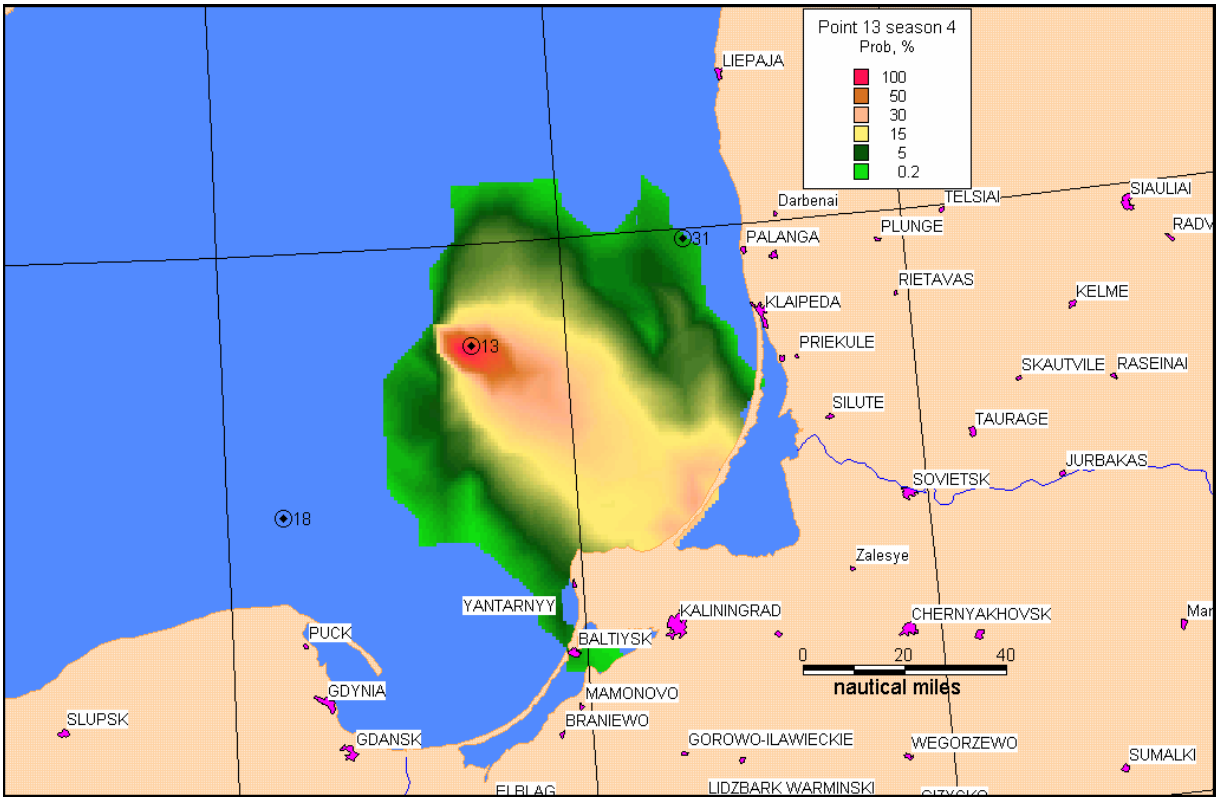

Figure 20 Probability of impact (%). Point 13. Summer season.

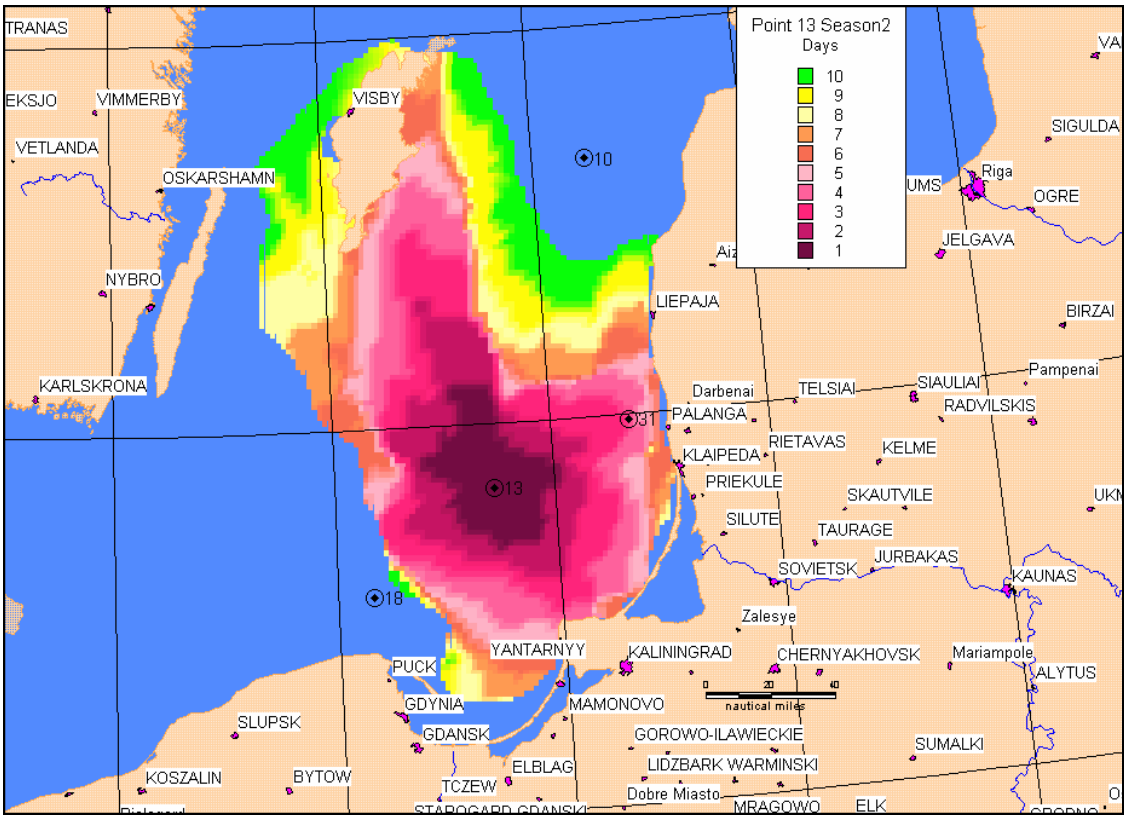

Figure 21 Risk zones for 1-10 days. Point 13. Autumn season.

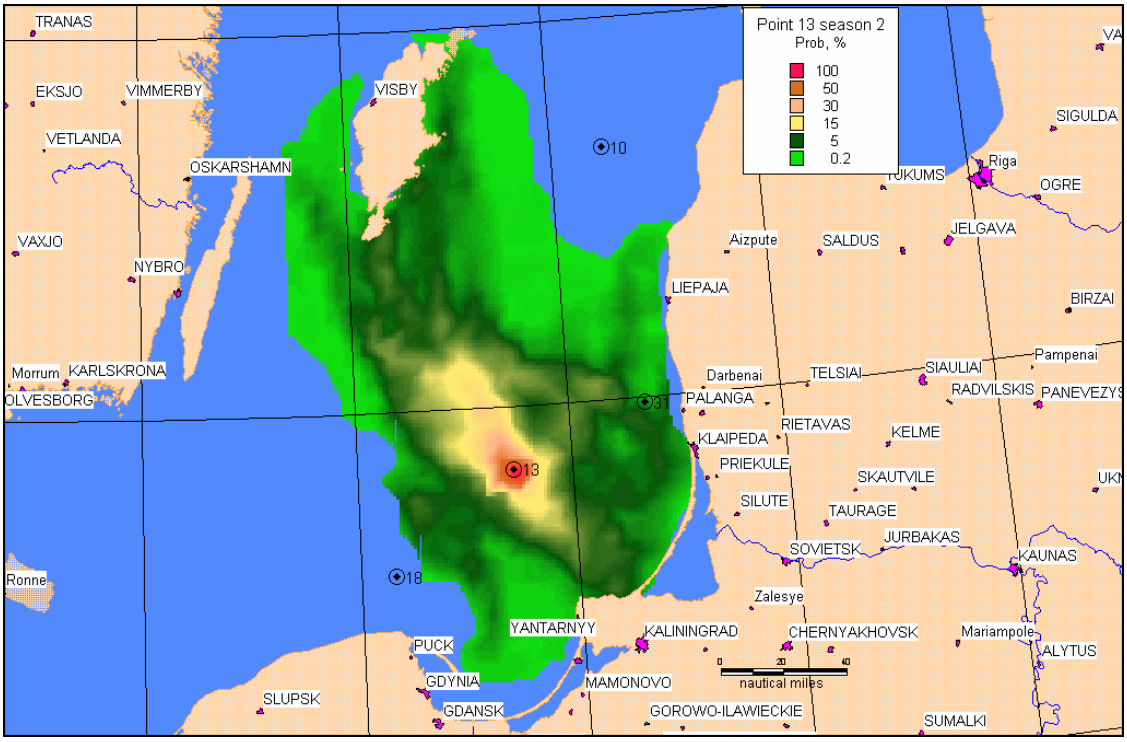

Figure 22 Probability of impact (%). Point 13. Autumn season.

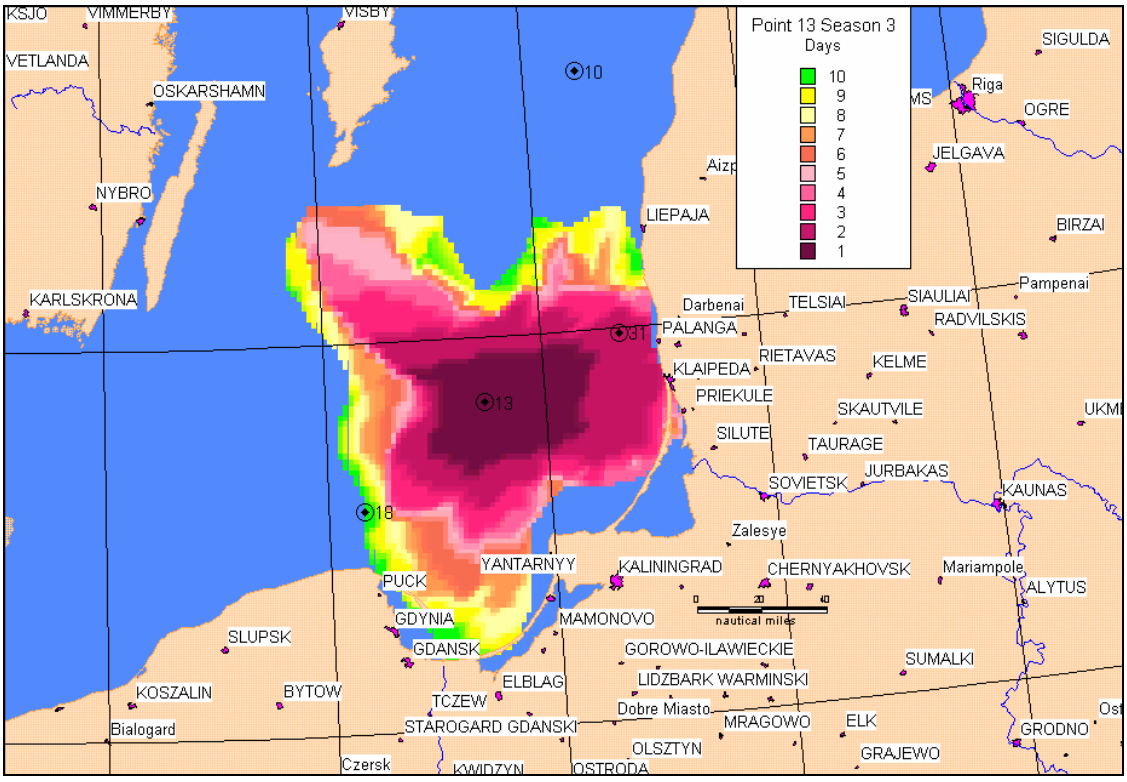

Figure 23 Risk zones for 1-10 days. Point 13. Spring season.

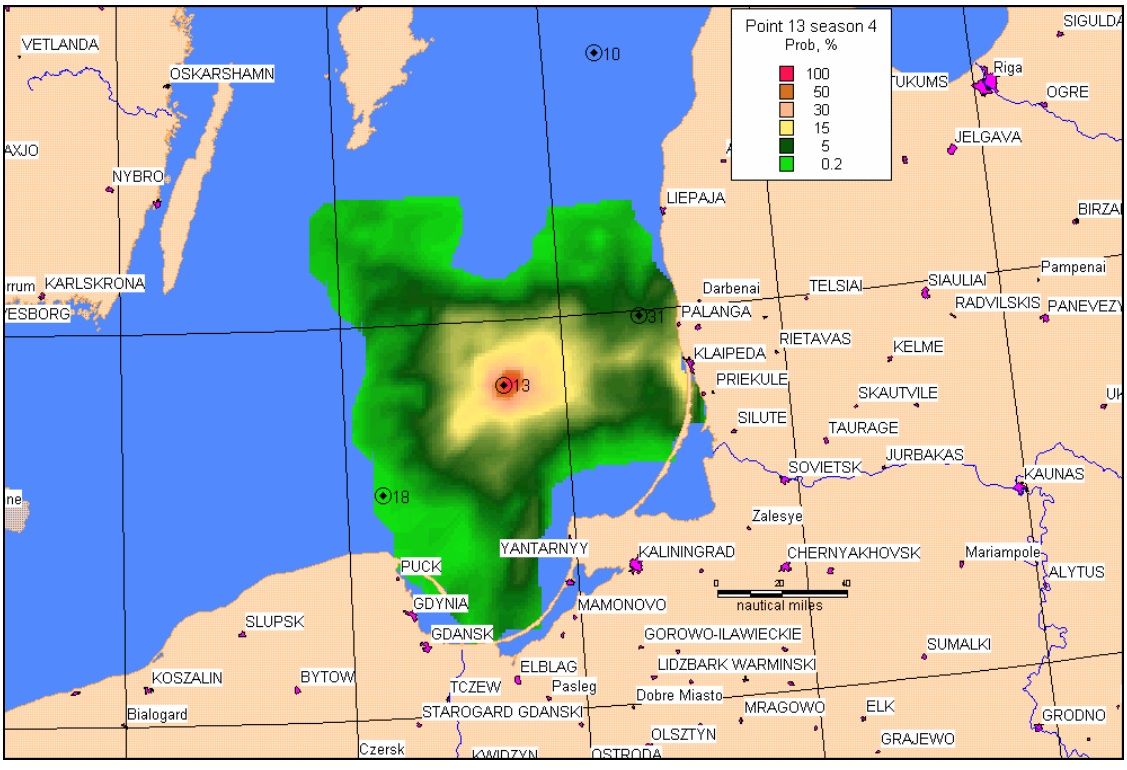

Figure 24 Probability of impact (%). Point 13. Spring season.

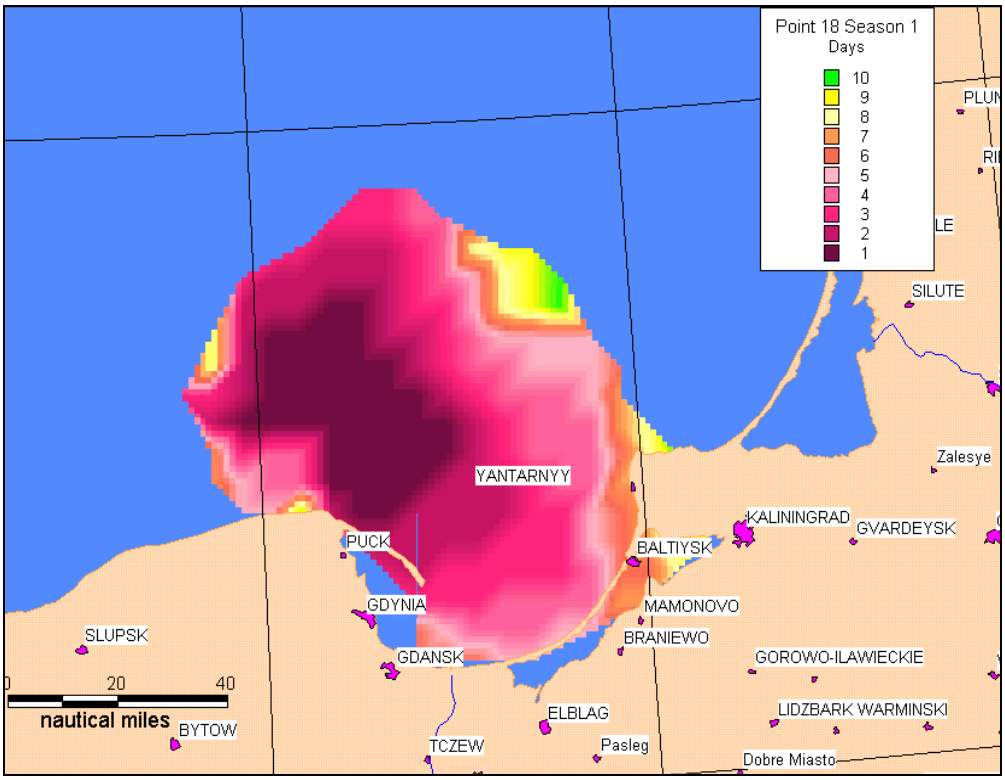

Figure 25 Risk zones for 1-10 days. Point 18. Summer season.

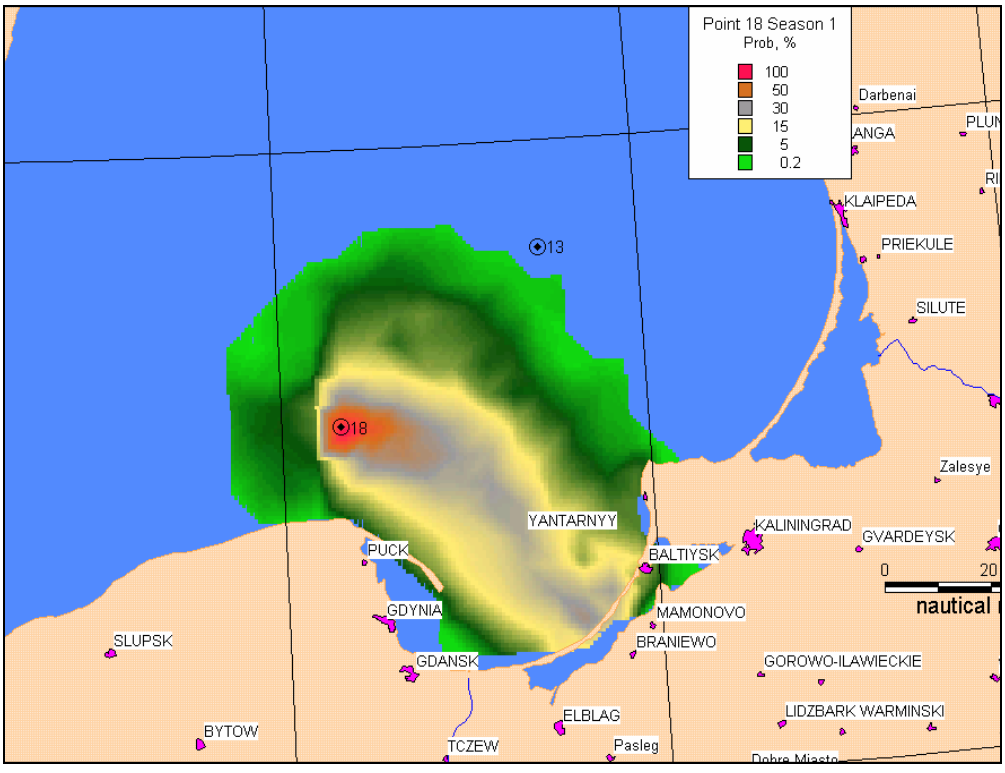

Figure 26 Probability of impact (%). Point 18. Summer season.

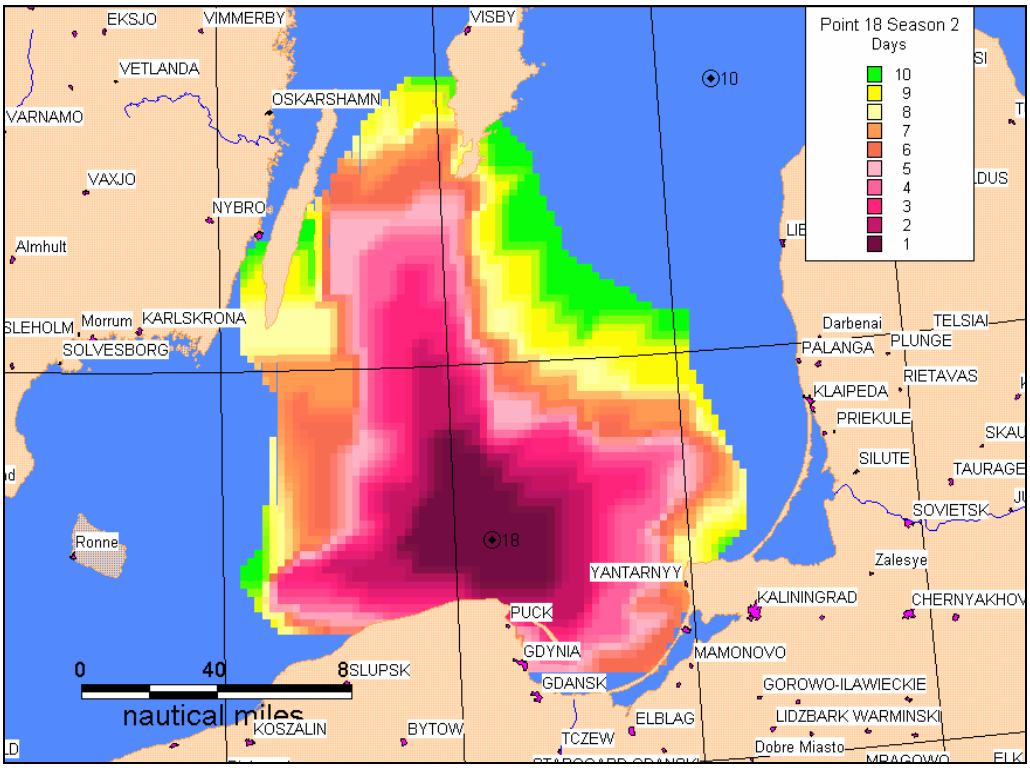

Figure 27 Risk zones for 1-10 days. Point 18. Autumn season.

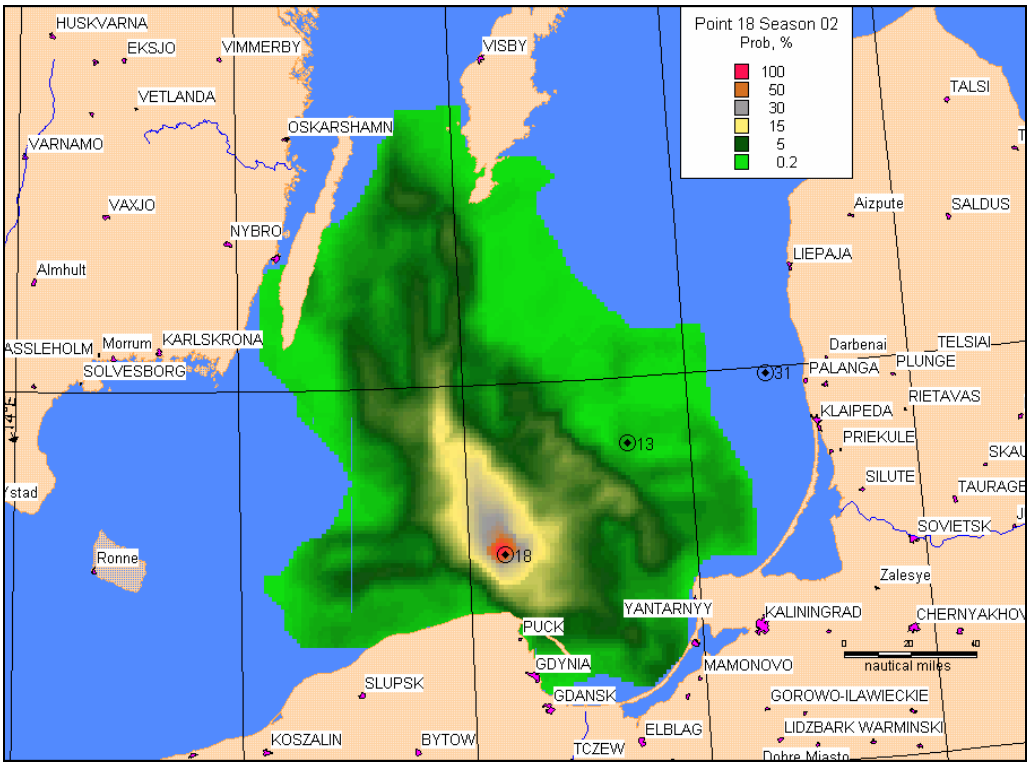

Figure 28 Probability of impact (%). Point 18. Autumn season.

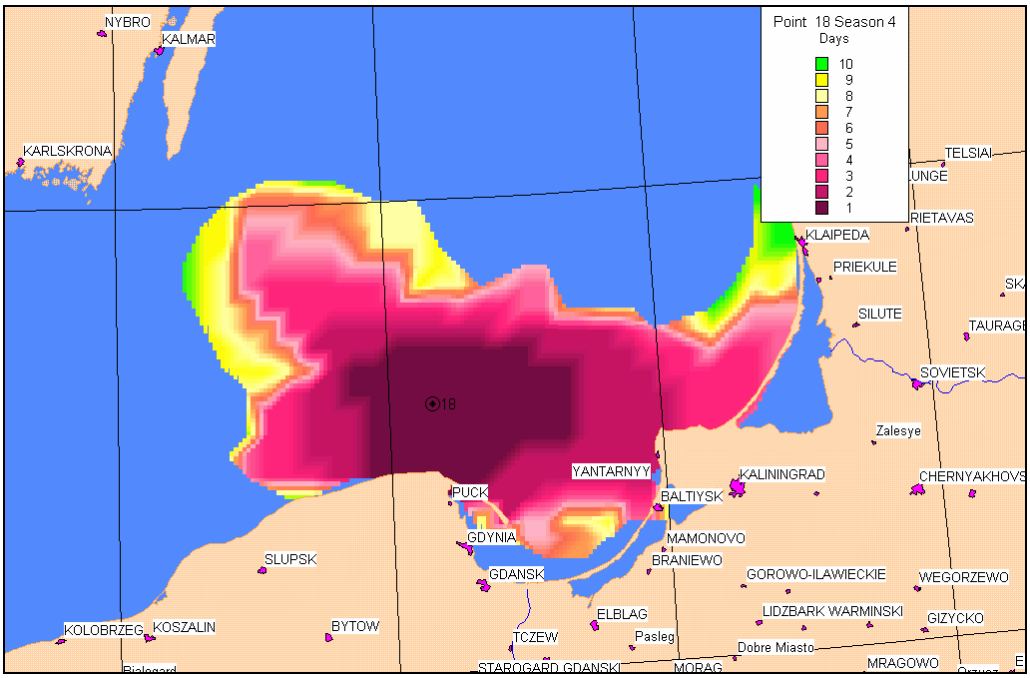

Figure 29 Risk zones for 1-10 days. Point 18. Spring season.

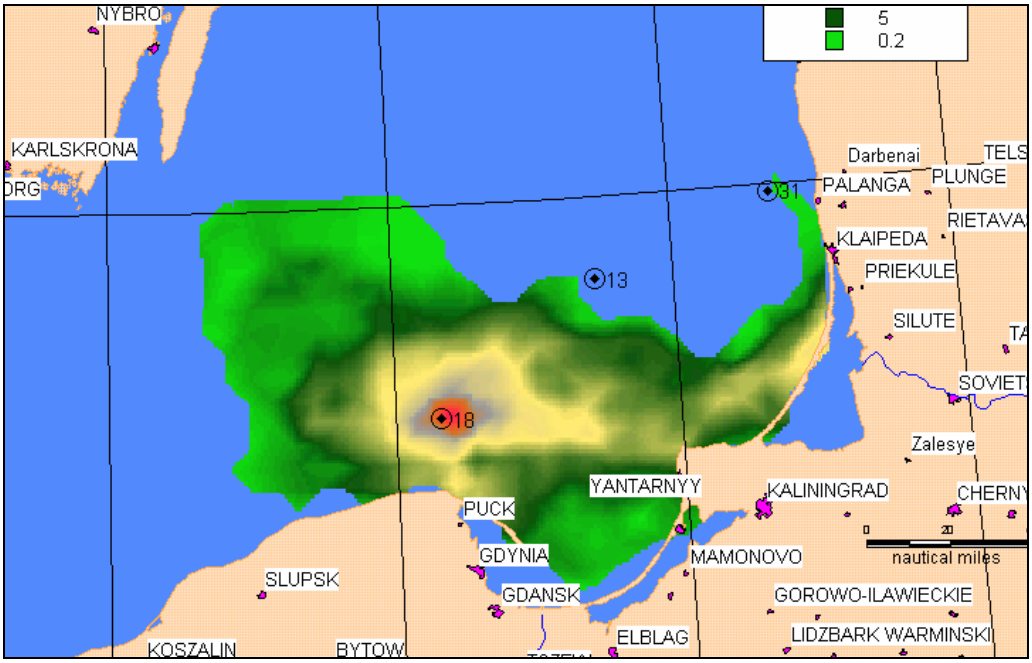

Figure 30 Probability of impact (%). Point 18. Spring season.

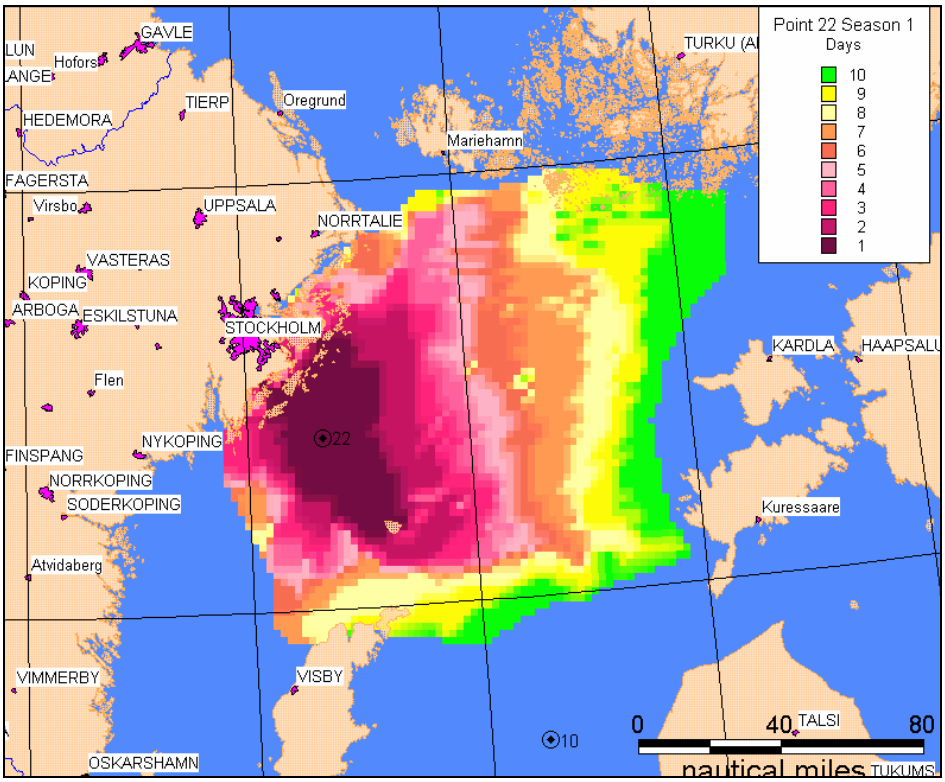

Figure 31 Risk zones for 1-10 days. Point 22. Summer season.

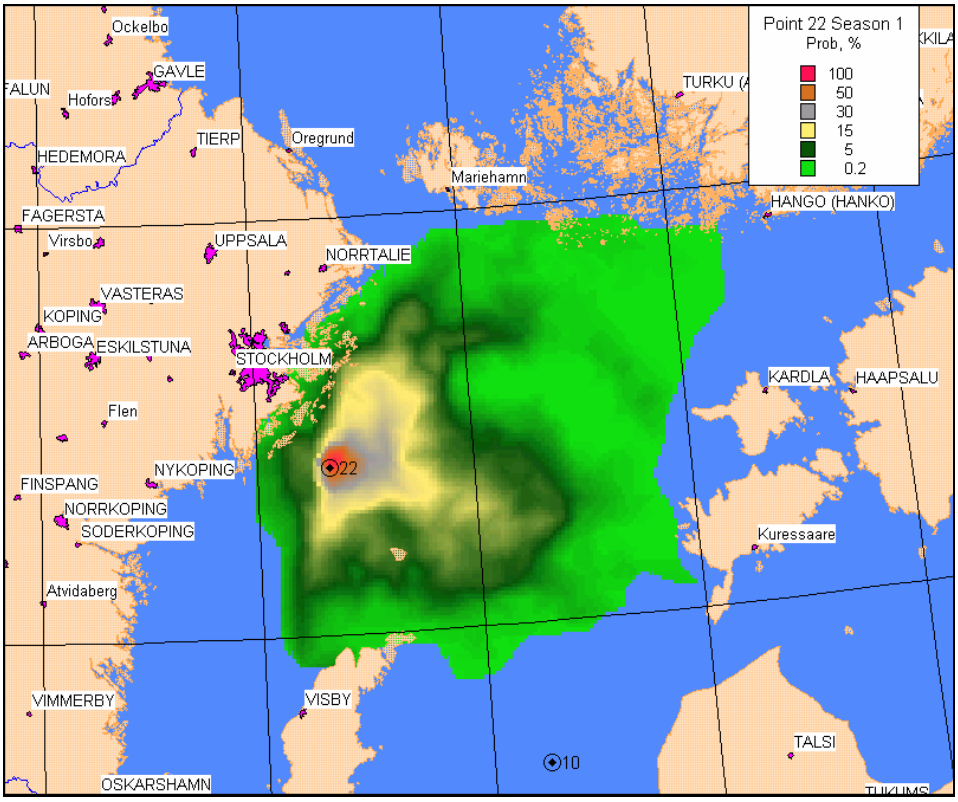

Figure 32 Probability of impact (%). Point 22. Summer season.

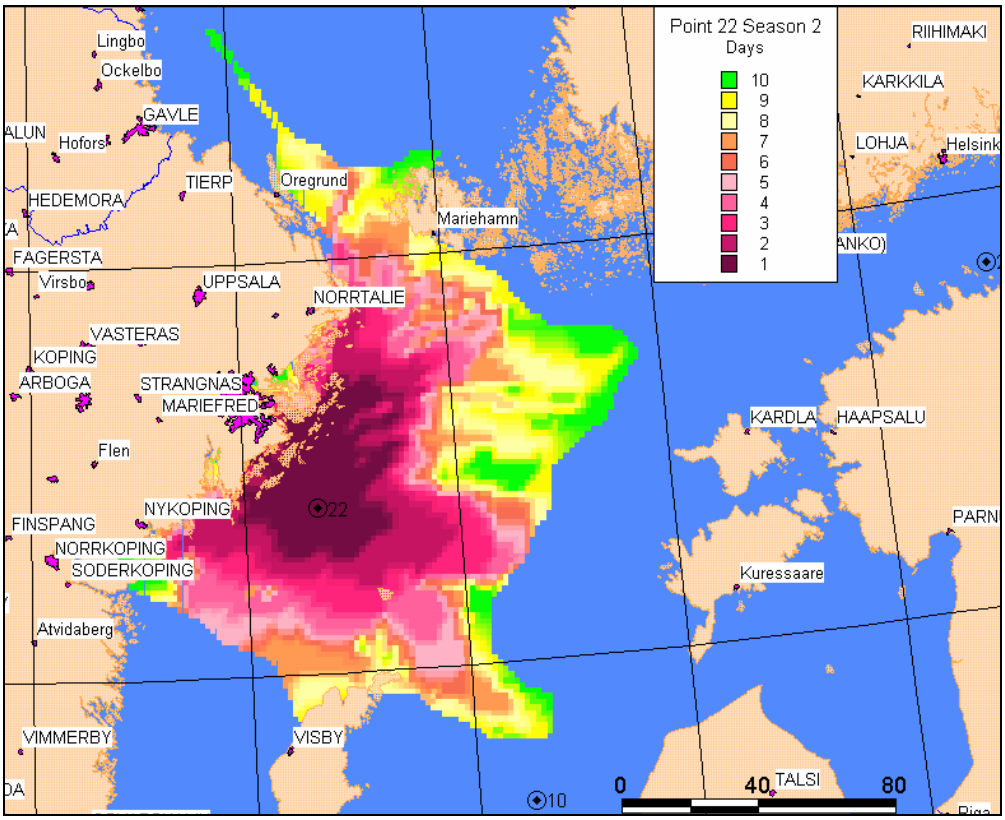

Figure 33 Risk zones for 1-10 days. Point 22. Autumn season.

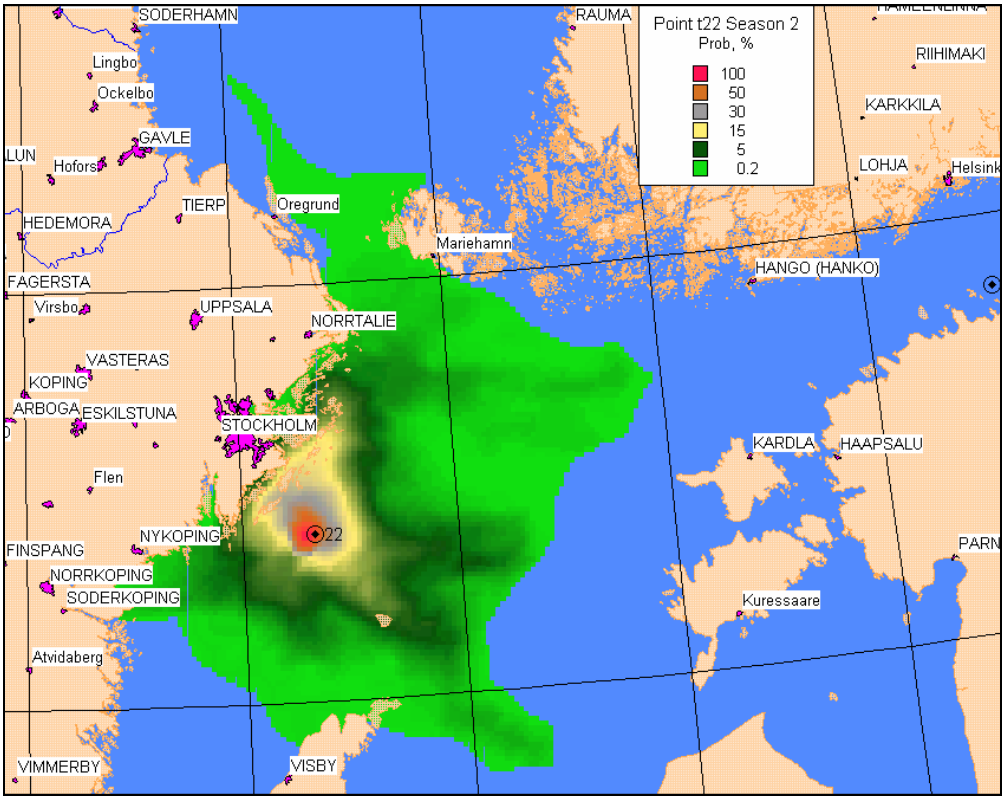

Figure 34 Probability of impact (%). Point 22. Autumn season.

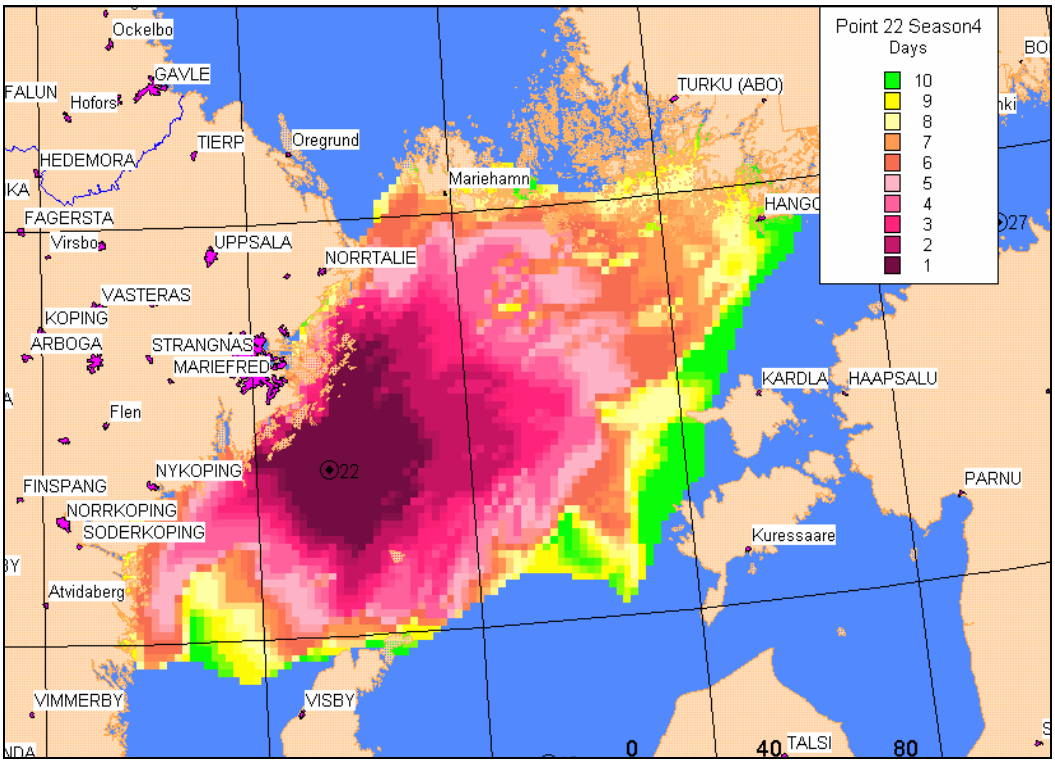

Figure 35 Risk zones for 1-10 days. Point 22. Spring season.

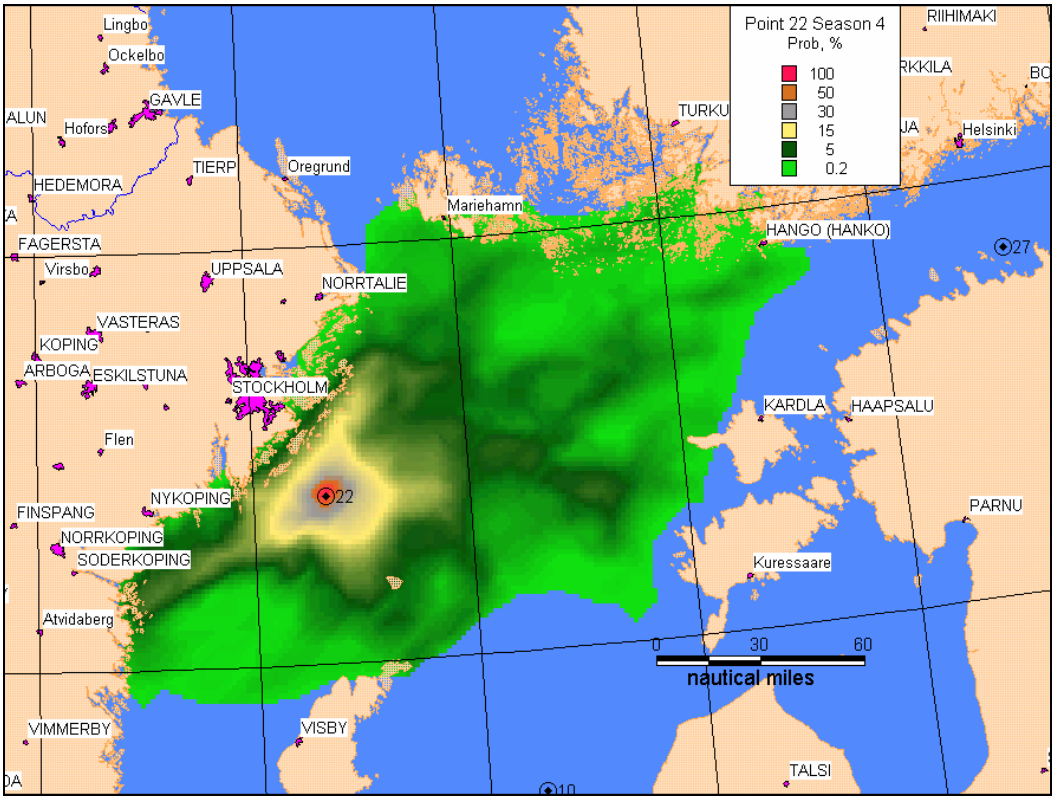

Figure 36 Probability of impact (%). Point 22. Spring season.

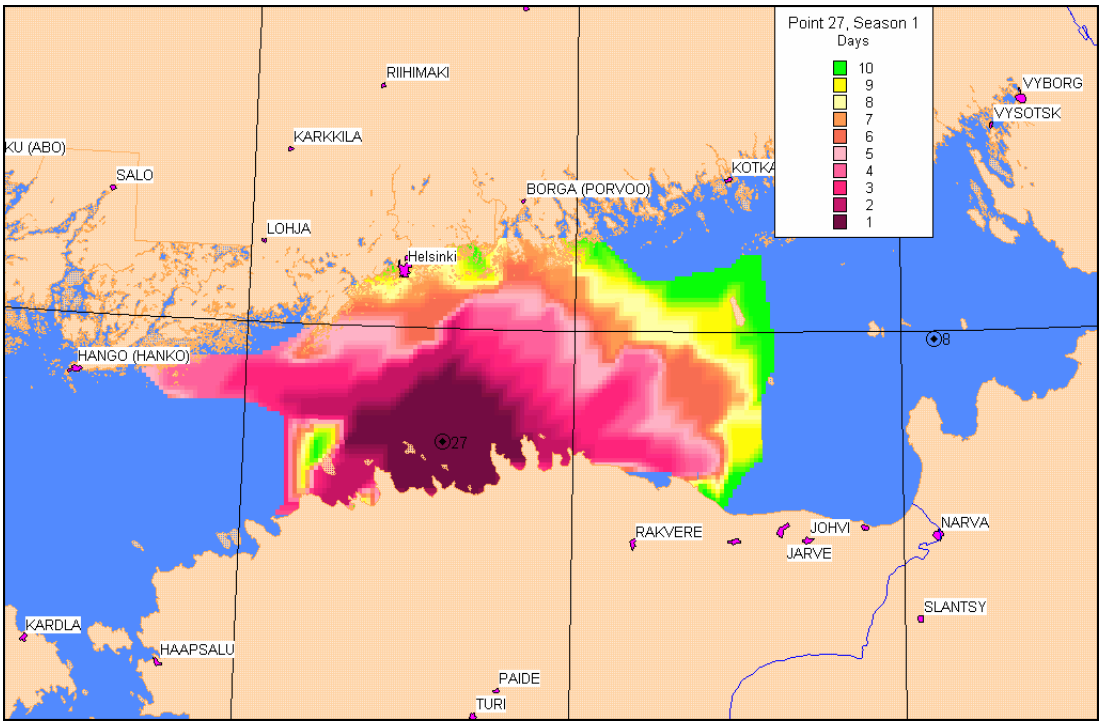

Figure 37 Risk zones for 1-10 days. Point 27. Summer season.

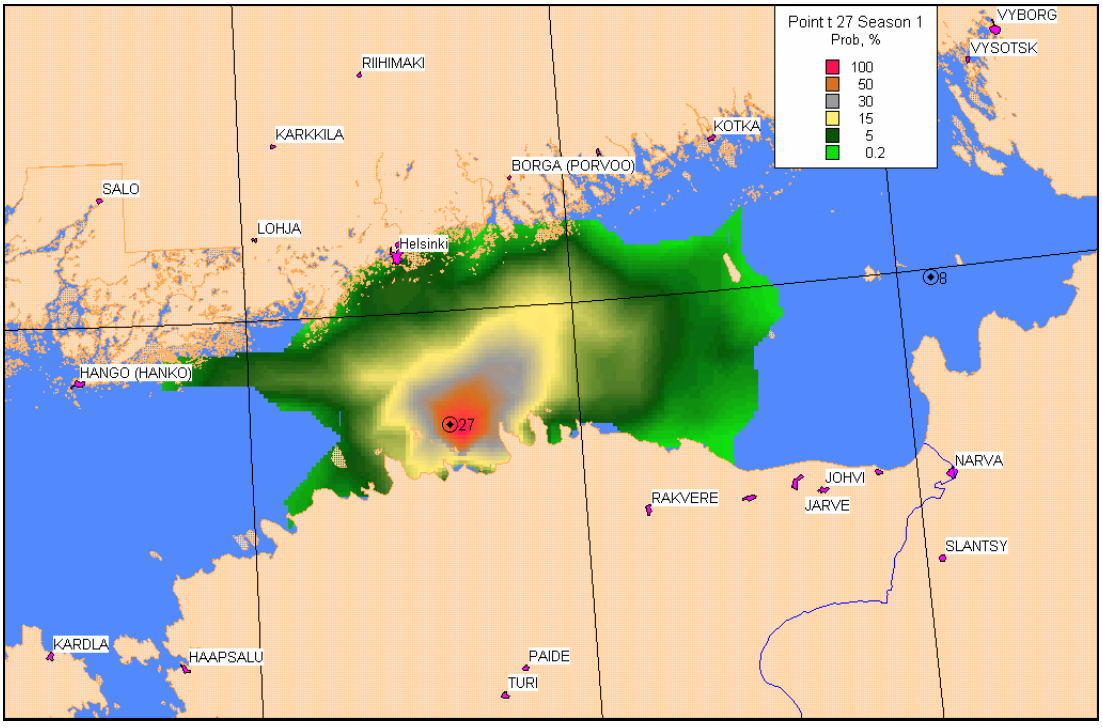

Figure 38 Probability of impact (%). Point 27. Summer season.

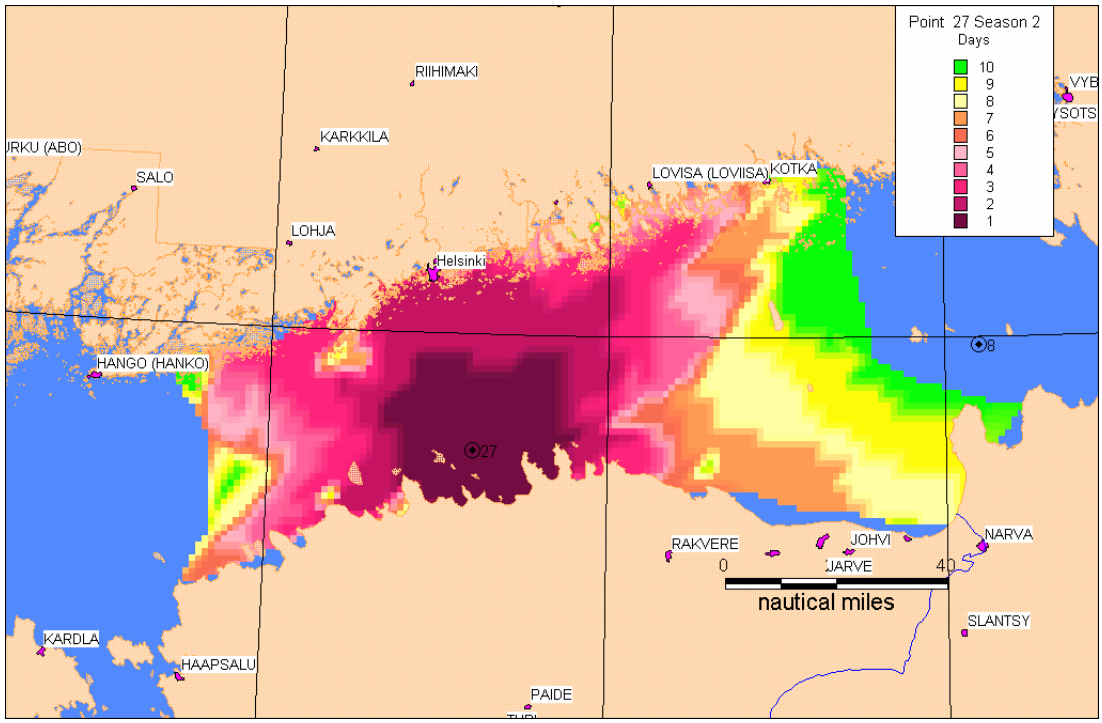

Figure 39 Risk zones for 1-10 days. Point 27. Autumn season.

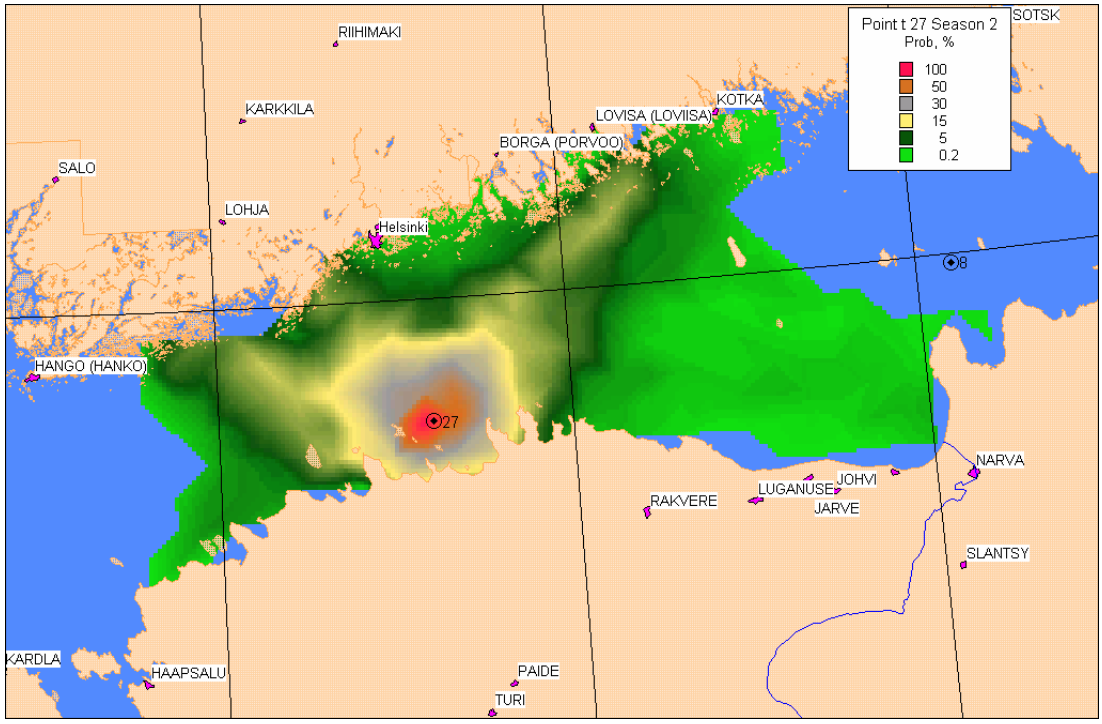

Figure 40 Probability of impact (%). Point 27. Autumn season.

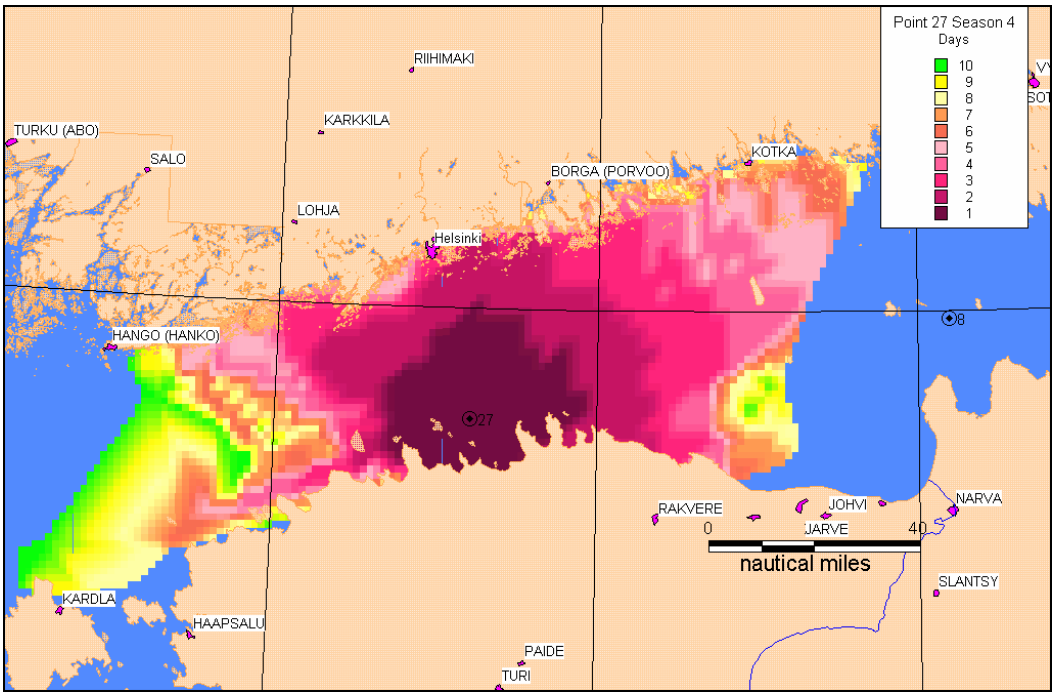

Figure 41 Risk zones for 1-10 days. Point 27. Spring season.

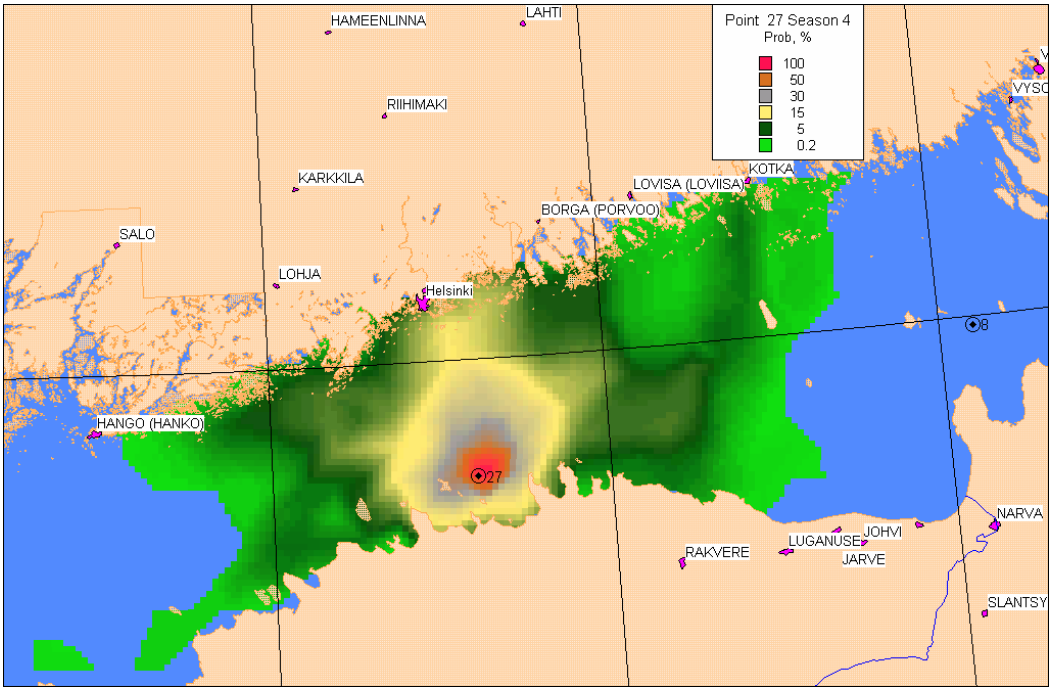

Figure 42 Probability of impact (%). Point 8. Spring season.

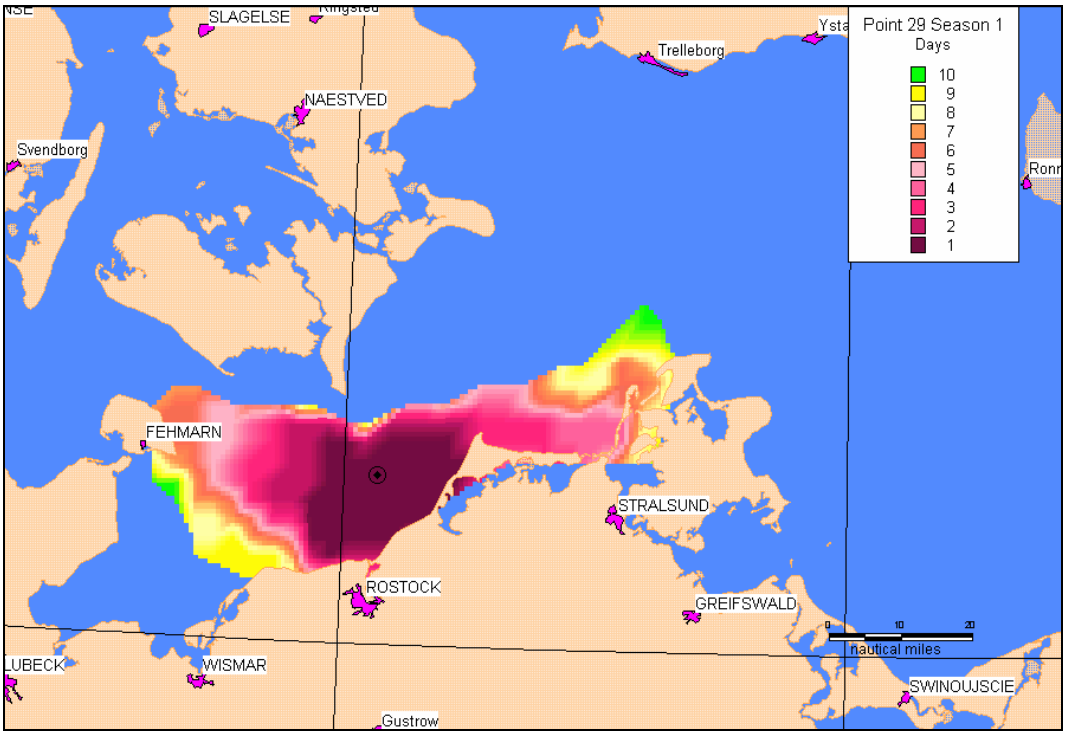

Figure 43 Risk zones for 1-10 days. Point 29. Summer season.

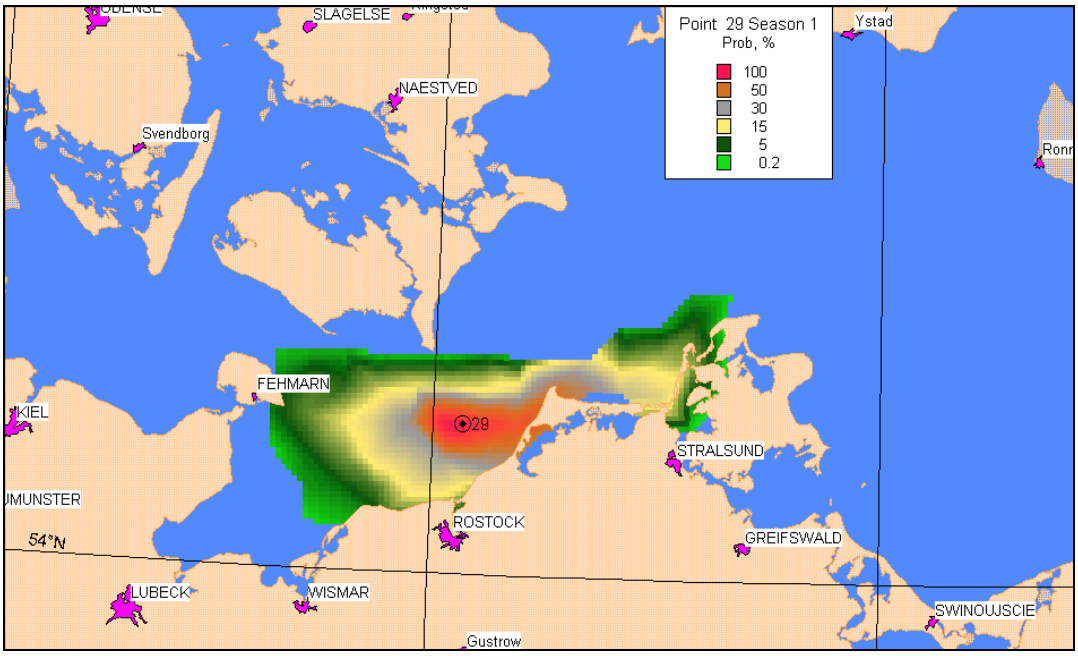

Figure 44 Probability of impact (%). Point 29. Summer season.

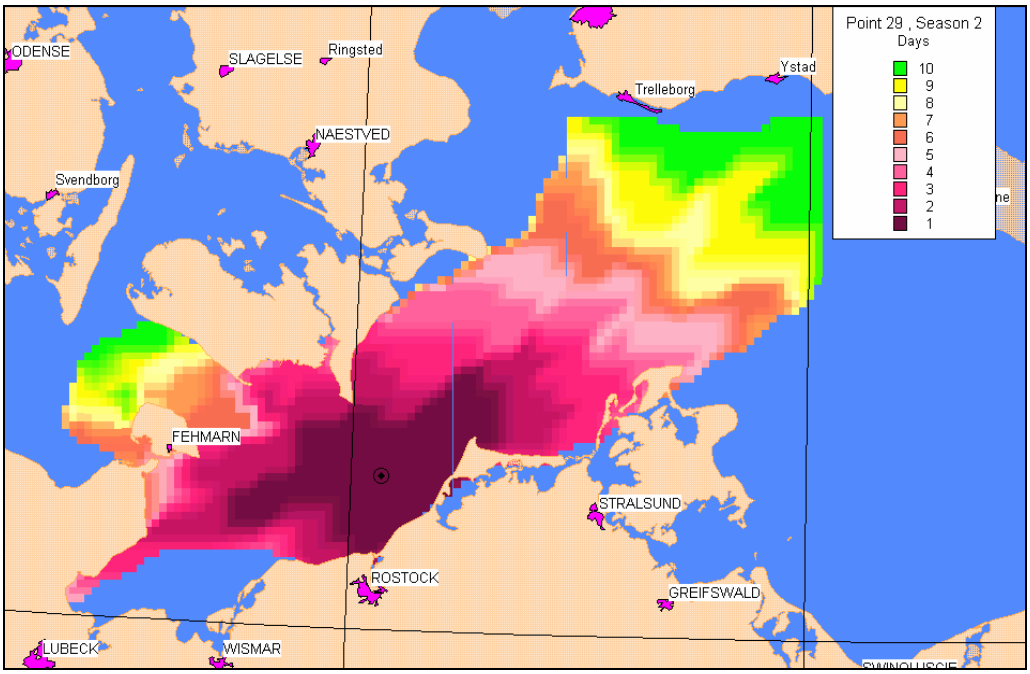

Figure 45 Risk zones for 1-10 days. Point 29. Autumn season.

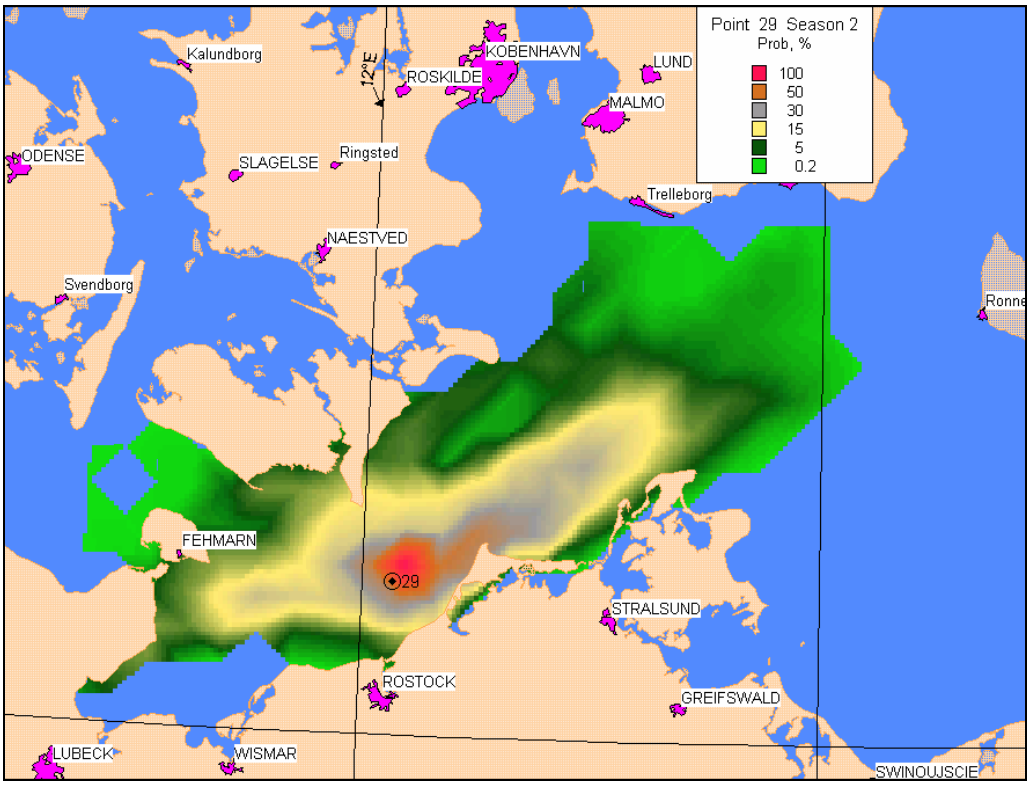

Figure 46 Probability of impact (%). Point 29. Autumn season.

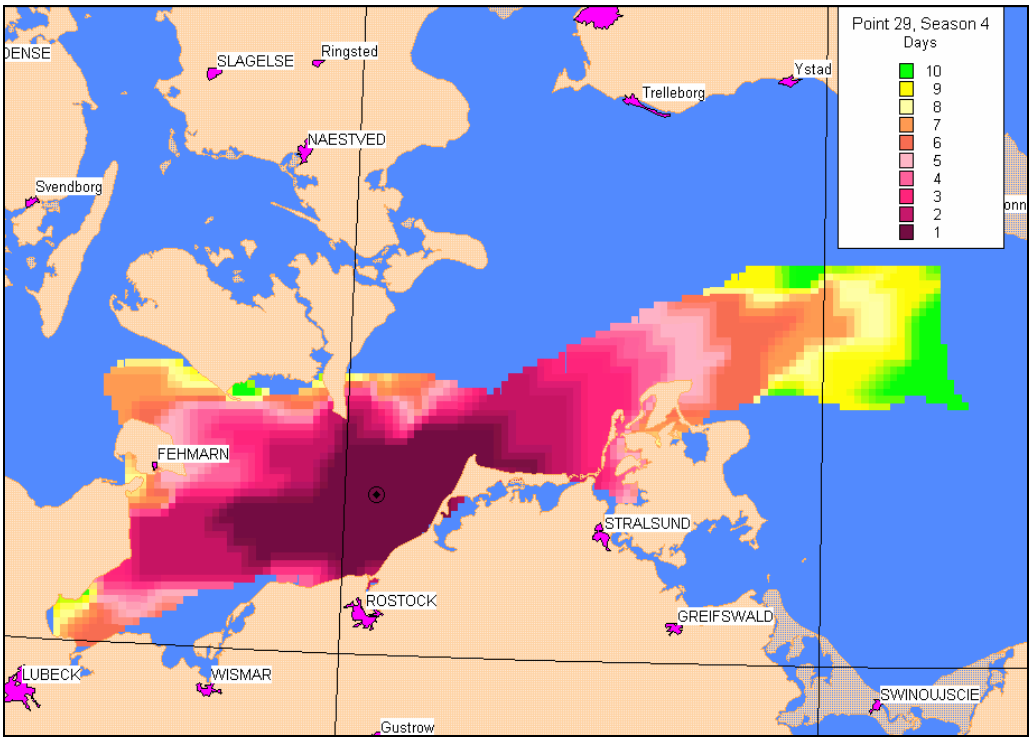

Figure 47 Risk zones for 1-10 days. Point 29. Spring season.

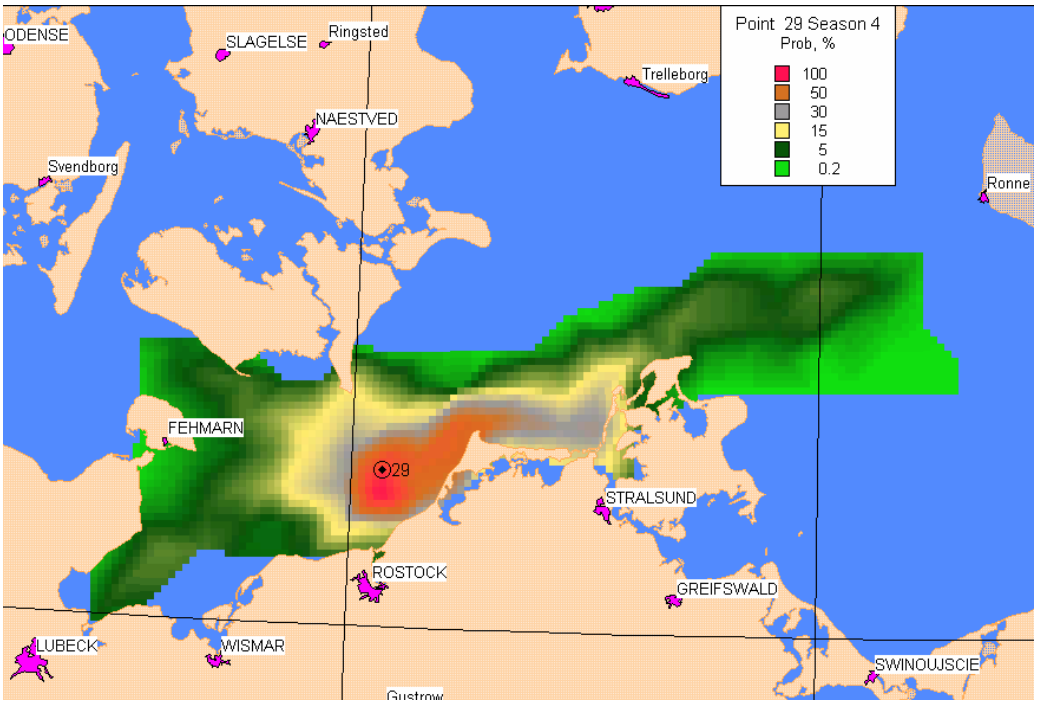

Figure 48 Probability of impact (%). Point 29. Spring season.

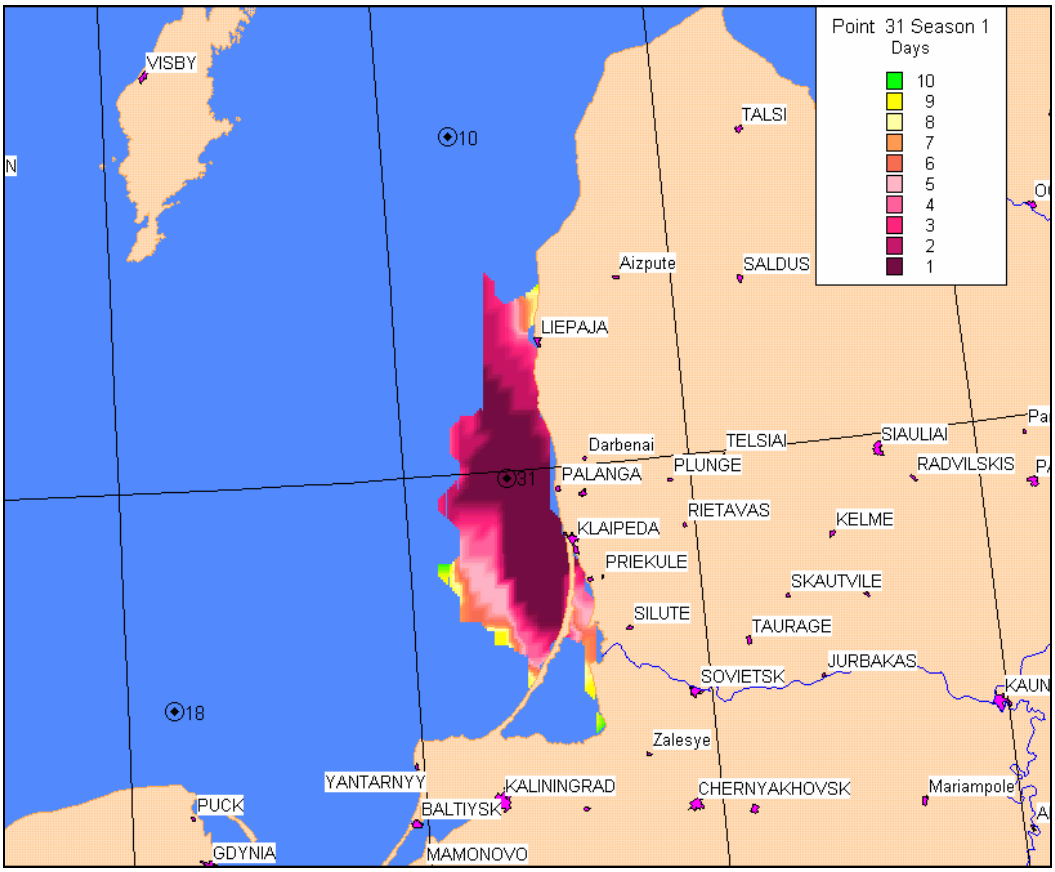

Figure 49 Risk zones for 1-10 days. Point 31. Summer season.

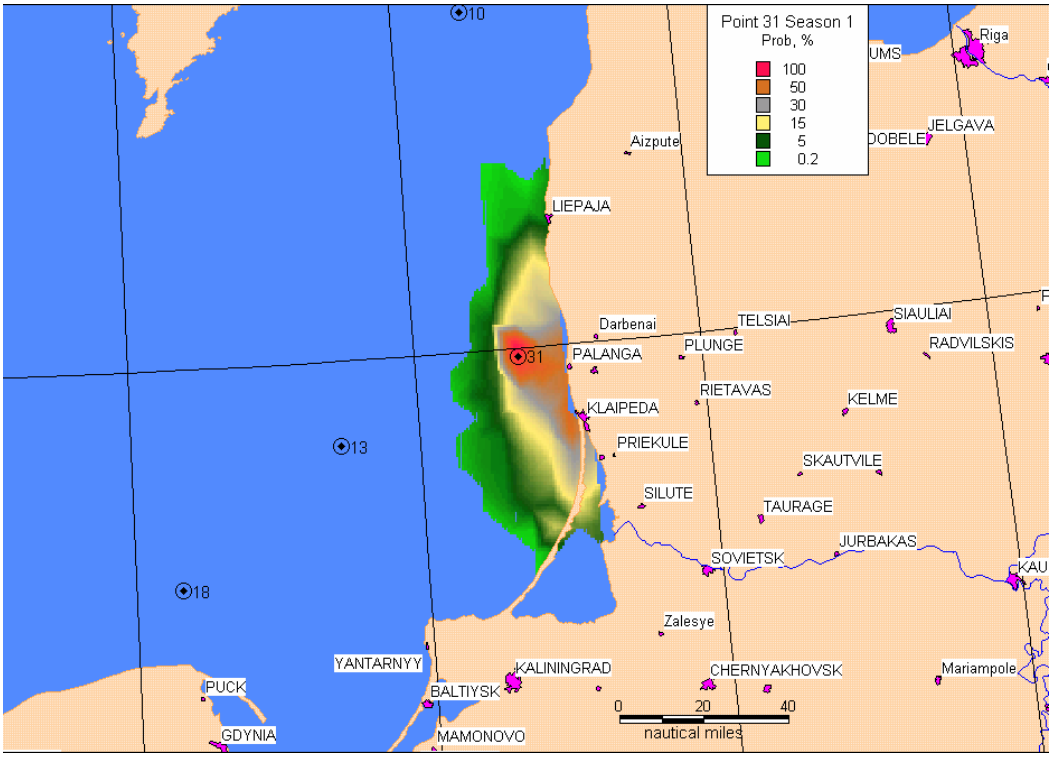

Figure 50 Probability of impact (%). Point 31. Summer season.

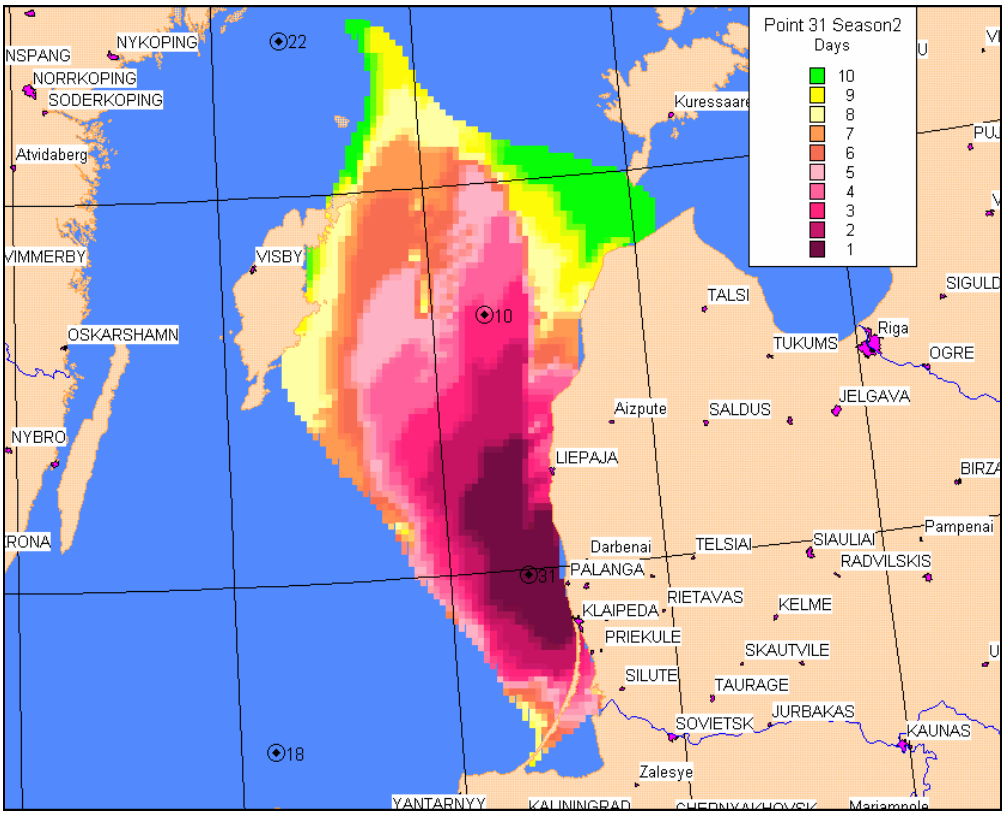

Figure 51 Risk zones for 1-10 days. Point 31. Autumn season.

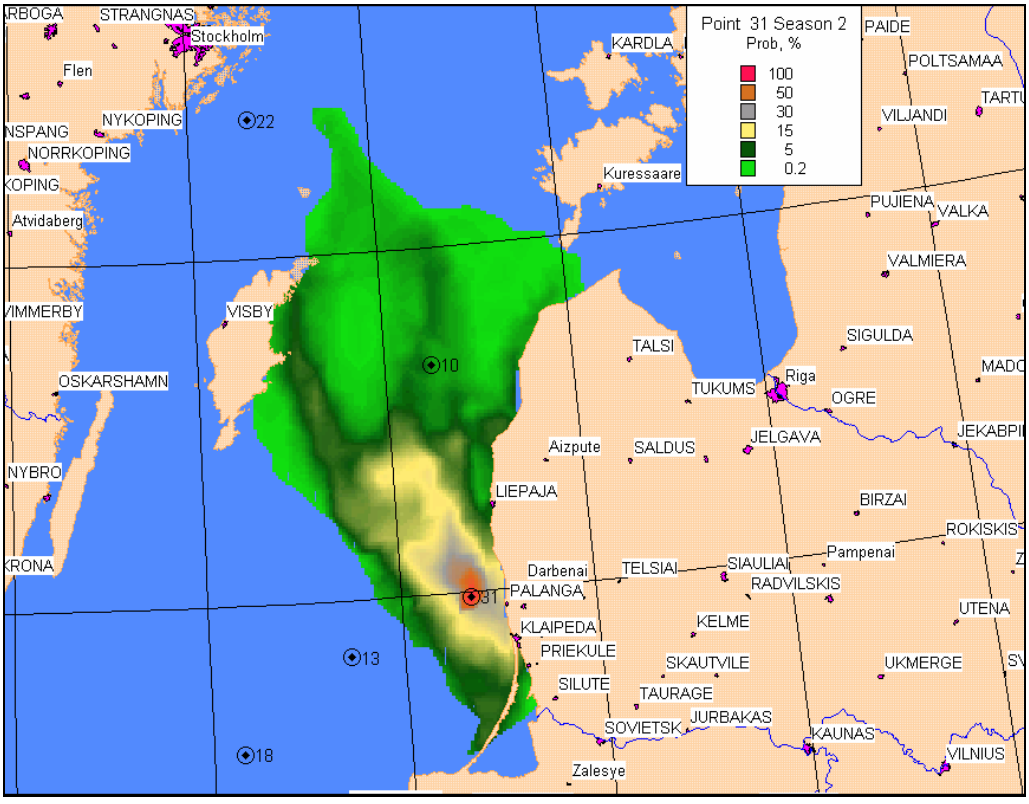

Figure 52 Probability of impact (%). Point 31. Autumn season.

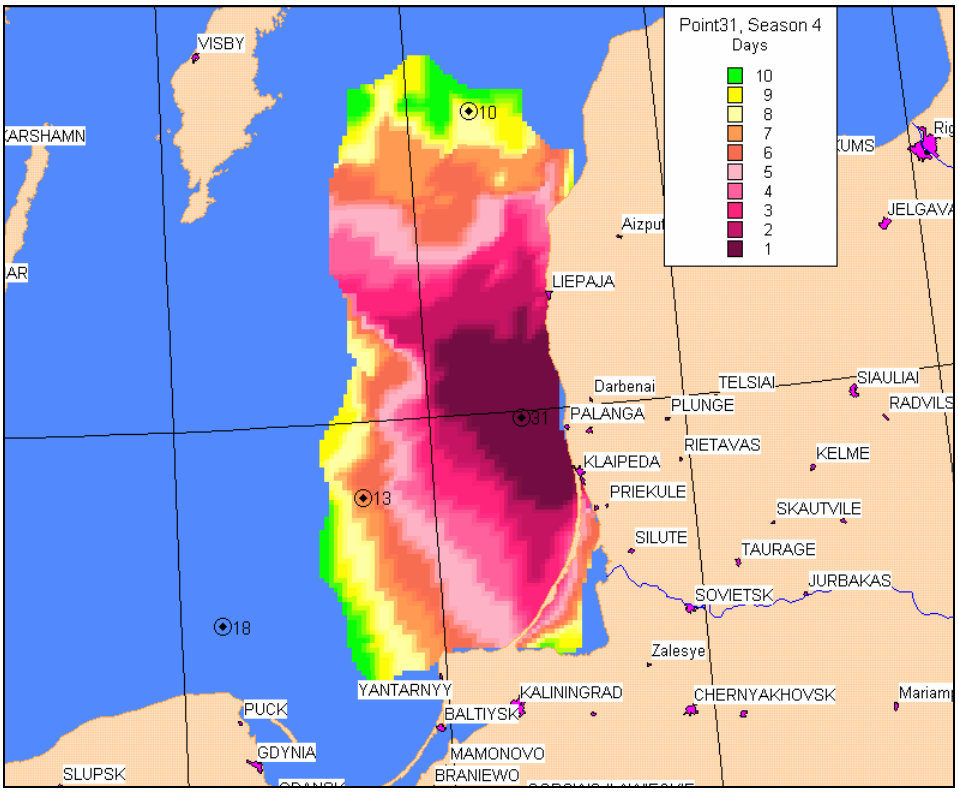

Figure 53 Risk zones for 1-10 days. Point 31. Spring season.

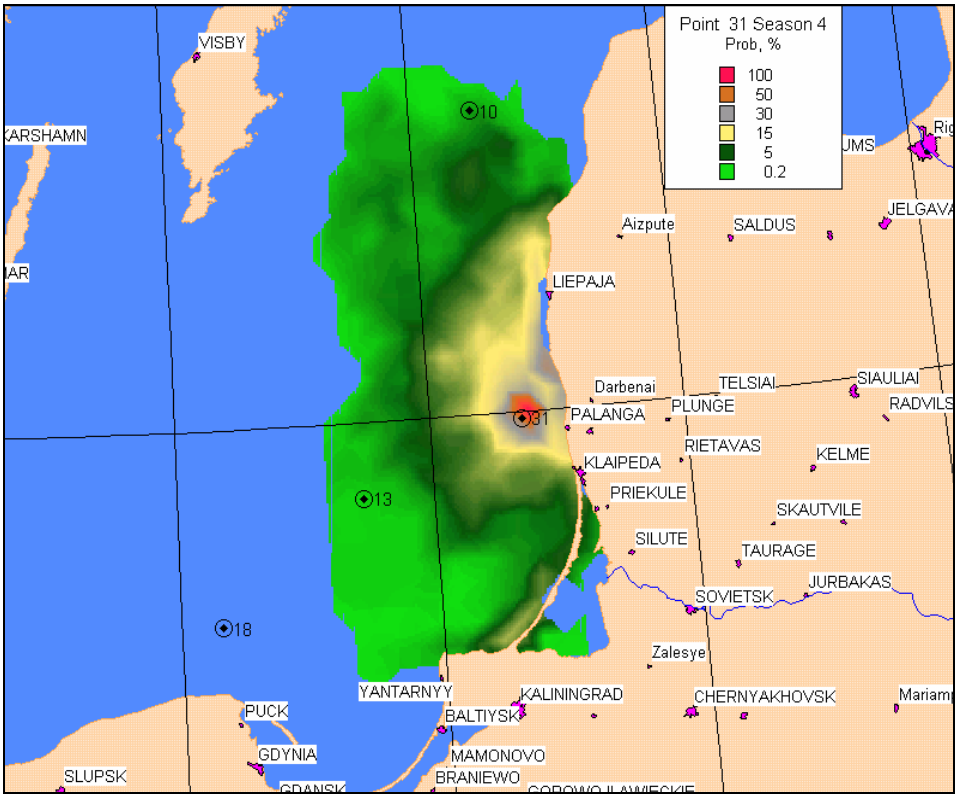

Figure 54 Probability of impact (%). Point 8. Spring season.

3.2. Weathering evaluation

The extent of oil spill impact on water area and shore depend on weathering intencity. The historical analysis of trajectories for the one-year period, using reconstructed metocean data, produced oil weathering results. This weathering is based on evaporation and dispersion into the water column and to the process of natural dispersion. Along with direct water-in-oil emulsion formation , oil evaporation causes an appreciable impact on changes in oil density on the sea surface and also changes in oil viscosity.

Figure 55-Figure 57 show the calculated limits of the weathering intencity in different Baltic areas for different seasons. Modeling results show that 20 to 50 % of the original oil weight is removed naturally in 10 days after spill. Key components of the oil weathering process are (i) evaporation of oil fractions to the atmosphere, and (ii) flow of oil droplets from the surface to the water column due to wave action and vertical mixing. Minimum weathering corresponds to periods with low wind speeds and almost entirely depends on the evaporation of volatile fractions from the oil slick. Maximum oil weathering occurs with strong wind, when most of the oil enters the water column in the form of droplets. The intensity and the final result of the evaporation of the volatile fractions of the oil slick depends, primarily, on the sea surface temperature and the oil properties.

Strong wind may remove oil slick from the sea surface almost completely, if oil have not sufficient amount of asphaltenes, which leads to water-in-oil emulsion making.

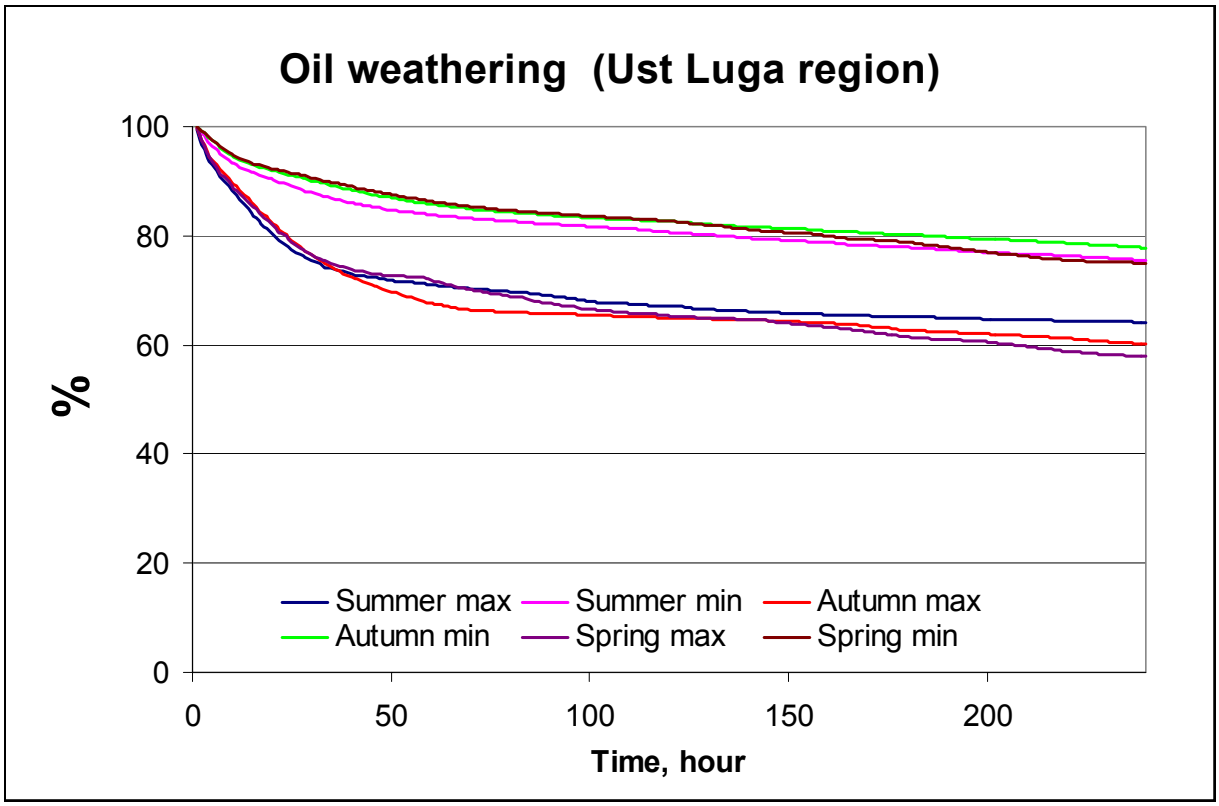

Figure 55 Oil at sea surface in percents to initial volume (Gulf of Finland)

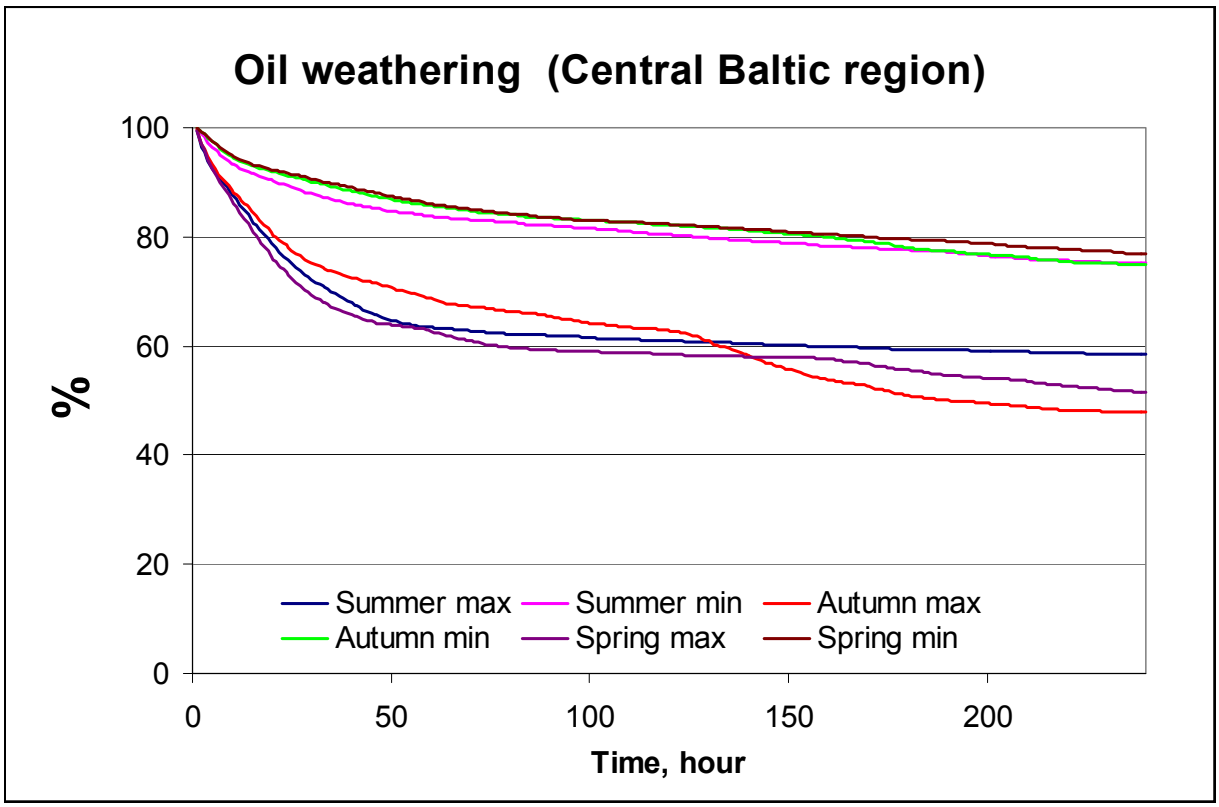

Figure 56 Oil at sea surface in percents to initial amount (Gotland area)

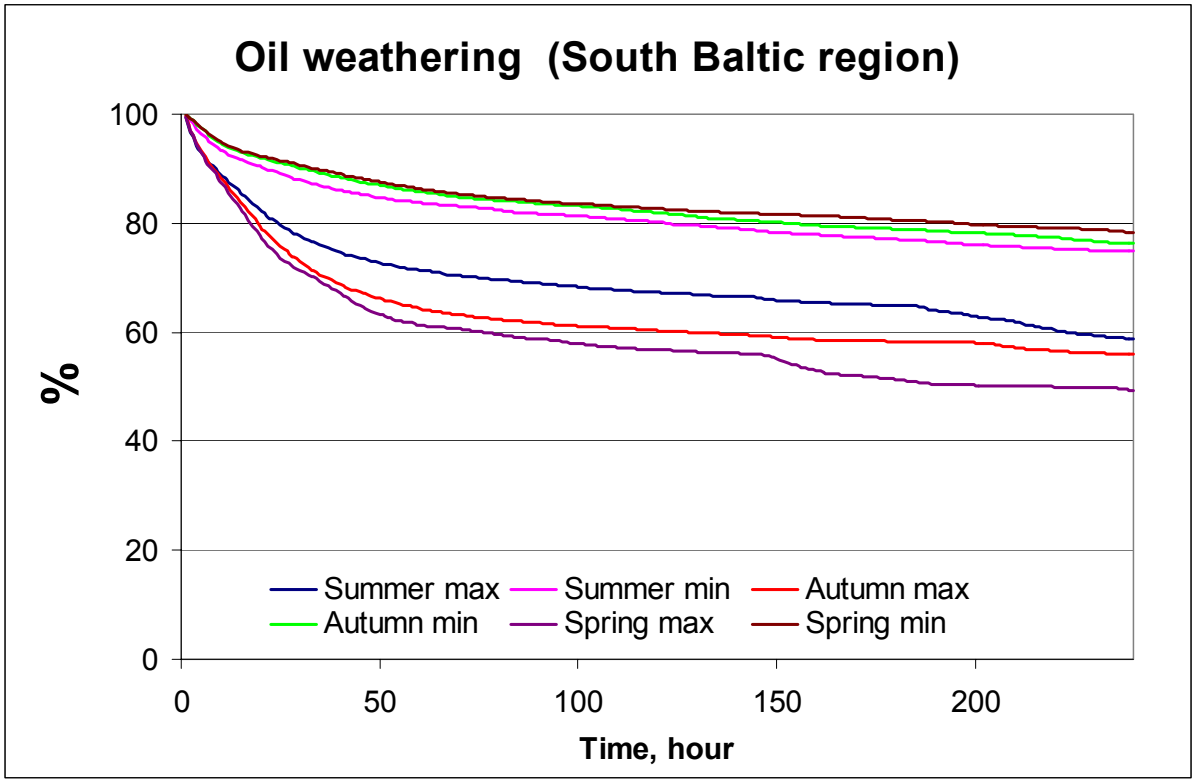

Figure 57 Oil at sea surface in percents to initial amount (South Baltic)

3.3. Probability of the shore impact

The Figures below show estimations of the possible shoreline impact intensity in 1, 3, 5 and 10 days after oil spill accident. The data are shown for eight (8) points of hypothetical accidents for *no ice* seasons. The figures represent conditional probability of the oil slick impact at the shoreline section of 20-kilometers length.

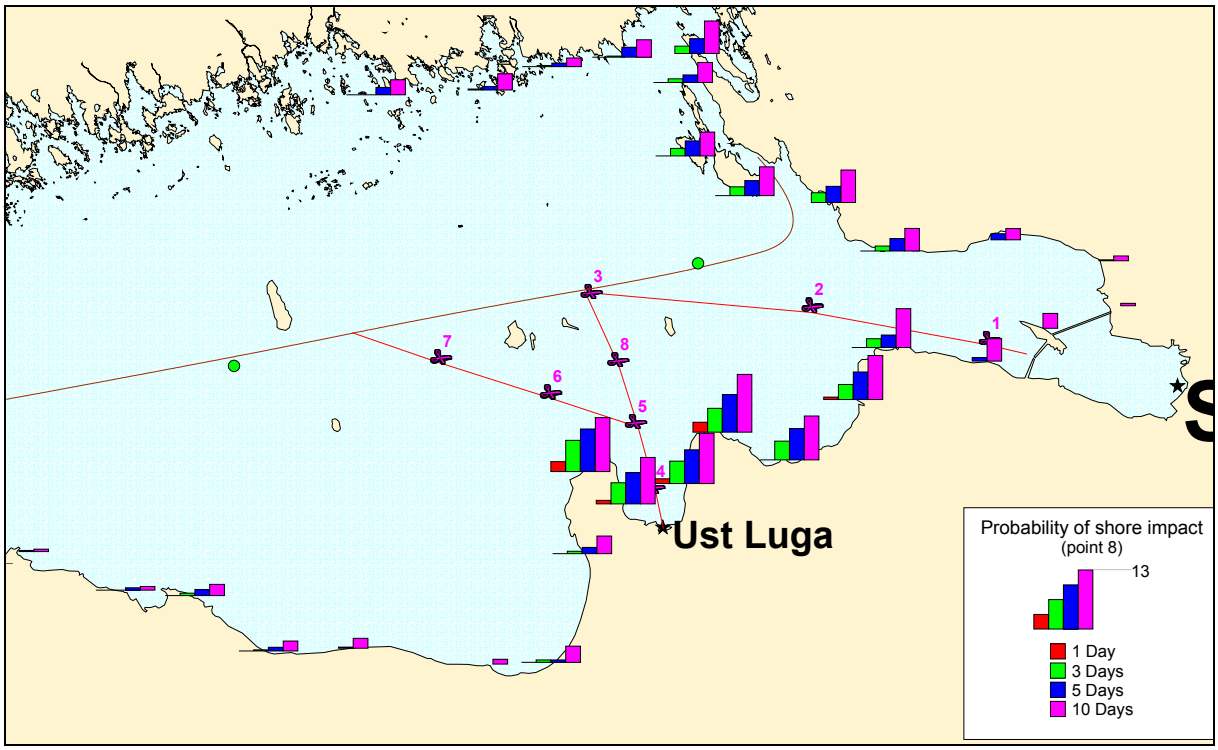

Figure 58 Probabilities of shoreline impact (point 8) (*Files p_coast8.*. Thematic map for YearDay1, YearDay3, YearDay5, YearDay10*)

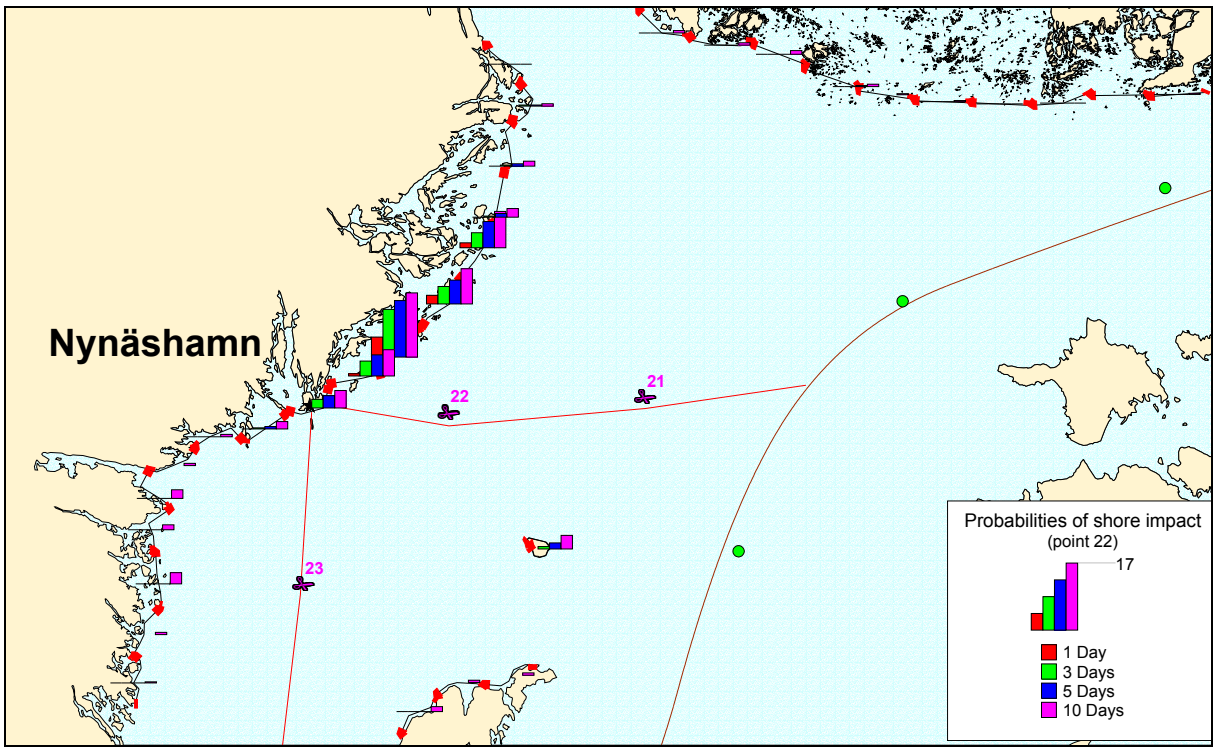

Figure 59 Probabilities of shoreline impact (point 22) *(Files p_coast22.*. Thematic map for YearDay1, YearDay3, YearDay5, YearDay10)*

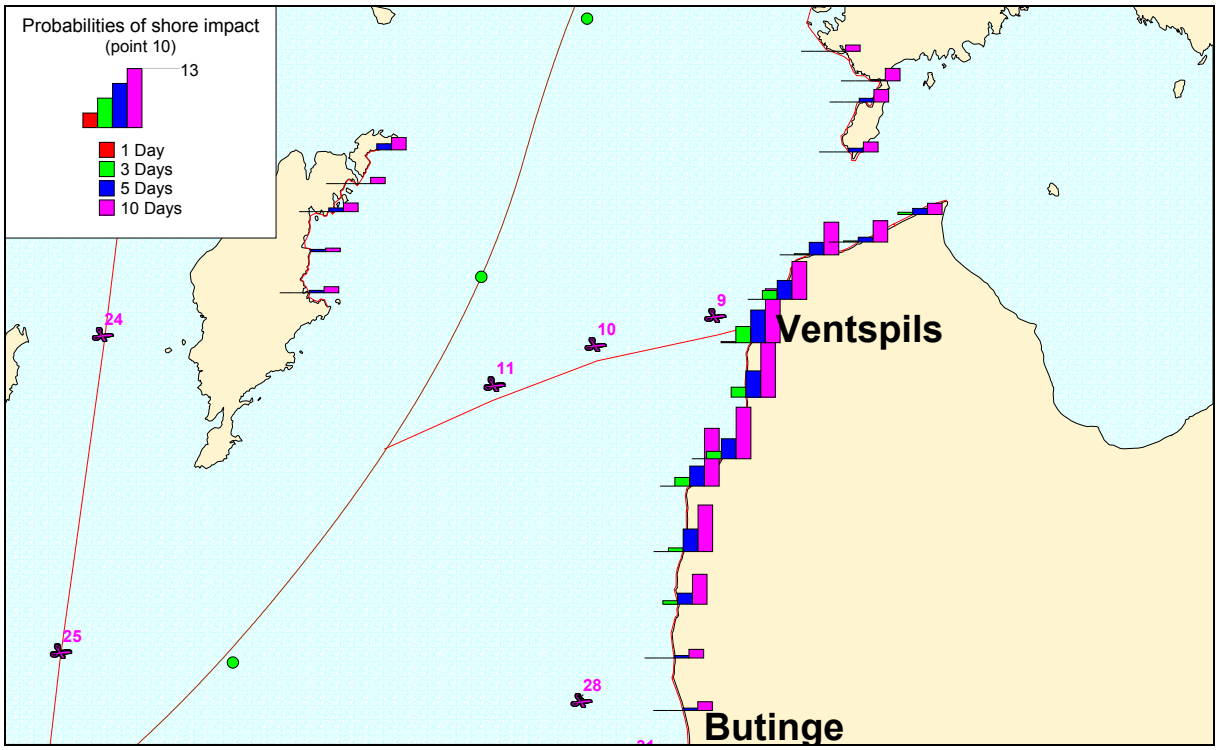

Figure 60 Probabilities of shoreline impact (point 10) ***(Files p_coast10.*. Thematic map for YearDay1, YearDay3, YearDay5, YearDay10)***

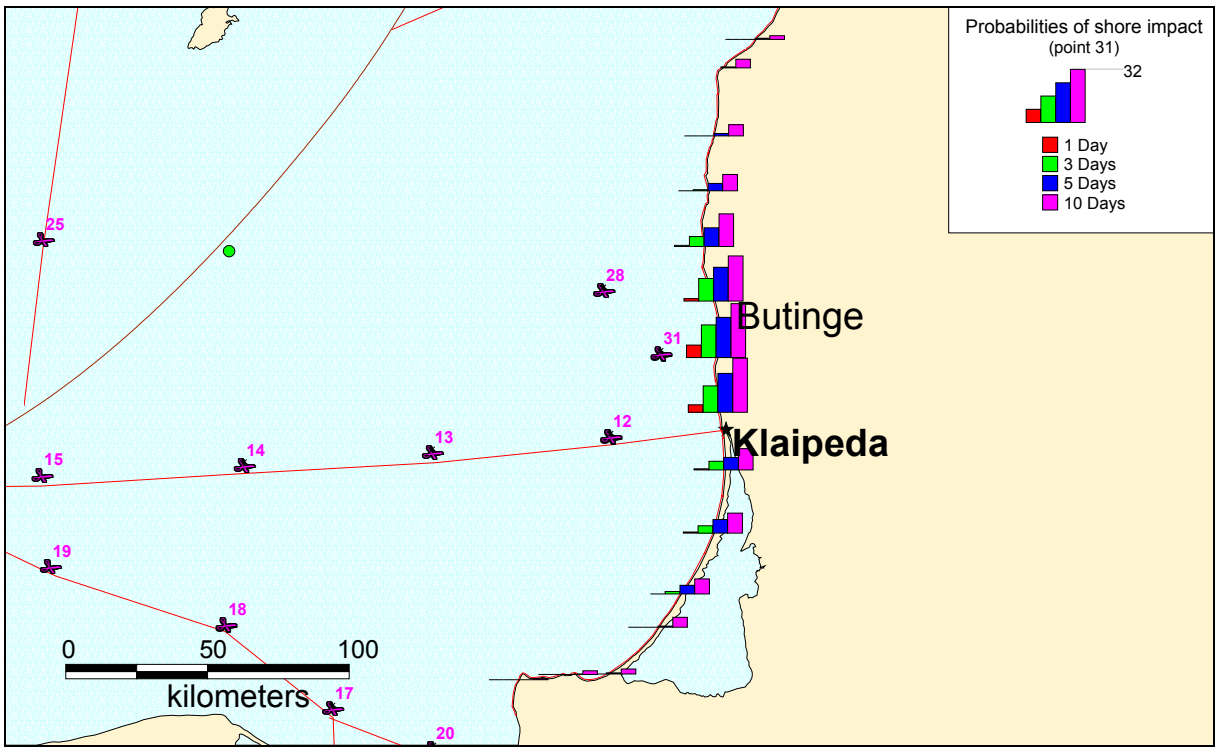

Figure 61 Probabilities of shoreline impact (point 31) ***(Files p_coast31.*. Thematic map for YearDay1, YearDay3, YearDay5, YearDay10)***

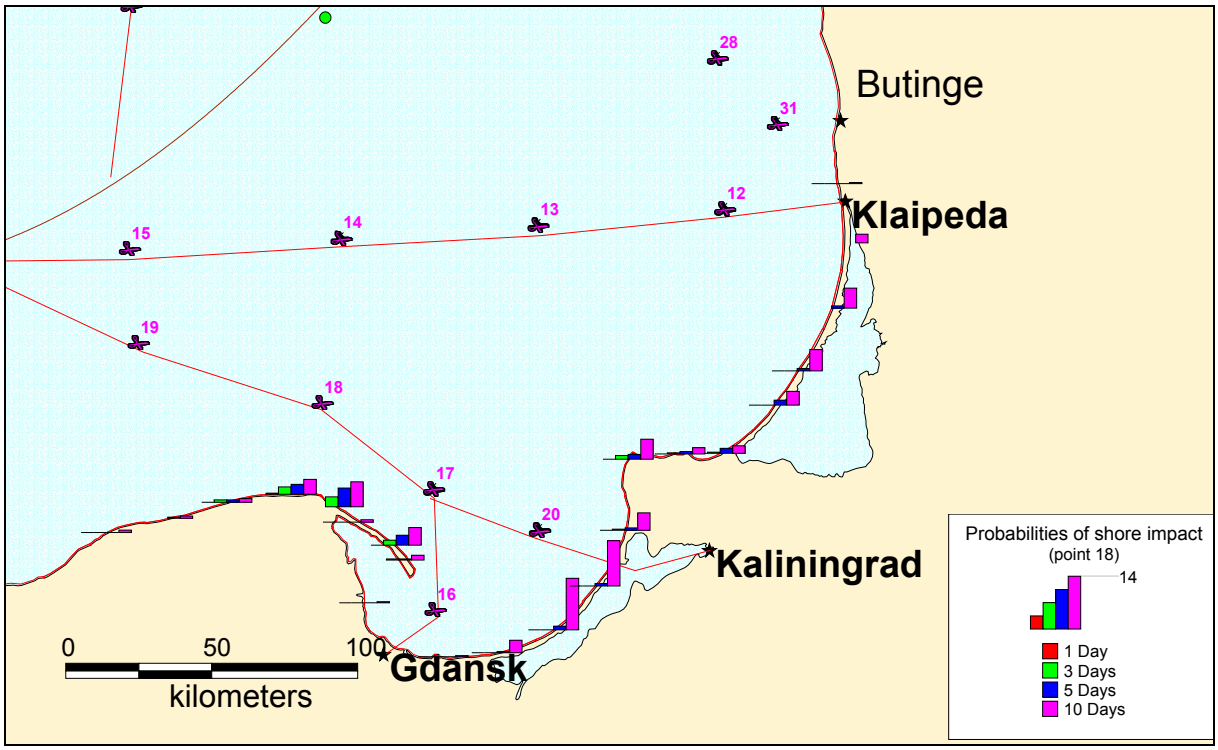

Figure 62 Probabilities of shoreline impact (point 18) ***(Files p_coast18.*. Thematic map for YearDay1, YearDay3, YearDay5, YearDay10)***

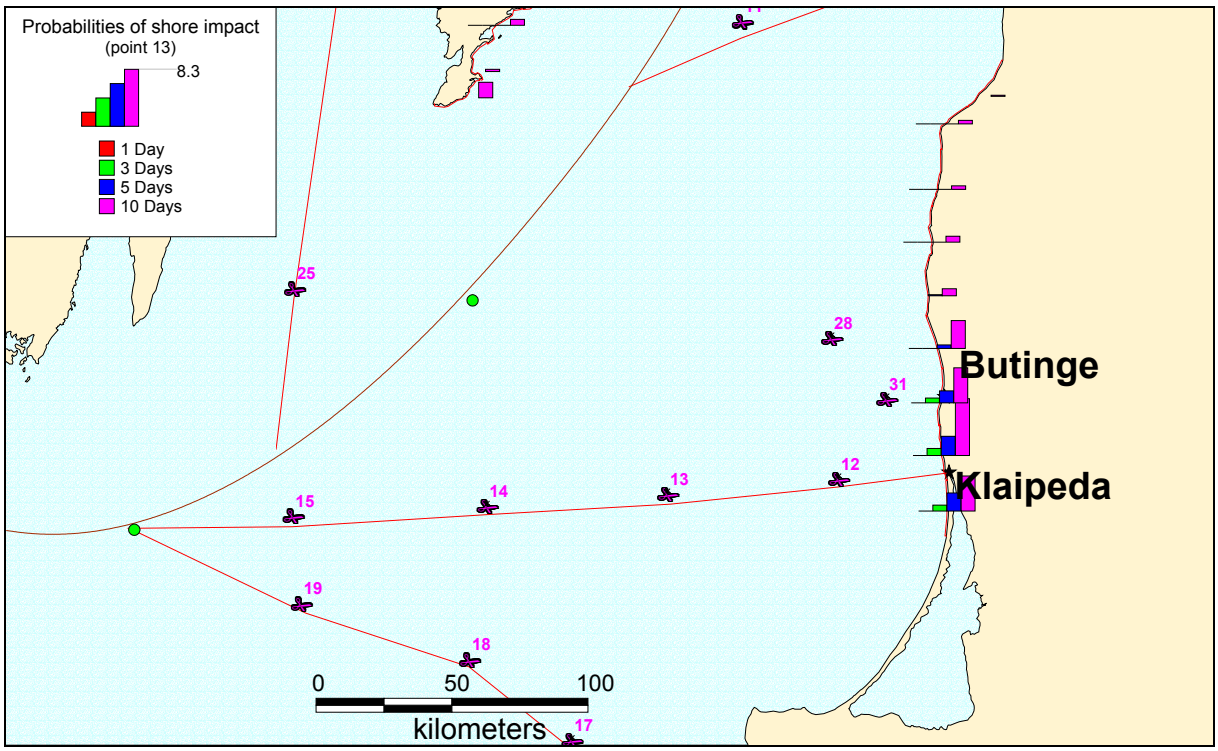

Figure 63 Probabilities of shoreline impact (point 13) ***(Files p_coast13.*. Thematic map for YearDay1, YearDay3, YearDay5, YearDay10)***

Table 3 Cumulative probabilities of shoreline impact for point of hypothetical spill (Files Spillpnt.mid)

Points	Summer				Autumn				Spring			
	Days after spill				Days after spill				Days after spill			
	1	3	5	10	1	3	5	10	1	3	5	10
1	42	87	97	100	66	90	98	100	64	98	100	100
2	7	46	68	93	22	72	89	97	26	75	87	97
3	8	31	55	90	10	53	74	96	6	51	78	97
4	58	86	91	98	77	94	96	100	57	79	94	100
5	17	50	66	93	29	69	84	96	16	52	76	96
6	5	36	53	91	18	54	78	91	16	46	73	93
7	3	33	46	82	7	37	65	93	6	39	61	88
8	10	38	58	92	18	56	74	93	6	47	75	94
9	10	58	81	98	9	28	40	67	13	40	48	61
10	0	14	38	87	0	5	23	58	0	13	33	46
11	0	2	18	69	0	6	18	46	0	8	27	51
12	1	30	60	91	0	21	34	63	4	27	39	59
13	0	5	22	63	0	0	6	47	0	8	20	36
14	0	0	2	52	0	0	8	20	0	0	8	29
15	0	0	0	9	0	3	6	33	0	0	2	22
16	21	75	87	94	19	63	71	83	20	71	90	96
17	0	13	50	82	1	11	27	53	3	29	61	76
18	0	2	8	62	0	3	7	17	1	11	26	48
19	0	5	11	29	0	2	10	35	0	0	4	33
20	10	60	80	98	3	39	51	66	13	53	73	85
21	0	0	1	10	0	10	28	51	0	1	11	41
22	2	10	17	28	17	50	62	79	4	25	33	60
23	0	4	19	43	0	31	55	82	0	14	35	64
24	2	55	76	90	1	31	65	91	7	51	76	90
25	0	0	1	4	0	14	28	51	0	10	21	58
26	28	54	65	82	30	57	76	94	25	65	85	99
27	17	45	56	83	26	50	75	97	20	58	81	98
28	1	31	57	88	0	19	32	61	4	27	31	47
29	7	66	78	95	8	40	58	79	27	63	77	91
30	0	15	52	88	0	31	55	74	2	36	56	74
31	14	53	77	93	5	33	41	65	17	43	54	67

The scale of impact evaluation

The scale of oil spill impact on shore and marine objects depend firstly on the amount of released oil. For large spills sea surface oiled area magnification lasts long time because of prolonged hydrodynamic stage of spreading. In case of small oil amounts oiled area increases

mainly for the expense of turbulent diffusion processes. The **Figure 64** and **Figure 65** show spill area increase for 30000 and 50 tons spills.

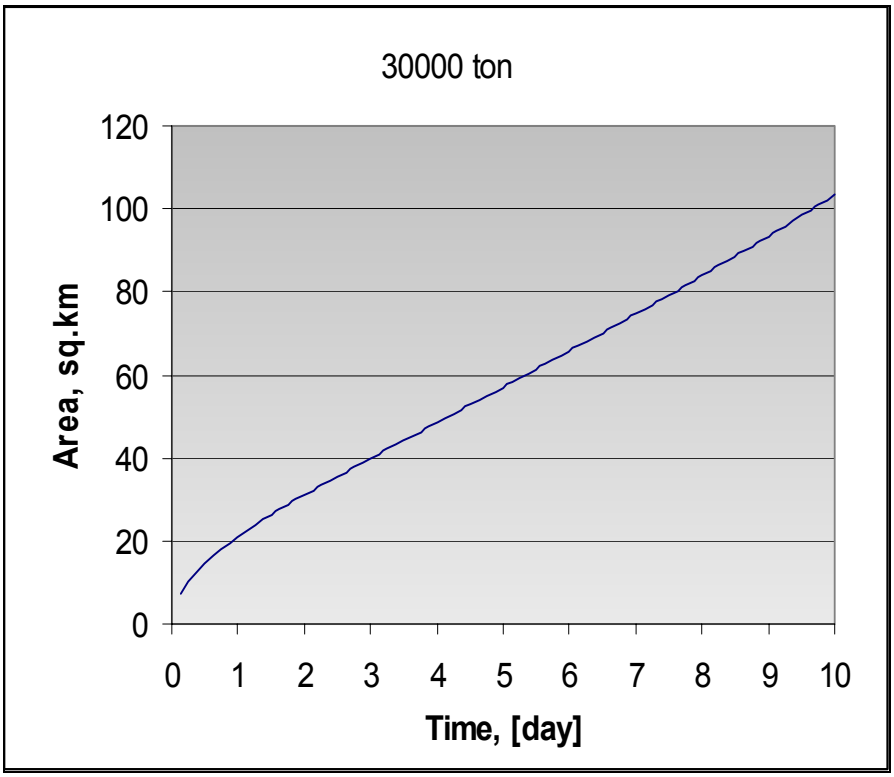

Figure 64 Spill area versus time for 30000 ton spill

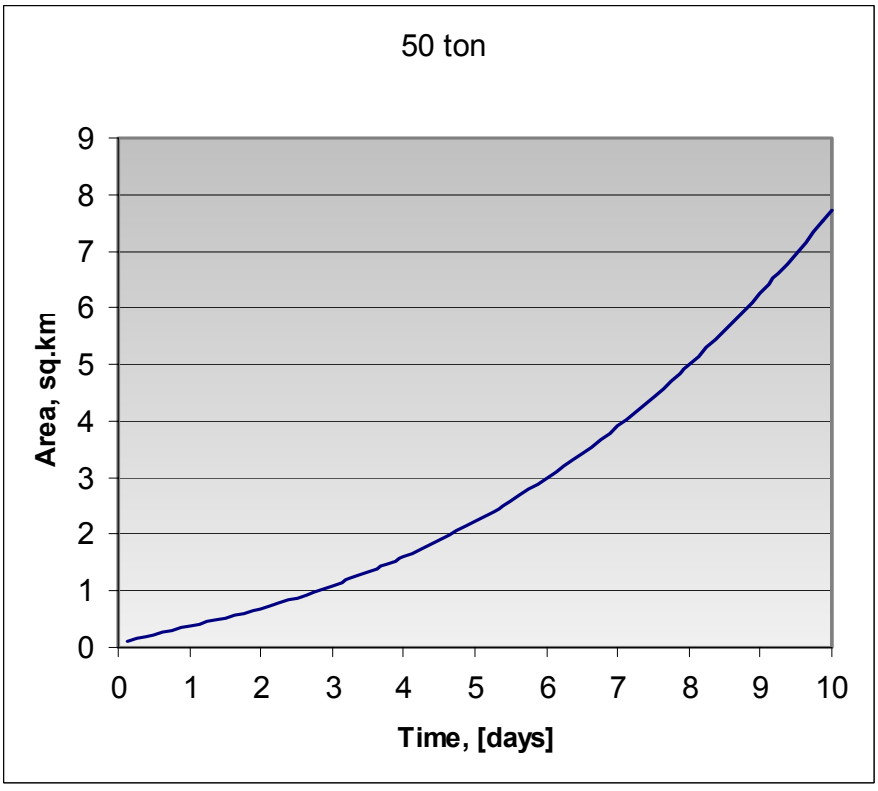

Figure 65 Spill area versus time for 50 tons

Figure 66-Figure 74 show *examples* of the consecutive position every 2 hours and configuration of the oil slick for the *potential* paths of oil slick movement following spills of 100 t, 1000 t and 10 000 t respectively.

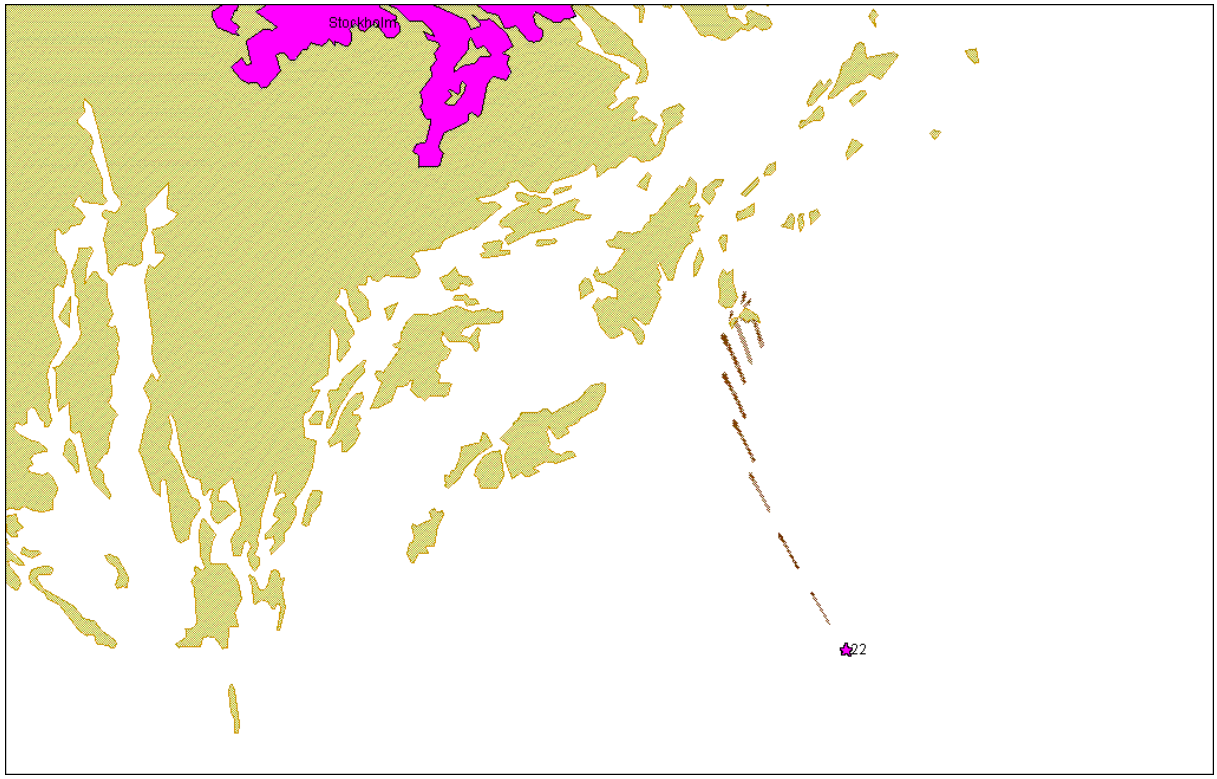

Figure 66 Oil spill 100t. Point 22. Trajectory 354.

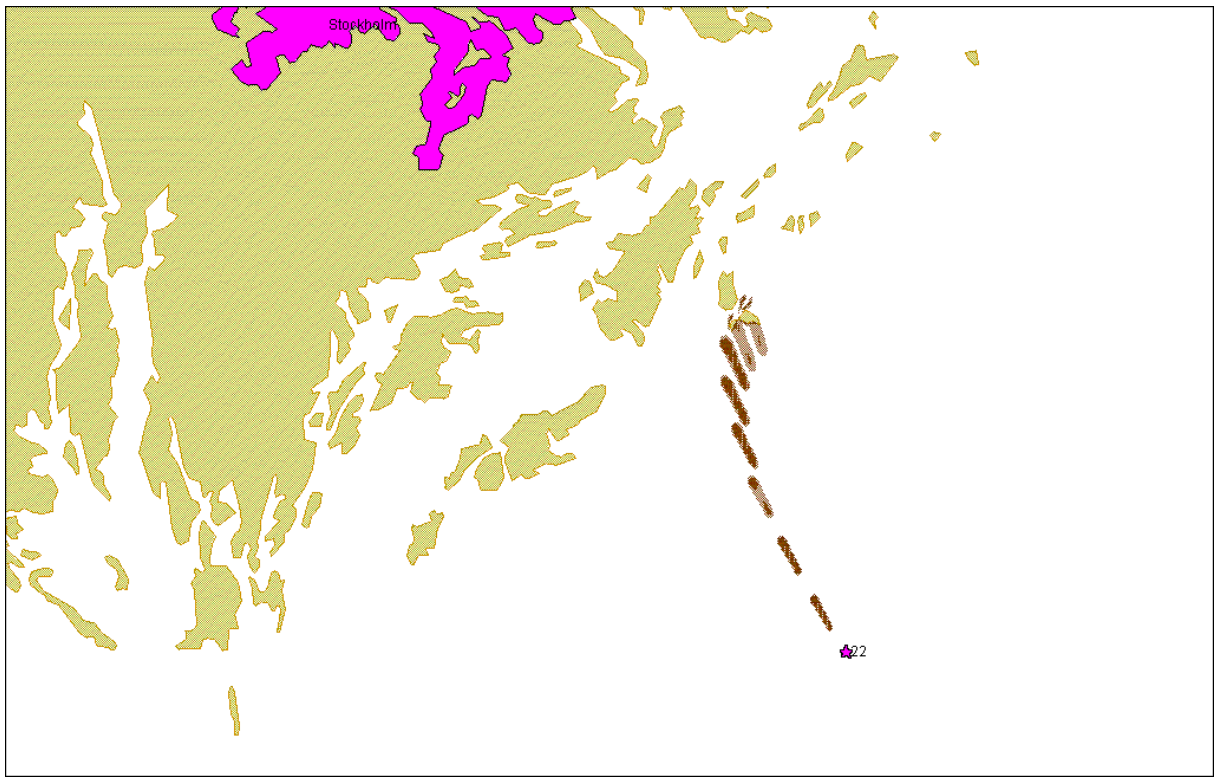

Figure 67 Oil spill 1000t. Point 22. Trajectory 354.

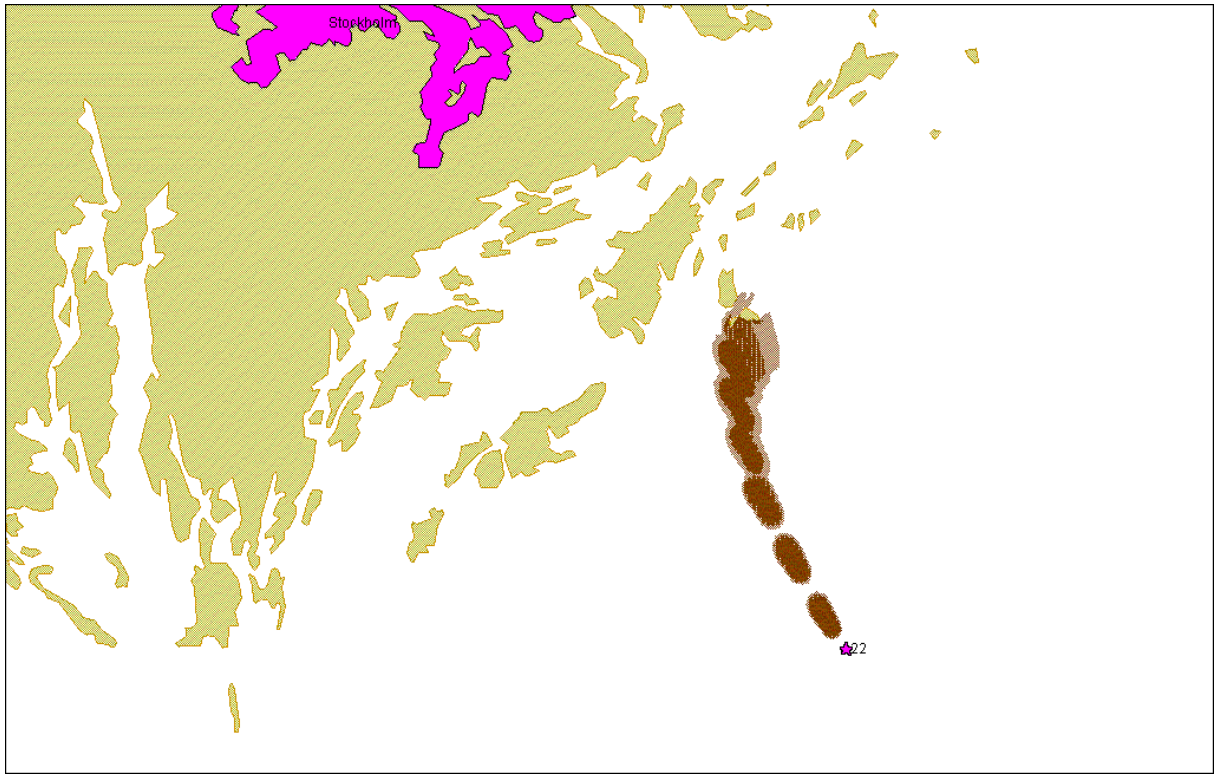

Figure 68 Oil spill 10000t. Point 22. Trajectory 354.

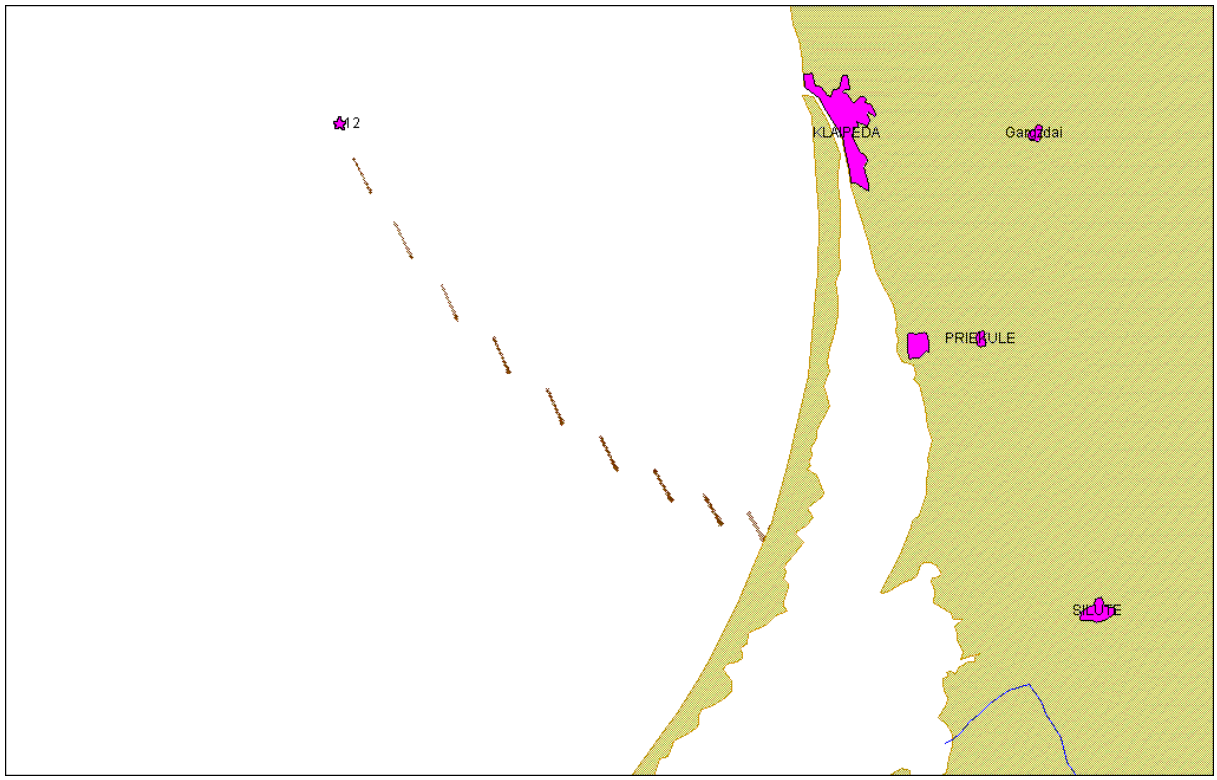

Figure 69 Oil spill 100t. Point 12. Trajectory 449.

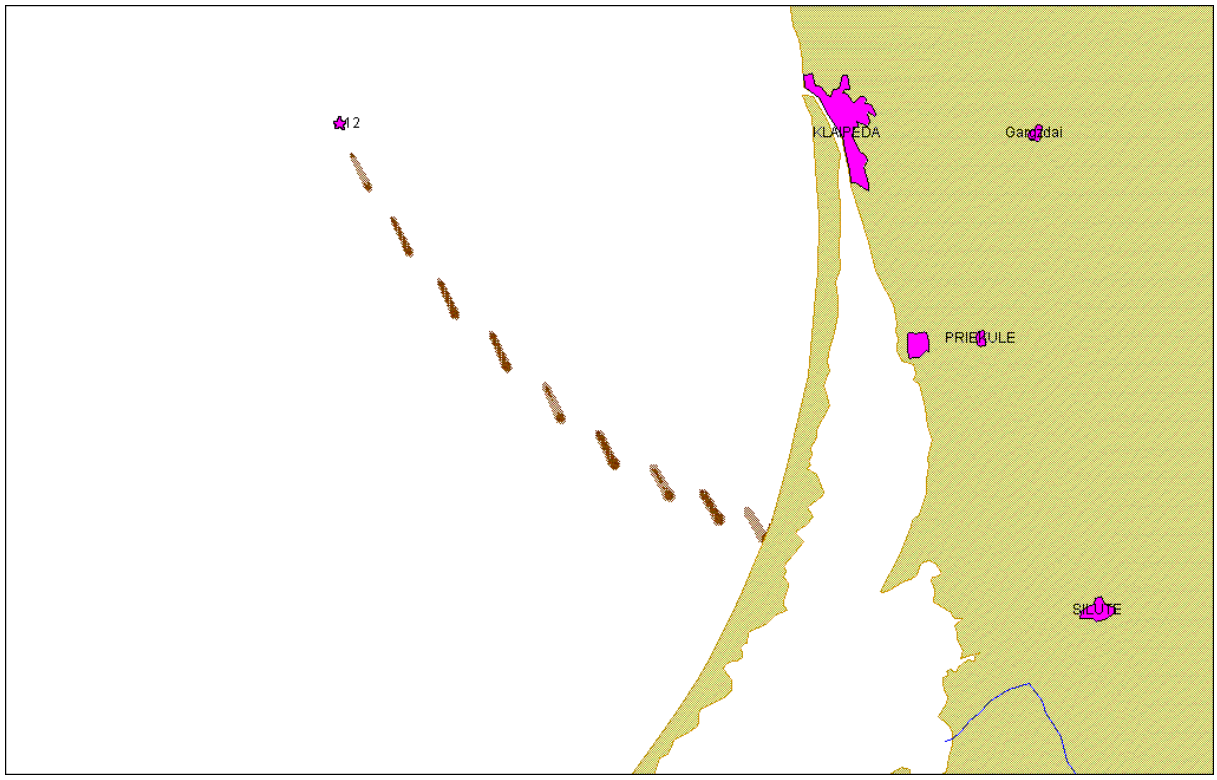

Figure 70 Oil spill 1000t. Point 12. Trajectory 449.

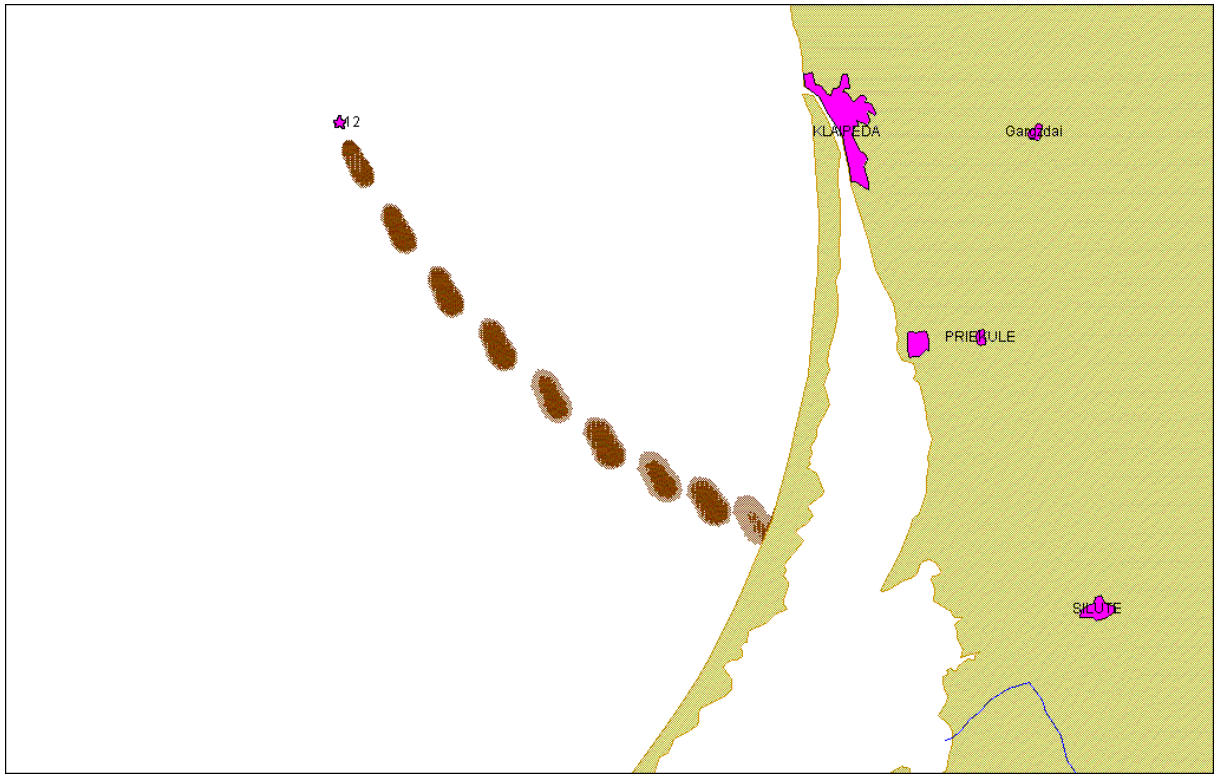

Figure 71 Oil spill 10000t. Point 12. Trajectory 449.

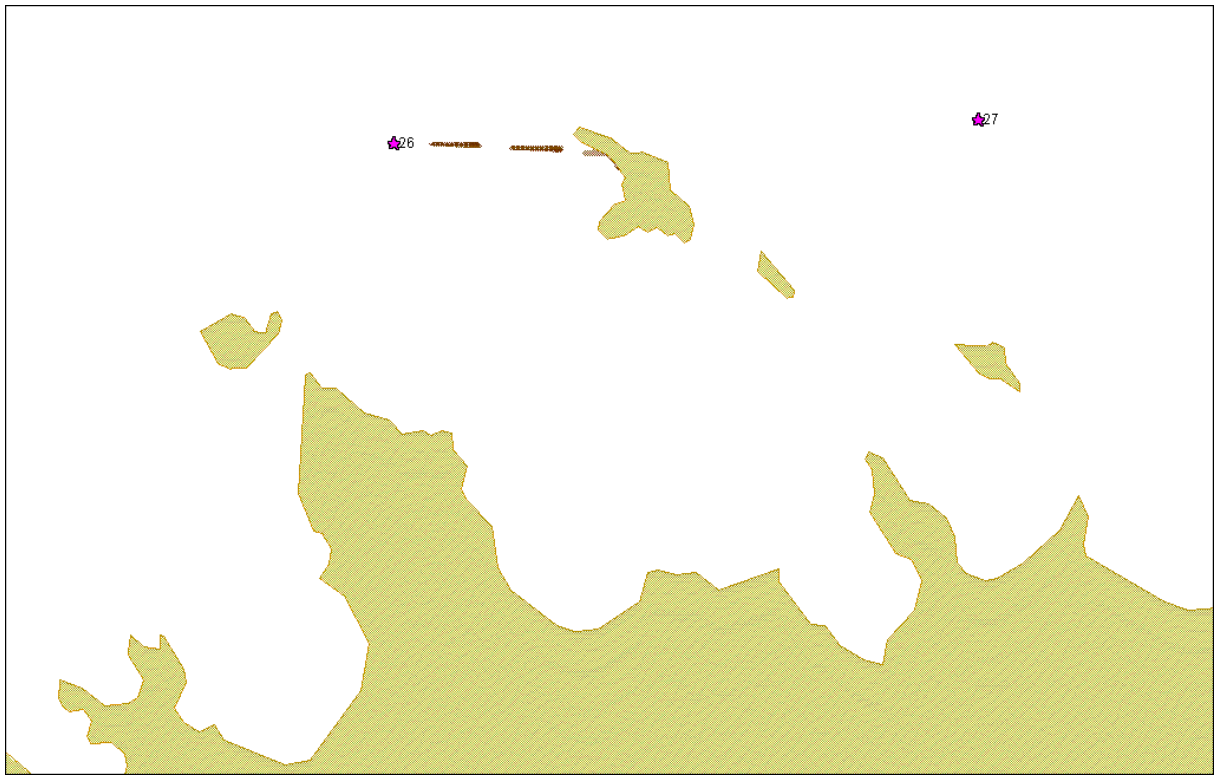

Figure 72 Oil spill 100t. Point 26. Trajectory 195.

Figure 73 Oil spill 1000t. Point 26. Trajectory 195.

Figure 74 Oil spill 10000t. Point 26. Trajectory 195.

Conclusions

The results of oil spill mathematical modelling at the sea surface are presented for possible oil spill emergency situations connected with oil transportation near selected Baltic seaports.

The mathematical modelling was carried out on the basis of a set of models reproducing typical for this region hydrometeorological conditions. The set of mathematical models includes:

· three-dimensional baroclinic model of currents dynamics in the Baltic sea

· model of dynamics of sea ice for the Baltic sea

· model of oil spill at the sea surface

For an estimation of risk zones, historical analysis of multiple equiprobable oil slick movement paths, as a function of metocean conditions in the region in question and oil discharge conditions were used.

The outcomes of mathematical modelling include:

- evaluation of risk zones, where oil slick may appear within the set time periods following the spill event , unless oil spill containment and response measures have been taken;

- estimation of oil weathering intencity for a typical seasons conditions

- estimation of possible risk zone of oil spills coastline impact in typical meteorological conditions

The calculations were carried out with a computer system OSMS, intended as for operative purposes in oil spills combatting, as for oil spill impact risk evaluation purposes.

4. Literature

1. Ovsienko S., Zatsepa S., Ivchenko A., (1995). *Oil spreading on snow/ice surface*, INSROP Working Papers, n.6
2. Ovsienko S., Zatsepa S., Ivchenko A., (1999). *Study and modelling of behavior and spreading of oil in cold water and in ice conditions* – Proc. POAC, Helsinki, Finland, 23-26 August
3. Zatsepa S., A.Ivchenko, S.Ovsienko, (1992). *A local operative model for oil drift and dispersion*, Proc. Combating marine oil spills in ice and cold conditions, Helsinki, Finland, 1-3 December, pp.189 -192
4. Zatsepa S., A.Ivchenko, S.Ovsienko, (1992). *Mathematical modelling of oil behavior in ice covered sea* - Proc. Combating marine oil spills in ice and cold conditions, Helsinki.
5. Mackay,D., Matsugy R.S. (1973), *Evaporation rate of liquid hydrocarbon spill on land and water*, Can.J.Chem.Eng., v.51, p.434-439
6. Kirstein,B.E., and R.T. Redding (1988) *Ocean-ice oil-weathering computer program user's manual*. U.S. Dep.Commer., NOAA, OCSEAP Final Rep. 59
7. INSROP Working Paper, No/5 -1994, I.5.1, pp. 58-61 - *Operational oil drift models.*
8. Belore,R., and Buist, I.A., (1988) *Modelling of oil spill in snow* ,Proc. of eleventh Arctic and marine oil spill program technical seminar, AMOP, June 7-9, 1988, Vancouver B.C.
9. Bachaus J.O, Hainbucher D. (1987) *A finite difference general circulation model for shelf seas and its application to low frequency variability on the north European shelf.* – Three- dimensional models of Marine and Estuarine dynamics, ed. Nihoul J.C.J. and Jamart B.M., Els. Oceanogr. ser., Amsterdam, p.221-244.
10. Bowden K.F., and Hamilton P. (1975) *Some experiments with a numerical model of circulation and mixing in a tidal estuary*. Estuar. Coast. Mar. Sci., vol.3, p.281-301.
11. Fang G, T.Ichiye. (1983) *On the vertical structure of tidal currents in a homogeneous sea.* Geophys. J.Roy. Astr. Soc, p.65-82.
12. Oey L.Y., Mellor G.L., Hires R.I. (1985) *A three-dimensional simulation of the Hudson-Raritan estuary*. Part 1. Description of the model and model simulations.// vol.15, N 11, p.1676-1692.
13. Ryabinin V.E., Zilberstein O.I. (1996) *Numerical prediction of storm surges – a review.* In: Storm Surges. Report N 33, WMO/TD – N 779, p.1-62.
14. Happala J., Lepparanta M. (1996) *Simulating the Baltic Sea ice season with a coupled ice-ocean model*, Tellus 48A, 5

Appendix A.

Mathematical Model of the Oil Spreading on the Sea Surface

The equations of model, representing certain development of traditional system of "shallow-water" equations, are derived by a method of perturbance by small parameter from initial 3-D problem, in which the movement within the layer of oil is described by Navier-Stokes equations for uncompressible Newtonian liquid.

Model features

- The oil spreading processes drawn by positive buoyancy of oil are described through the complete equations of hydrodynamics. For their solution a set of adaptive (self-adapting) grids - Lagrangian and Eulerian is formed, it allows parametrical description of evaporation, emulsification, aging processes, as well as sedimentation and interaction with driving booms. Polygonal approximation of a coastline makes possible a wide range of electronic maps use.
- The mathematical statement of the problem and unusual Eulerian-Lagrangian computing process allows to consider spills of oil from diverse sources, including lengthy and multiple ones.
- Dynamics of very thin films of oil (about several molecular layers) is not considered in the model. The parameterizations of this process can be included in a system, however from practical point of view these films are insignificant, for they contain small (less than 5-10 %) amount of spilled oil.

Wind waves parameters are calculated by local wind for oil dispersion in the water column parameterization. Waves affect on emulsification process and mechanic and chemical combating means effectivity.

Oil slick, being in contact with a shore or port buildings, partially falls out on their surface. The amounts of oil, delayed or stranding at a coast, are calculated in the model. The elements of a coastline have varying swallowing ability, and the rate of sedimentation is supposed to be a proportional to thickness of oil, contacting with shore.

For use in a model oil or petroleum product should be defined through its physical properties - density, viscosity and surface tension, and fractional structure. Typically the oil is

represented as a mixture of well known hydrocarbon fractions. The partition can be various. In this model oil is represented as a mixture of several (8-20) components with known temperatures of boiling (true boiling point) and density of fractions.

Main equations.

Let us consider 2-D area Ω(t,x,y) with boundary dΩ. Oil occupies sub area Ω‘, generally speaking, multispanned. In sub area Ω‘ ∈ Ω the source is , providing flow of oil - Q on sea surface. The area is bounded by the set of linear functions, approximating coast line shape. The main equations of model, for area Ω‘ are as follows:

$$H(\frac{\partial \mathbf{u}}{\partial t} + \mathbf{u}\nabla\mathbf{u}) = -Hg'\nabla H - \beta(\mathbf{u} - (\mathbf{u}_d + \mathbf{u}_c))|\mathbf{u} - (\mathbf{u}_d + \mathbf{u}_c)| + \frac{1}{\rho_o}\nabla.\mathbf{T} \qquad \text{(A1)}$$

$$\frac{\partial H}{\partial t} + \nabla.(H\mathbf{u}) = -\frac{k_e + k_d - Q}{\rho_o} \qquad \text{(A2)}$$

where ρ_o is oil density, $\mathbf{u}$ is vertically averaged velocity of oil, $\mathbf{u}_d$ is velocity of surface wind drift current, , $\mathbf{u}_c$ is tide, storm surge and drift current velocity on horizon 2 m (possibly, received from the circulation model), H is thickness of oil, k_e is mass flux due to evaporation, k_d is mass flux due to waves breaking, Q is flow of oil on surface from source of spill, **T** is a tensor of viscous stresses in the layer of oil; $\nabla.$ is operator of a horizontal divergence, ∇ is operator of a horizontal gradient, g is gravity acceleration, $g' = g\frac{\rho_w - \rho_o}{\rho_w}$, ρ_w is water density. Viscous stresses can be represented as

$$T_{xx} = \mu H(4\frac{\partial U}{\partial x} + 2\frac{\partial V}{\partial y}) \qquad T_{xy} = \mu H(\frac{\partial U}{\partial y} + \frac{\partial V}{\partial x})$$

$$T_{yx} = \mu H(\frac{\partial U}{\partial y} + \frac{\partial V}{\partial x}) \qquad T_{yy} = \mu H(2\frac{\partial U}{\partial x} + 4\frac{\partial V}{\partial y}) \qquad \text{(A3)}$$

If the boundary of area Ω(t, x, y) is L (t, x, y) and L=L_1 (t, x, y) ∪ L_2 (x, y), where L_1 - free boundary and L_2 - contact boundary, the system of equations (1) - (2) should be complemented by the following boundary conditions:

kinematics condition

$$L_1: \qquad R_t + u\nabla R - \frac{(k_e + k_d)}{\rho}\frac{|\nabla H||\nabla R|}{(\nabla H \nabla R)}\nabla R = 0 \qquad \text{(A4)}$$

where R (t, x, y) =0 - equation of free boundary;

And **dynamic condition**

$$L_1: \qquad H=0 \qquad \text{(A5)}$$

$$\partial \mathbf{u}_\tau / \partial \mathbf{n} = 0$$

where $\mathbf{u}_\tau$ is tangential to boundary oil velocity component , **n** is normal vector to considered part of boundary.

First two terms in equation (4) are traditional and describe movement of boundary as movement of particles its making. The last term describes movement of boundary due to drain of mass, stipulated by processes of evaporation of oil and filtration.

On fixed (contact) boundary L_2 (if any) the following condition should be stated

$$L_2: \quad \mathbf{u}_n = 0 \qquad (6)$$

where $\mathbf{u}_n$ - normal to L_2 component **u**.

When contact boundary (booms or extended ice flow) is moved with velocity V_b, the boundary condition (A6) transforms as

$$L_2: \qquad \mathbf{u}_n = V_{bn} \qquad \text{(A7)}$$

Parameterizations

Parameterization of velocity $\mathbf{u}_d$ and turn angle α_d of a surface drift current is chosen as

$$\mathbf{u}_d = 0.03 W_{10} \qquad \text{(A8)}$$

$$\alpha_d = (1.-\exp(-H_d/H_o))\,[40^o - 8x(W_{10})^{0.5}], \quad W_{10} \le 25 \text{ m/c}$$

$$\alpha_d = 0 \qquad W_{10} > 25 \text{ m/c}$$

Where W_{10} –wind velocity at 10m, H_d - depth in oil slick location, H_o - reference depth.

Oil is represented as a mixture of several (8-20) components with known temperatures of boiling (true boiling point) and densities of fractions. Peculiarities of oil types are defined by the various percentage parity of components in mixture.

The mass flux due to evaporation is represented as:

$$k_e = k\sum_k \frac{MW_k VP_k X_k}{RT} \qquad \text{(A9)}$$

Where k is empirical factor, VP_k is partial vapor pressure of a fraction of oil, MW_k is molecular weight of a fraction, X_k is molar concentration of a fraction, R is universal gas constant, T is water surface temperature.

$$k = 0.0018(\mathbf{W}_{10})^{0.78} \quad \text{if } \mathbf{W}_{10} > 4 \text{ m/s} \qquad \text{(A10)}$$

$$k = 0.005 \quad \text{if } \mathbf{W}_{10} < 4 \text{ m/s}$$

At high sea state the additional factor of reduction of surface concentration of oil is a flow of drops in marine environment due to breaking waves. This flux can be entered parametrically as follows

$\rho\frac{\partial h}{\partial t} = -\rho h R \cdot F(r_0)$	1	Oil thickness on the sea surface change due to dispersion of oil h - averaged thickness of oil
$F(r_0) = V_d \int_0^{r_0} \frac{P(r)dr}{w(r)+V_d}$; $V_d = 0.0015 \cdot W_{10}$	2	$F(r_0)$ - function, indicating which part of oil from volume, penetrated under water surface will not return to surface V_d – conventional “diffusion” velocity of drops of oil
$w(r) = \frac{2}{9}\frac{(\rho_w - \rho)}{\rho_w}\frac{gr^2}{\nu_w}$	3	$w(r)$ - vertical velocity of a drop of oil with radius r due to buoyancy effect. ν_w - kinematics viscosity of water g - gravitational constant

$P(r) = 1.7\frac{r^{0.7}}{r_0^{1.7}}$	4	$P(r)$ - cumulative distribution function of volume of the dispersed oil by the drops sizes
$r_0 = \max(r_{d\max}, \bar{\bar{h}})$	5	r_0 – conventional maximum size of drops of oil
$r_{d\max} = r_{d0} \cdot k_d$,	6	r_{d0} - maximum size of drops of standard oil $r_{d\max}$ - maximum size of drops of considered oil
$\bar{\bar{h}} = k_d \cdot h$	7	k_d - coefficient $\bar{\bar{h}}$ - conditional thickness of a slick
$k_d = \frac{\sigma}{\sigma_0}(\frac{\mu}{\mu_0})^{\frac{3}{8}}$	8	σ, μ - surface tension and viscosity of oil σ_0, μ_0 - surface tension and viscosity of standard oil
$\sigma(\alpha) = \sigma_1 + (\sigma_0 - \sigma_1) \cdot 10^{-\alpha}$	9	σ_1 - surface tension oil - water after the powder dispenser impact $(\sigma_1 = 1)$
$\alpha = 20 \cdot \frac{\Omega_d}{\tilde{\Omega}_{oil}}$	10	$\Omega_{\hat{a}}$ - amount of the powder dispenser [m3] $\tilde{\Omega}$ - volume of handled oil
$\tilde{\Omega}_{oil} = h \cdot \tilde{S}_{oil}$	11	$\tilde{S}_{oil}$ - slick area, treated by the powder dispenser
$R = k\frac{g}{C_T^4}V_*^3 = k_1 \cdot W_{10}^3$ $k_1 = 0.014\frac{9.8}{6.4^4}(C_u)^{\frac{3}{2}}$ $C_u = 10^{-3}(1 + 0.07 \cdot W_{10})$	12	C_u - drag coefficient of a water surface R - "rate of rotation" of sea surface without an oil film W_{10} - wind velocity on 10 m horizont $C_T = 0.8 \cdot W_{10crit}$ W_{10crit} is critical wind velocity, when breaking waves appear.

Content of water in oil (during water-in-oil emulsification process) is parameterized as follows

$$(1 - k_2 F_w)\exp\left[\frac{2.5F_w}{1 - k_1 F_w}\right] = \exp(k_3 t) \qquad \text{(A11)}$$

The modification of viscosity of oil due to penetration of water in oil is described by relation

(A12)

Where F_w is volume part of water in oil, k_2 is inversed maximum volume part of water in oil. Typically, $k_3 = 2 \cdot 10^{-6} (W_{10})^2$, $k_1 = 0.65$

When the thickness of oil layer becomes less than ~0.05 mm, its area increases mainly by the processes of a turbulent diffusion. The mathematical formalization of this stage is

$$\frac{\partial C}{\partial t} + \mathbf{u}_c \nabla C = \nabla . k_T \nabla C \qquad \text{(A13)}$$

where C is the surface concentration of oil at sea surface, $\mathbf{u}_c$ - a velocity of a surface layer of water, k_T is the turbulent diffusion coefficient, depending on a space scale of phenomena and hydro meteorological conditions, with a boundary condition on contact boundary

$$L_2: \qquad \frac{\partial C}{\partial \mathbf{n}} = Q \qquad \text{(A14)}$$

Where Q - oil mass flux due to sedimentation on a shore.

Loss of a mass of oil, which can be absorbed and is strand on a various type of coast, are calculated with the following algorithm

$$L_2: \qquad Q \approx k_S H u_n(\delta) \qquad \text{(A15)}$$

Where k_S - empirical coefficient, depending on a coast morphological structure, $u_n(\delta)$ - component of a velocity of oil, normal to coastline on some distance δ from a shore.

At initial moment of time oil thickness distribution is *H* (x, y, 0) and velocity **u**(x, y, 0) and area Ω‘(0) are assumed known. It is required to determine *H* (x, y, t), **u**(x,y,t) and Ω (t,x,y) at t> 0.

The problem of oil spreading on sea surface partially covered by ice is natural for considering in two limiting cases. If (*a*) characteristic scale of spill is much less than characteristic floes sizes, that can probably be realized near fast ice boundaries, the following boundary condition is necessary to add, having flow of oil $Q_{oil\text{-}in\text{-}ice}$ in column of an ice cover

$$L_2: \qquad \mathbf{u}_n = 0 \qquad \text{(A16)}$$

$$Q_{oil\text{-}in\text{-}ice} = Q_{oil\text{-}in\text{-}ice}(\mathbf{u}, H, \mu, E, ...) \qquad (A17)$$

where E is the porosity of an ice cover.

If ice cover with characteristic floe sizes, considerably exceeding scales of oil spill is moving, the boundary condition is necessary to replace by

$$L_2: \qquad \mathbf{u}_n = \mathbf{u}_{in} \qquad (A18)$$

Where $\mathbf{u}_{in}$- normal to L_2 a component of ice velocity.

The conditions (A16) and (A17) should be complemented by a slip condition for component of velocity of an oil field tangential to L_2, if the role of the viscous stresses in equation (A1) is significant.

As other limiting case (*b*) it is natural to consider a situation, when the size of oil spill are much greater than characteristic floes sizes. In this situation a spreading of oil on surface of the sea will depend also on compactness of an ice cover.

The equations of momentum balance for oil *on sea surface* in this case will be written as

$$\rho(1-S)H\left(\frac{\partial \mathbf{u}}{\partial t} + \mathbf{u}\nabla\mathbf{u}\right) = -\rho g' H\nabla H - B_1(\mathbf{u} - (\mathbf{u}_d + \mathbf{u}_T))\left|\mathbf{u} - (\mathbf{u}_d + \mathbf{u}_T)\right| + B_2(\mathbf{u}_i - \mathbf{u}) \quad (A1a)$$

$$\frac{\partial H}{\partial t} + \nabla.(H\mathbf{u}) + H\frac{S}{1-S}\nabla.\mathbf{u}_i = -\frac{k_e + k_d}{\rho}F(S) - \frac{Q}{\rho(1-S)} \qquad (A2a)$$

The quantity of oil on unit of the area of a sea surface in considered situation is $(1-S)H$, as only the part of a surface of the sea, namely $(1-S)$ can be covered by spreading oil .

Two last terms in equation of the momentum balance (1a) describe effects of resistance to oil movement, and if the first term $B_1(\mathbf{u} - (\mathbf{u}_d + \mathbf{u}_T))\left|\mathbf{u} - (\mathbf{u}_d + \mathbf{u}_T)\right|$ describes " friction between oil and water ", and $B_1 \propto \beta_1(1\text{-}S)$, the second term $B_2(\mathbf{u}_i - \mathbf{u})$ describes dynamic effect of ice on oil field. Moving ice "bring" oil spill, and $B_2 \propto H\left[\frac{S}{d}\right]^{-1}$, where β_1,

β_2 is empirical parameters, d - characteristic floes size. The expression in square brackets $\left[\frac{S}{d}\right]$ is essentially lengths of a line of "lateral" interaction of a oil field with ice.

From physical reasons it is clear, that the velocity of a spreading will also depend on parameter, for instance ω , describing average distance between ice floes. It is clear also that the resistance to oil spreading will be greater when ice compactness $S = S_{crit}$ increases. The critical value of ice compactness, after which the oil spreading is stopped completely depend on geometrical properties of ice floes. For example, S_{crit} is about 0.91 for hexagonal packing of ice floes.

The last term in left part of an equation (A2a) occurs by virtue of that the changes of thickness of oil in "point" of sea covered by ice depend not only on dynamics of oil but also from change of ice field compactness.

The function F (S) in equation of the oil mass balance describes effects of reduction of the oil evaporation rate and penetration of the oil drops in water by the compact ice by the " wind shadow " or others, not taking into account in parameterizations mentioned above.

It is need to note, that in case of ice of enough large compactness presence, transport of oil pollution will largely depend on dynamics of ice cover and use of ice dynamics model, coupled with model of circulation of considered sea region is required.

Numerical technique

Numerical technique was developed to solve "shallow-water-like" two dimensional system of equation with free boundaries. This technique referred here as Eulerian-Lagrangian numerical technology is development of well-known Particles-In-Cells (PIC) method. Numerical technique was successfully used for oil spill forecasting in different hydro meteorological conditions, ice dynamics and investigations of introthermocline eddy lenses dynamics.

One of the most difficult problems in solving the system of equations (A1)-(A2) with boundary conditions (A3)-(A5), is that area where solution must be determined is generally unknown and should be calculated during the modeling process. A traditional Eulerian grid method use is inconvenient here, and it is preferable to work with a Eulerian-Lagrangian technique. The related method of calculations is known as particles-in-cells (PIC) method, but in fact the technique described here differs sufficiently from the original one developed by [Harlow, 1964]. However, one of the common features of this technologies is the use of two types of media representation - Lagrangian and Eulerian.

The object of modeling (oil) may be represented as a set of particles with several inherent parameters, such as space coordinates (z_i), velocity (v_i) and mass (m_i). The initial condition is stated as:

$$\{\mathbf{x}_i\} = \{\mathbf{x}_i(x,y,0)\}\ ,\ \{v_i\} = \{v_i(x,y,0)\}\ ,\ \{m_i\} = \{m_i\}\quad ;\quad \{\mathbf{x}_i\} \in \Omega_o\ ; \qquad \text{(A36)}$$

where Ω_o - initial configuration of oil spill. The number of particles must be sufficient to describe the boundary of area Ω_o , and later $\Omega(t)$, with required accuracy.

As far as coordinates of the particles are known, we superpose rectangular Eulerian grid on particles configuration in such way that it contains all particles. Then we can determine process characteristics U(x,y,t) and H(x,y,t) in grid representation . The example of grid configuration convenient for restoration of a field of velocity and thickness from particles in units of a grid is shown on Fig. 2

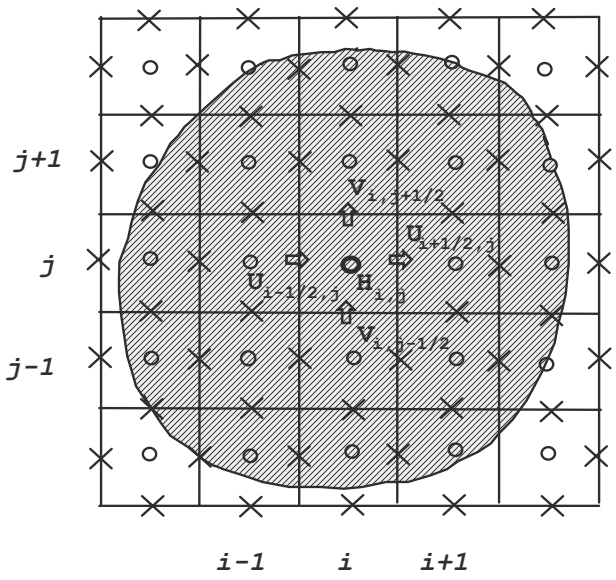

Figure 75. Schematic pattern of Eulerian grid.

The grid which is used in this technology is not quite Eulerian, because it is necessary to rebuild it at each time step. In traditional representation an Eulerian grid is defined by fixed in space points, but here these "fixed" points are changeable. Nevertheless we will call it a "Eulerian grid" for simplicity. As soon as the Eulerian grid has been constructed, we can transport all properties of the media from particles to grid, and the values of H(x,y,t) and U(x,y,t) as grid's functions will be determined at fixed space points.

$$H_{i,j} = \frac{\rho_o}{\gamma \Delta x \Delta y} \sum_{k}^{N_{ij}} m_k \tag{A37}$$

The following basic calculation steps are:

I. Calculation of intermediate values of $\mathbf{u}$ and H by the equations:

$$\Omega\text{‘}: \; H\frac{\partial \mathbf{u}}{\partial t} = -Hg'\nabla H - \beta(\mathbf{u} - (\mathbf{u}_d + \mathbf{u}_c))\left|\mathbf{u} - (\mathbf{u}_d + \mathbf{u}_c)\right| + \frac{1}{\rho_o}\nabla.\mathbf{T} \tag{A38}$$

$$\frac{\partial H}{\partial t} = 0$$

where all effects, associated with movement of media and mass fluxes are neglected . At this stage all necessary characteristics of media are described in Eulerian representation.

II. New values of the mass of particles are calculated in accordance with the following relationship:

$$m_i(t+\Delta t) = m_i(t) + \Delta t(k_e + k_d)S_p \qquad \text{(A39)}$$

where S_p - area of individual particle. This parameter does not have a physical meaning, but it is a suitable computational variable. The second step is finished with interpolation of **u** from grid to particles. At the end of this step media characteristics may be described in Lagrangian representation completely.

III. The third step is started from transport of particles with their properties across the Eulerian grid and new values of H and U are calculated to comply with the basic conservation laws for mass and momentum for every cell of the new Eulerian grid.

When the trajectory of particle cross the fixed (shoreline) boundary, the special technique (omitted here) is used to determine its new position. The mass of such particle is calculated in accordance with relationship (A15).

Step III represents the approximation of transport part of equations (A1) ,(A2):

$$\frac{\partial \mathbf{u}}{\partial t} + \mathbf{u}\nabla\mathbf{u} = 0 \qquad \text{(A1")}$$

$$\frac{\partial H}{\partial t} + \nabla.(H\mathbf{u}) = Q \qquad \text{(A2")}$$

At the end of this step media characteristics are transmitted from Lagrangian representation back to the Eulerian one.

Using the oil surface concentration gradient, the model calculates also “diffusion velocity”, which is subsequently added to the advective velocity field (obtained from a circulation model or available currents data).

Appendix B.

3D baroclinic model with free surface for currents calculation

Equations of motion

The initial system of equations with free surface in Cartesian coordinate system in hydrostatic approximation and in f-plane may be written as [Oey et al., 1985]:

$$\frac{\partial u}{\partial x}+\frac{\partial v}{\partial y}+\frac{\partial w}{\partial z}=0, \qquad \text{(B1)}$$

$$\frac{\partial u}{\partial t}+\frac{\partial}{\partial x}u^2+\frac{\partial}{\partial y}vu+\frac{\partial}{\partial z}wu-fv=-g\frac{\partial \zeta}{\partial x}-\frac{1}{\rho_0}\frac{\partial p_s}{\partial x}+N_h\left(\frac{\partial^2 u}{\partial x^2}+\frac{\partial^2 u}{\partial y^2}\right)+N_z\frac{\partial^2 u}{\partial z^2}, \qquad \text{(B2)}$$

$$\frac{\partial v}{\partial t}+\frac{\partial}{\partial x}vu+\frac{\partial}{\partial y}v^2+\frac{\partial}{\partial z}wv+fu=-g\frac{\partial \zeta}{\partial y}-\frac{1}{\rho_0}\frac{\partial p_s}{\partial y}+N_h\left(\frac{\partial^2 v}{\partial x^2}+\frac{\partial^2 v}{\partial y^2}\right)+N_z\frac{\partial^2 v}{\partial z^2}, \qquad \text{(B3)}$$

$$\frac{\partial \rho}{\partial t}+\frac{\partial}{\partial x}u\rho+\frac{\partial}{\partial y}v\rho+\frac{\partial}{\partial z}w\rho=K_z\frac{\partial^2 \rho}{\partial z^2}\ . \qquad \text{(B4)}$$

The coordinate system origin is placed at undisturbed sea surface, z axis is directed vertically upward, y axis – northward, x axis – eastward. The following definitions are used: f – Coriolis parameter, p-pressure, ρ - density, ρ_o – reference density value, u, v, w- velocity vector components by x, y, z axes, g- gravitation acceleration.

Pressure is written with hydrostatic condition used:

$$p=\int_z^{\zeta}\rho g dz=\rho_0\zeta+\int_z^{0}\rho g dz=\rho_0 g\zeta+p_s, \qquad \text{(B5)}$$

where ζ - free surface deviation from undisturbed condition,

$$p_s=\int_z^{0}\rho\, g dz\ .$$

N_h, N_z – horizontal and vertical turbulent viscosity coefficients, K_z-vertical turbulent diffusion coefficient.

Boundary conditions

At sea surface the tangential wind tractions are stated, cinematic condition and buoyancy flux absence condition as well:

$$N_z \frac{\partial u}{\partial z} = \tau_{sx}, \quad N_z \frac{\partial v}{\partial z} = \tau_{sy}, \quad \frac{\partial \zeta}{\partial t} + u \frac{\partial \zeta}{\partial x} + v \frac{\partial \zeta}{\partial y} = w, \quad K_z \frac{\partial \rho}{\partial z} = 0. \qquad \text{(B6)}$$

The quadratic tension law is adopted at bottom, and cinematic condition of current flow round the bottom relief roughness $H(x, y)$ and buoyancy flux absence condition:

$$N_z \frac{\partial u}{\partial z} = \tau_{bx}, N_z \frac{\partial v}{\partial z} = \tau_{by}, u \frac{\partial H}{\partial x} + v \frac{\partial H}{\partial y} = w, K_z \frac{\partial \rho}{\partial z} = 0. \qquad \text{(B7)}$$

In (B-6), (B-7) :

$$(\tau_{sx}, \tau_{sy}) = (C_d U_{ax} |\vec{U}_a|, C_d U_{ay} |\vec{U}_a|), \quad \vec{U}_a - \text{ wind velocity}, \quad C_d = 3{,}2 \cdot 10^{-6}, \qquad \text{(B8)}$$

$$(\tau_{bx}, \tau_{by}) = (\alpha u_b |\vec{U}_b|, \alpha v_b |\vec{U}_b|), \vec{U}_b - \text{velocity at bottom}, \alpha = 2{,}5 \cdot 10^{-3}. \qquad \text{(B9)}$$

Finite difference equations

In order to construct numerical scheme, a rectilinear mesh x_i, y_j, z_k is introduced covering all reference area. Side boundaries are approximated by the vertical planes, passing through the grid nodes. The upper boundary of the surface cells is changing in time, and the lower boundary of the bottom cells id defined by the bottom relief. The number of layers is defined by the depth of place and is changing spatially from 1 (upper and lower layers coincide) up to 18.

The semi-implicit approximation leap-frog scheme is used for temporal approximation. The velocity components are calculated at even time steps, and density and surface level - at odd ones. The equations terms with vertical turbulent viscosity and diffusion have been approximated implicitly, it allows to avoid time step restriction inherent to explicit time scheme:

$$\Delta t \le \Delta z^2 / 2N_z. \qquad \text{(B10)}$$

The most strong restriction is posed by explicit approximation of terms describing the long gravity waves propagation:

$$\Delta t \le \Delta x / (2gH)^{1/2}. \qquad \text{(B11)}$$

The velocity components u, v, w are calculated at cells sides, density and level – at centers, what is typical for the "C" mesh [Mesinger, Aracawa, 1979]. For spatial approximation the integral – interpolation method is used[Samarskii, 1989]. The initial equations are integrated through cells, the continual functions are replaced by their discrete

analogues, and fluxes through cell boundaries – correspondent finite difference approximations. The resulting finite-difference equations system appears like this:

The continuity equation:

$$\delta_k \cdot \left(\zeta^{n+3} - \zeta^{n+1}\right)_{i+1/2,j+1/2} / \Delta t + \left(\sigma_{i+1}^{n+1} \cdot \mathrm{u}_{i+1}^{n+2} - \sigma_i^{n+1} \cdot \mathrm{u}_i^{n+2}\right)_{j+1/2,k+1/2} / \Delta \mathrm{x} + \left(\sigma_{j+1}^{n+1} \cdot \mathrm{v}_{j+1}^{n+2} - \sigma_j^{n+1} \cdot \mathrm{v}_j^{n+2}\right)_{i+1/2,k+1/2} / \Delta \mathrm{y} + \left(\omega_{k+1}^{n+2} - \omega_k^{n+2}\right)_{i+1/2,j+1/2} = 0. \quad \text{(B12)}$$

Equation for u velocity component:

$$\left(\sigma^{n+1}\mathrm{u}^{n+2} - \sigma^{n+1}\mathrm{u}^{n}\right)_{\mathrm{i,j+1/2,k+1/2}} / \Delta \mathrm{t} + \left(\sigma_{\mathrm{i+1/2}}^{\mathrm{n+1}} \bar{\mathrm{u}}_{\mathrm{i+1/2}}^{\mathrm{n}} \mathrm{u}_{\mathrm{a,i}}^{\mathrm{n}} - \sigma_{\mathrm{i-1/2}}^{\mathrm{n+1}} \bar{\mathrm{u}}_{\mathrm{i-1/2}}^{\mathrm{n}} \mathrm{u}_{\mathrm{b,i}}^{\mathrm{n}}\right)_{\mathrm{j+1/2,k+1/2}} / \Delta \mathrm{x} + \left(\sigma_{\mathrm{j+1}}^{\mathrm{n+1}} \bar{\mathrm{v}}_{\mathrm{j+1}}^{\mathrm{n}} \mathrm{u}_{\mathrm{c,j+1/2}}^{\mathrm{n}} - \sigma_{\mathrm{j}}^{\mathrm{n+1}} \bar{\mathrm{v}}_{\mathrm{j}}^{\mathrm{n}} \mathrm{u}_{\mathrm{d,j+1/2}}^{\mathrm{n}}\right)_{\mathrm{i,k+1/2}} / \Delta \mathrm{y} + \left(\bar{\omega}_{\mathrm{k}}^{\mathrm{n}} \mathrm{u}_{\mathrm{e,k+1/2}}^{\mathrm{n}} - \bar{\omega}_{\mathrm{k+1}}^{\mathrm{n}} \mathrm{u}_{\mathrm{f,k+1/2}}^{\mathrm{n}}\right)_{\mathrm{i,j+1/2}} =$$
$$= \sigma_{\mathrm{i,j+1/2,k+1/2}}^{\mathrm{n+1}} \cdot [-\mathrm{g} \cdot (\zeta_{\mathrm{i+1/2}}^{\mathrm{n+1}} - \zeta_{\mathrm{i-1/2}}^{\mathrm{n+1}})_{\mathrm{j+1/2}} / \Delta \mathrm{x} - (\mathrm{P}_{\mathrm{s,i+1/2}}^{\mathrm{n+1}} - \mathrm{P}_{\mathrm{s,i-1/2}}^{\mathrm{n+1}})_{\mathrm{j+1/2,}} / \Delta \mathrm{x} + \mathrm{f} \cdot \bar{\mathrm{v}}_{\mathrm{i,j+1/2}}^{\mathrm{n}} \quad \text{(B13)}$$
$$+ \mathrm{N_h} \cdot (\mathrm{u}_{\mathrm{i+1}} - 2\,\mathrm{u}_{\mathrm{i}} + \mathrm{u}_{\mathrm{i-1}})_{\mathrm{j+1/2}}^{\mathrm{n}} / \Delta \mathrm{x}^2 + \mathrm{N_h} \cdot (\mathrm{u}_{\mathrm{j+3/2}} - 2\,\mathrm{u}_{\mathrm{j+1/2}} + \mathrm{u}_{\mathrm{j-1/2}})_{\mathrm{i}}^{\mathrm{n}} / \Delta \mathrm{y}^2]_{\mathrm{k+1/2}}$$
$$+ (\tau_{\mathrm{xk}}^{\mathrm{n+2}} - \tau_{\mathrm{xk+1}}^{\mathrm{n+2}})_{\mathrm{i,j+1/2}}.$$

Equation for v velocity component:

$$\left(\sigma^{\mathrm{n+1}}\mathrm{v}^{\mathrm{n+2}} - \sigma^{\mathrm{n+1}}\mathrm{v}^{\mathrm{n}}\right)_{\mathrm{i+1/2,j,k+1/2}} / \Delta \mathrm{t} + \left(\sigma_{\mathrm{i+1}}^{\mathrm{n+1}} \bar{\mathrm{u}}_{\mathrm{i+1}}^{\mathrm{n}} \mathrm{v}_{\mathrm{a,i+1/2}}^{\mathrm{n}} - \sigma_{\mathrm{i}}^{\mathrm{n+1}} \bar{\mathrm{u}}_{\mathrm{i}}^{\mathrm{n}} \mathrm{v}_{\mathrm{b,i+1/2}}^{\mathrm{n}}\right)_{\mathrm{j,k+1/2}} / \Delta \mathrm{x} + \left(\sigma_{\mathrm{j+1/2}}^{\mathrm{n+1}} \bar{\mathrm{v}}_{\mathrm{j+1/2}}^{\mathrm{n}} \mathrm{v}_{\mathrm{c,j}}^{\mathrm{n}} - \sigma_{\mathrm{j-1/2}}^{\mathrm{n+1}} \bar{\mathrm{v}}_{\mathrm{j-1/2}}^{\mathrm{n}} \mathrm{v}_{\mathrm{d,j}}^{\mathrm{n}}\right)_{\mathrm{i+1/2,k+1/2}} / \Delta \mathrm{y} + \left(\bar{\omega}_{\mathrm{k}}^{\mathrm{n}} \mathrm{v}_{\mathrm{e,k+1/2}}^{\mathrm{n}} - \bar{\omega}_{\mathrm{k+1}}^{\mathrm{n}} \mathrm{v}_{\mathrm{f,k+1/2}}^{\mathrm{n}}\right)_{\mathrm{i+1/2,j}} =$$
$$= \sigma_{\mathrm{i+1/2,j,k+1/2}}^{\mathrm{n+1}} \cdot [-\mathrm{g} \cdot (\zeta_{\mathrm{j+1/2}}^{\mathrm{n+1}} - \zeta_{\mathrm{j-1/2}}^{\mathrm{n+1}})_{\mathrm{i+1/2}} / \Delta \mathrm{y} + (\mathrm{P}_{\mathrm{s,j+1/2}}^{\mathrm{n+1}} - \mathrm{P}_{\mathrm{s,j-1/2}}^{\mathrm{n+1}})_{\mathrm{i+1/2}} / \Delta \mathrm{y} - \mathrm{f} \cdot \hat{\mathrm{u}}_{\mathrm{i+1/2,j}}^{\mathrm{n}} + \quad \text{(B14)}$$
$$+ \mathrm{N_h} \cdot (\mathrm{v}_{\mathrm{i+3/2}} - 2\mathrm{v}_{\mathrm{i+1/2}} + \mathrm{v}_{\mathrm{i-1/2}})_{\mathrm{j}}^{\mathrm{n}} / \Delta \mathrm{x}^2 + \mathrm{N_h} \cdot (\mathrm{v}_{\mathrm{j+1}} - 2\mathrm{v}_{\mathrm{j}} + \mathrm{v}_{\mathrm{j-1}})_{\mathrm{i+1/2}}^{\mathrm{n}} / \Delta \mathrm{y}^2]_{\mathrm{k+1/2}}$$
$$+ (\tau_{\mathrm{y,k}}^{\mathrm{n+2}} - \tau_{\mathrm{y,k+1}}^{\mathrm{n+2}})_{\mathrm{i+1/2,j}}.$$

Equation for density:

$$(\sigma^{n+3}\rho^{n+3} - \sigma^{n+1}\rho^{n+1})_{i+1/2,j+1/2,k+1/2} / \Delta t + (\sigma_{i+1}^{n+1} u_{i+1}^{n+2} \rho_{a,i+1/2}^{n+1} - \sigma_i^{n+1} u_i^{n+2} \rho_{b,i+1/2}^{n+1})_{j+1/2,k+1/2} / \Delta x +$$
$$(\sigma_{j+1}^{n+1} v_{j+1}^{n+2} \rho_{c,j+1/2}^{n+1} - \sigma_j^{n+1} v_j^{n+2} \rho_{d,j+1/2}^{n+1})_{i+1/2,k+1/2} / \Delta y + (\omega_k^{n+2} \rho_{e,k+1/2}^{n+3} - \omega_{k+1}^{n+2} \rho_{f,k+1/2}^{n+3})_{i+1/2,j+1/2} =$$
$$K_{z,k} (\rho_{k+1/2}^{n+3} - \rho_{k-1/2}^{n+3})_{i+1/2,j+1/2} / \Delta\sigma_k - K_{z,k+1} (\rho_{k+3/2}^{n+3} - \rho_{k+1/2}^{n+3})_{i+1/2,j+1/2} / \Delta\sigma_{k+1}. \quad \text{(B15)}$$

The following definitions have been introduced in (B11-B15):

$$\delta_k = 1, k = 0; \delta_k = 0, k = 1,\ldots,B-1; \omega_k = w_k, k = 1,\ldots B-1; \omega_0 = 0, \omega_B = 0;$$
$$\sigma_{k+1/2} = z_k - z_{k+1}, k = 1,\ldots.B-2; \sigma_{1/2} = z - z_1, \sigma_{B-1/2} = z_{B-1} + H;$$
$$(\tau_{xk}, \tau_{y,k}) = N_{zk}\left(\frac{u_{k+1/2} - u_{k-1/2}}{\sigma_k}, \frac{v_{k+1/2} - v_{k-1/2}}{\sigma_k}\right); \sigma_k = (\sigma_{k+1/2} - \sigma_{k-1/2}) / 2, k = 1,\ldots B-1$$
$$(\tau_{Bx}, \tau_{By}) = \alpha\left|\vec{U}_B\right|^n (u_B, v_B)^{n+2}; (\tau_{sx}, \tau_{sy}) = C_d\left|\vec{U}_a\right|^{n+2} (U_{ax}, U_{ay})^{n+2}.$$
$$i = 1,\ldots\ldots M \qquad j = 1,\ldots\ldots\ldots\ldots N$$

The line on top defines the averaging by two netboring points e.g.:

$$\overline{u}_{i+1/2} = (u_{i+1} + u_i) / 2,$$

and «top cover» - averaging by four netbour points:

$$\overline{v}_{i,j+1/2,k+1/2} = (v_{i-1/2,j,k+1/2} + v_{i+1/2,j,k+1/2} + v_{i-1/2,j+1,k+1/2} + v_{i+1/2,j+1,k+1/2}) / 4.$$

In advective nonlinear terms for velocity and density equations variables with a, b, c, d, e, f indexes depend on velocity sign at the cell side and are defined through conservative scheme with oriented differences [Rouch, 1980], e.g.:

$$\rho_{a,i+1/2} = \rho_{i+1/2}, \quad u_{i+1} \geq 0; \quad \rho_{a,i+1/2} = \rho_{i+3/2}, \quad u_{i+1} \leq 0;$$
$$\rho_{b,i+1/2} = \rho_{i+1/2}, \quad u_i \leq 0; \quad \rho_{b,i+1/2} = \rho_{i-1/2}, \quad u_i \geq 0.$$

The vertical turbulence viscosity coefficient is depth dependent. The following approximation is used [Backhaus, Hainbucher, 1987; Ryabinin, Zilberstein, 1996]:

$$N_z = k_{\min} + k_0 k_s, \qquad \text{(B16)}$$

where $k_{min} = 25$ cm^2/c,

$$k_0 = kH\left|\vec{U}_i\right|, \qquad \text{(B17)}$$

where H – total depth, $\left|\vec{U}_i\right|$ - averaged through the i –th layer thickness module of the current velocity,

k – dimensionless coefficient, called as Bowden turbulence coefficient [Bowden, Hamilton, 1975]. Its value is chosen there as 2,7 10^{-3} [Fang, Ichiye, 1983].

$$k_s = (1 + \sigma \mathrm{Ri}_i)^{-p}, \qquad \text{(B18)}$$

where Ri_i is Richardson number for i th layer, $\sigma = 7$, $p = 0.25$

So, the turbulent mixing rate depend as on current velocity, as on stratification.

At the liquid boundary the tide level variations are complemented by level values defined by inverse barometer law.

At sea surface the atmospheric pressure gradients and tangential wind stresses have been stated.

Appendix D.

List of files

File name	Brief description	Comments
Bs(01:31)(01,02,04).* Sample – Fig. -----	Oil spill trajectories for season for each spill points	Bs0101.* – a set of oil spill trajectories from point number 01 during season number 01
Tr_all(01:31).* Sample – Fig.-----	Oil spill trajectories combined for three seasons for each spill points	Tr_all01.* - a set of oil spill trajectories from point number 01, processed for each days. Processed information include: **Numtraj** – number of trajectories **Season** – number of season (1-summer, 2 - autumn, 3 -spring) **Day -** days after spill accident S_oil - surface oil, % D_oil - dispersed oil, % E_oil - evaporated oil, % Thick_mm - average oil thickness for *15000* oil discharged, mm Windm_mc - maximum wind speed for day Area_sqkm - square of spill area for *15000* oil discharged, sq. km CtimeHour – time to shore impact for this trajectories

Prob(01:31)(01,02,04).* Sample – Fig.-----	Probability of area impact (%) for each spill points	Day_1- probability of oil spill impact to 10x10 km sea area during *first* day after spill accident, Day_2 - probability of oil spill impact to 10x10 km sea area during *second* day after spill accident, ……. P_10t - probability of oil spill impact to 10x10 km sea area during *10 days* after spill accident Risk_Zone – *minimum days* after spill accident to impact 10x10 km sea area
Pr_all(01:31) Sample – Fig.-----	Probability of area impact (%) combined for each spill points	Just the same for 3 seasons
Pd_cst(01:31) Sample – Fig.-----		Probabilities of shore inpact for individual days, %
Pr_cst(01:31) Sample – Fig.-----		Summarized probabilities of shore impact for days after spill, %

P_coast8.* P_coast10.* P_coast13.* P_coast18.* P_coast27.* P_coast31.* P_coast22.* P_coast29.* Sample – Fig.7	Ust Luga Ventspils Klaipeda Gdansk-Kaliningrad Muuga Butinge Nynashamn Rostock	Probabilities of oil impact to 20 km segnent of shoreline around the point of hypothetical spill. YearDay1 - probability to contact with selected shoreline segment during the first day after accident througt 3 “no ice” seasons YearDay3 - …during first 3 days… YearDay5 - …during first 5 days… YearDay10 - …during first 5 days…

Comments:

1. In all files **Seasons** means – 01/summer, 02/autumn, 04/spring except of files Tr_all(01:31).* as mentioned above.
2. Parameters (Thick_mm, area_sqkm) in files Tr_all(01:31).* are related to oil discharge 15000 ton choosen as a sample in statistical calculations.
   All files above have been designed in MAPINFO format.

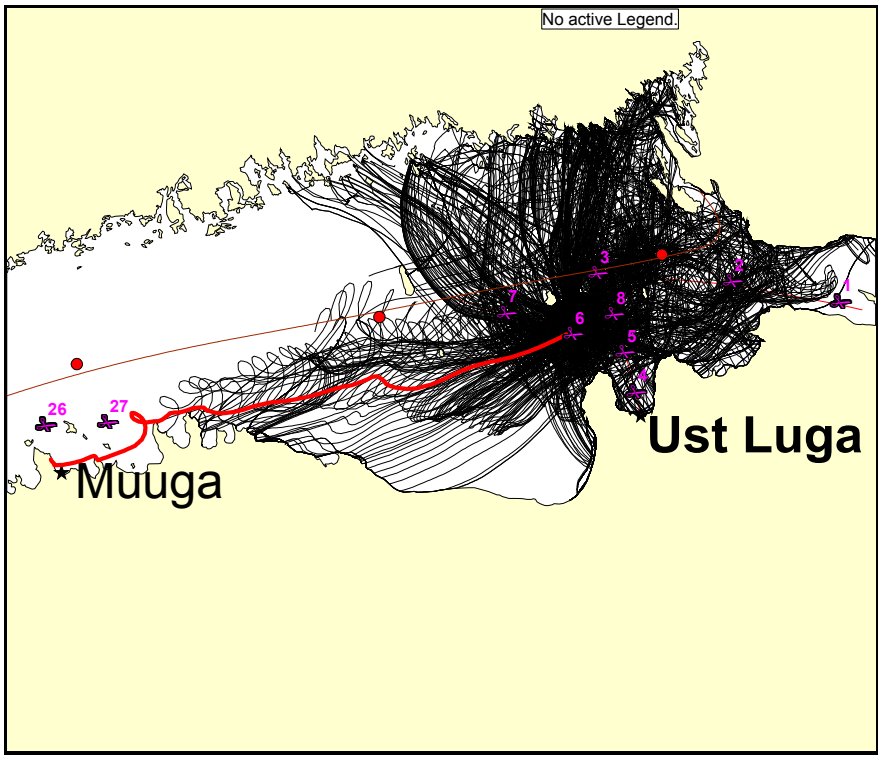

Fig.1 A set of trajectories from point 6 for spring. One individual trajectory is marked as thick red line. (*Files Bs0604.**)

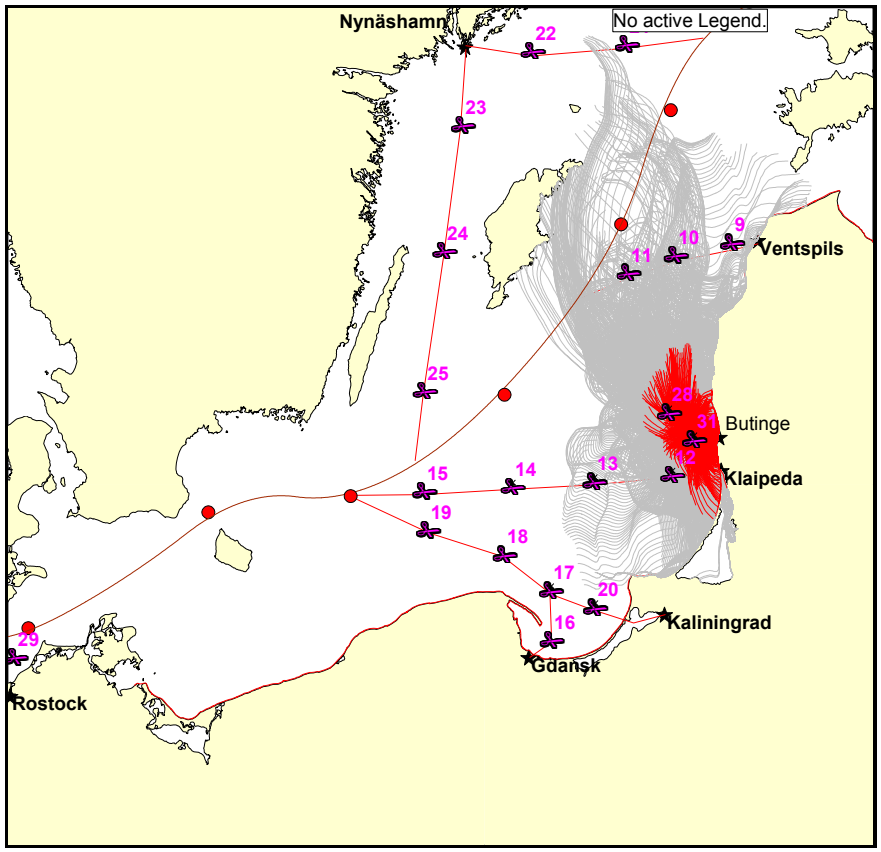

Fig.2 A set of trajectories of oil spill movement from point 31. Selected red color shows the 1 day after spill accident trajectories. (*Files Tr_all31.**)

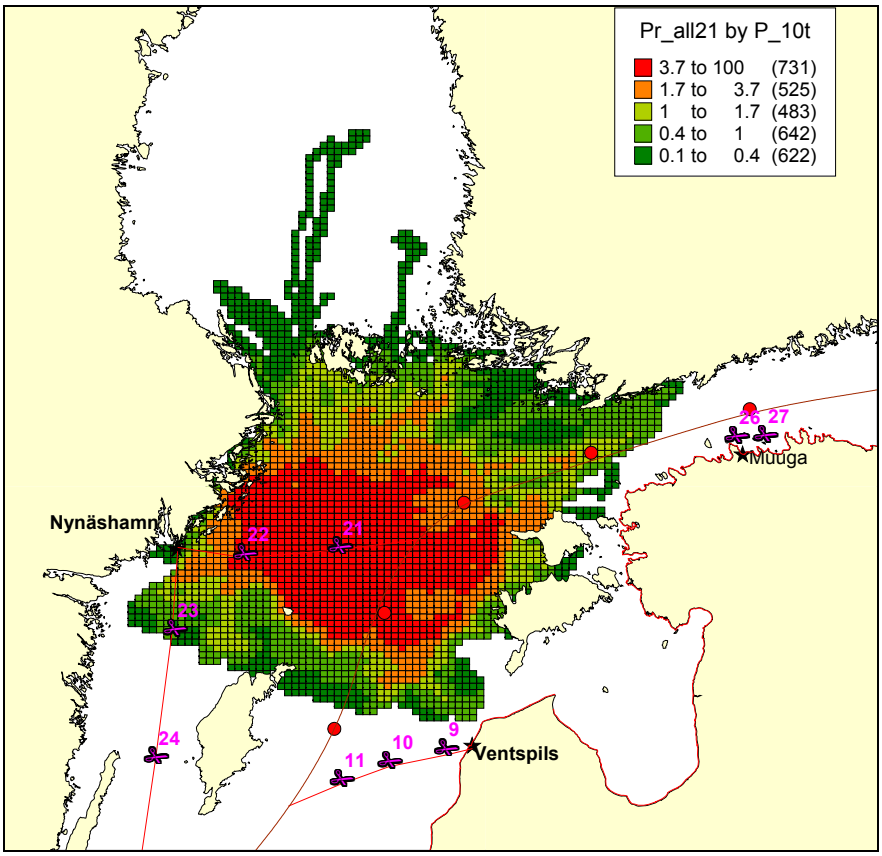

Fig.3.1 Probabilities of sea area impact for point 21(*Files Pr_all21.* Thematic map for P_10t)*

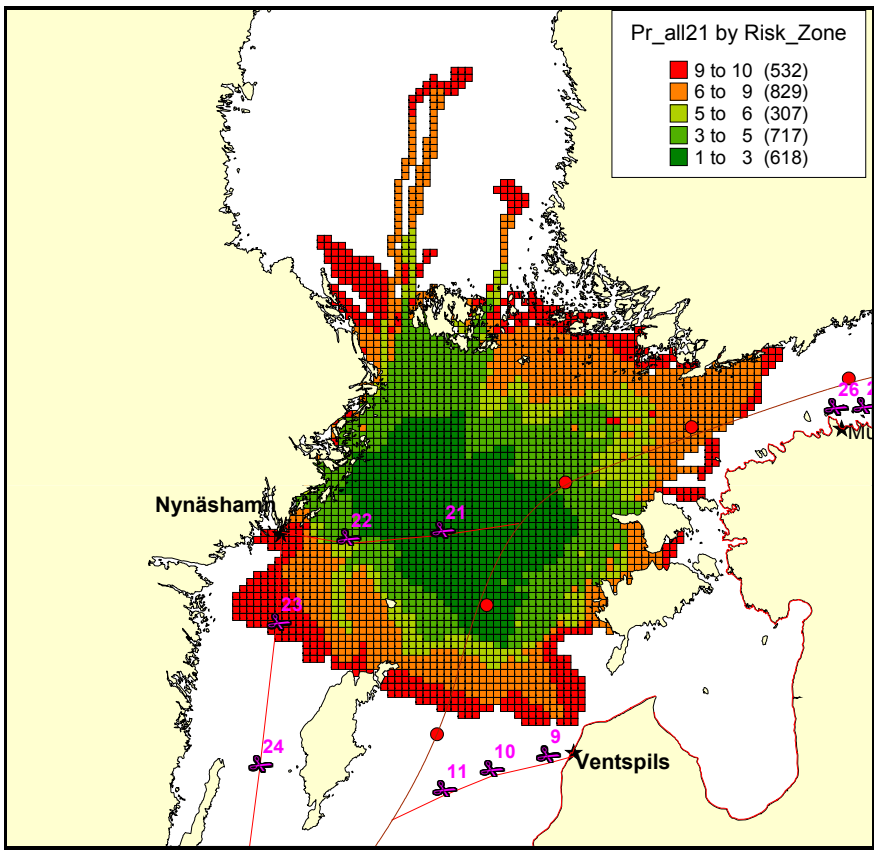

Fig. 3.2. Risk zone for point 21 (*Files Pr_all21.*. Thematic map for Risk_zone)*

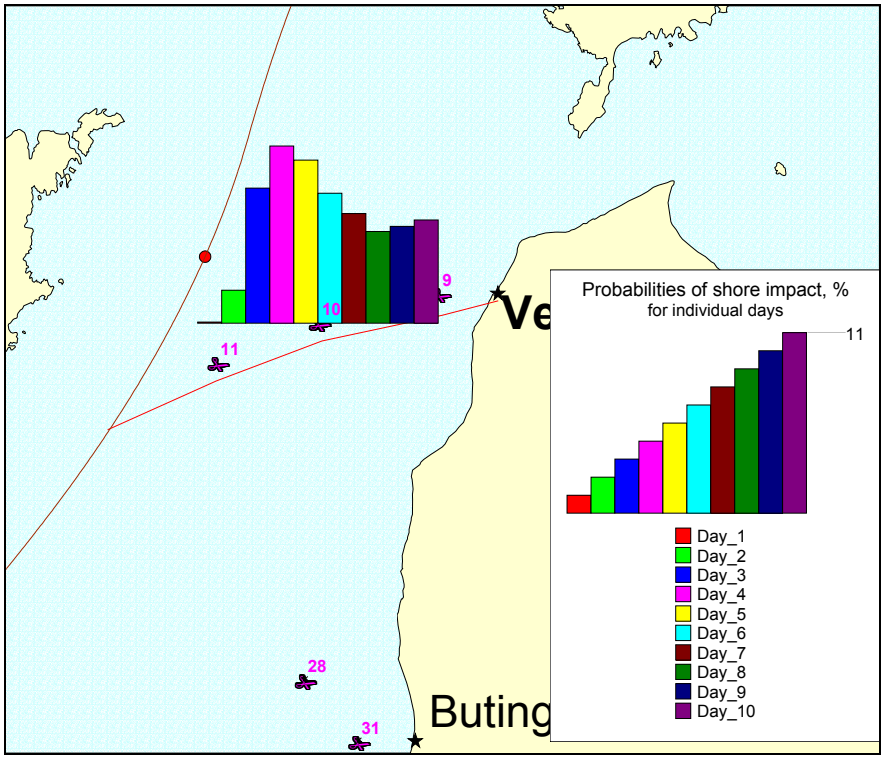

Fig. 5 Probabilities of shore inpact for individual days, % *(Files Pd_cst10.*. Thematic map for Day_1-Day_10)*

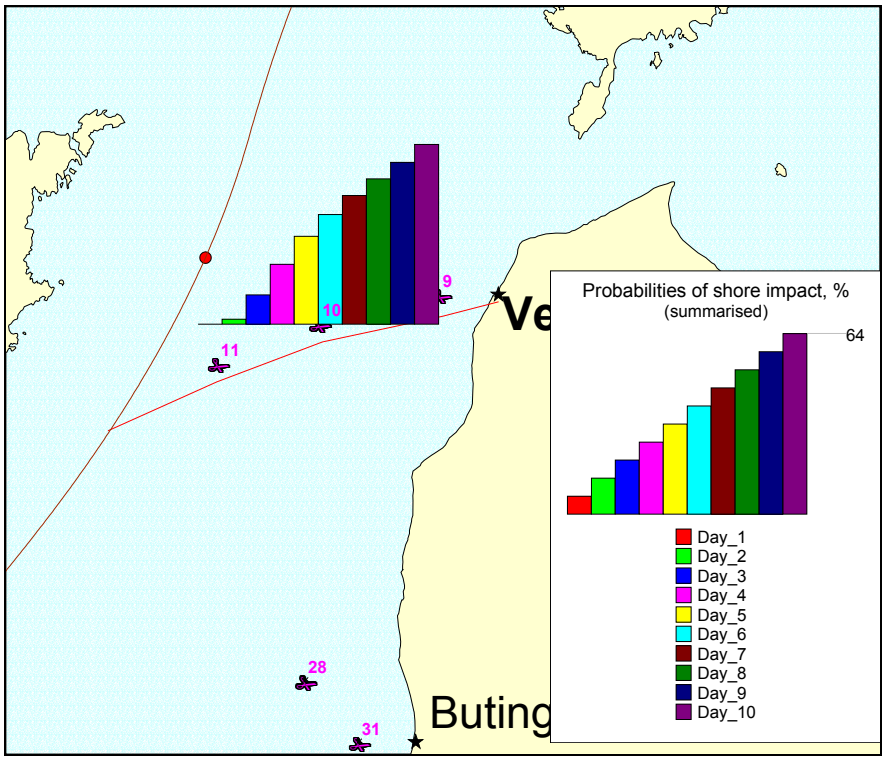

Fig.6 Summarized probabilities of shore impact for days after spill, %*(Files Pr_cst10.*. Thematic map for Day_1-Day_10)*

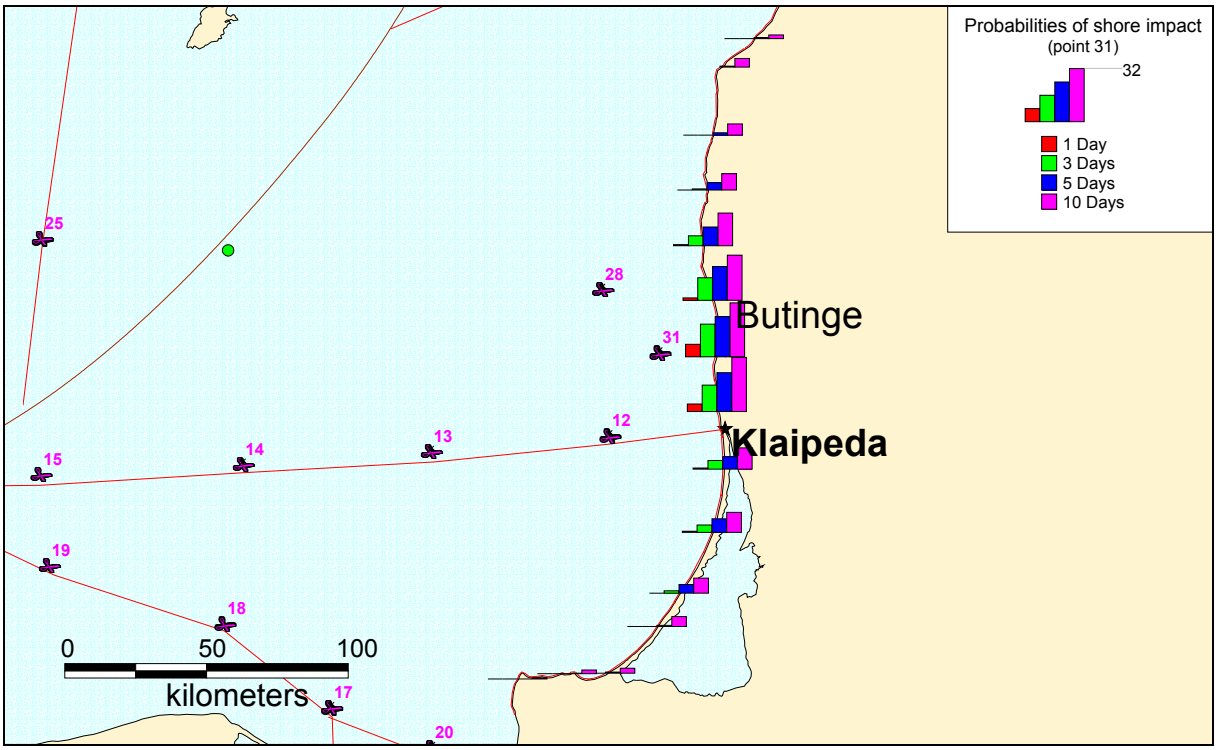

Fig. Probabilities of shoreline impact (point 31) *(Files p_coast31.*. Thematic map for YearDay1, YearDay3, YearDay5, YearDay10)*